

Random Walkers & Electrodiffusion: A Primer



Random Walk with Drift (Marius Lehene)

Christopher Bergevin

York University, Dept. of Physics & Astronomy

Slides available at:

<http://www.yorku.ca/cberge/>

References/Acknowledgements

- Weiss TF (1996) *Cellular Biophysics vols.1&2* (MIT Press)
- Bialek W (2012) *Biophysics: Searching for Principles* (Princeton UP)
- Murray JD (2003) *Mathematical Biology vols.1&2* (Springer)
- Keener J & Sneyd J (1998) *Mathematical Physiology* (Springer)
- Nelson P (2002) *Biological Physics* (WH Freeman)
- Dennis Freeman (MIT) <https://ocw.mit.edu/courses/electrical-engineering-and-computer-science/6-021j-quantitative-physiology-cells-and-tissues-fall-2004/>

Starting Point: Quiz



How many neurons are there in the human brain? Synapses?

Human brain contains $\sim 10^{11}$ (100 billion) neurons!
(with 100 trillion+ connections inbetween)


“Grand Challenge”

U.S. Department of Health & Human Services

NIH National Institutes of Health
Turning Discovery Into Health

The BRAIN Initiative® About | Resources | Funding | BRAIN & News | **BRAIN Update¹** | Contact Us

The BRAIN Initiative®



BRAIN Update
New Funding Opportunity Announcements and a Pre-Application Webinar for the BRAIN Initiative Advanced Postdoctoral Career Transition Award to Promote Diversity (K99/R00)
 Program for BRAIN Initiative K99/R00 Career Transition Award to Promote Diversity

Cell Type **Circuit Diagrams** **Monitor Neural Activity** **Interventional Tools** **Theory and Data Analysis Tools** **Human Neuroscience** **Integrated Approaches**

WHAT IS THE BRAIN INITIATIVE?

The Brain Research through Advancing Innovative Neurotechnologies® (BRAIN) Initiative is aimed at revolutionizing our understanding of the human brain. By accelerating the development and application of innovative technologies, researchers will be able to produce a revolutionary new dynamic picture of the brain that, for the first time, shows how individual cells and complex neural circuits interact in both time and space. Long desired by researchers seeking new ways to treat, cure, and even prevent brain disorders, this picture will fill major gaps in our current knowledge and provide unprecedented opportunities for exploring exactly how the brain enables the human body to record, process, utilize, store, and retrieve vast quantities of information, all at the speed of thought.

Highlights of The BRAIN Initiative®

- Re-visiting BRAIN's Strategic Plan**
Accepting input using BRAINfeedback@nih.gov
- 2017 Funded Awards**

- BRAIN Initiative Funding Opportunities**


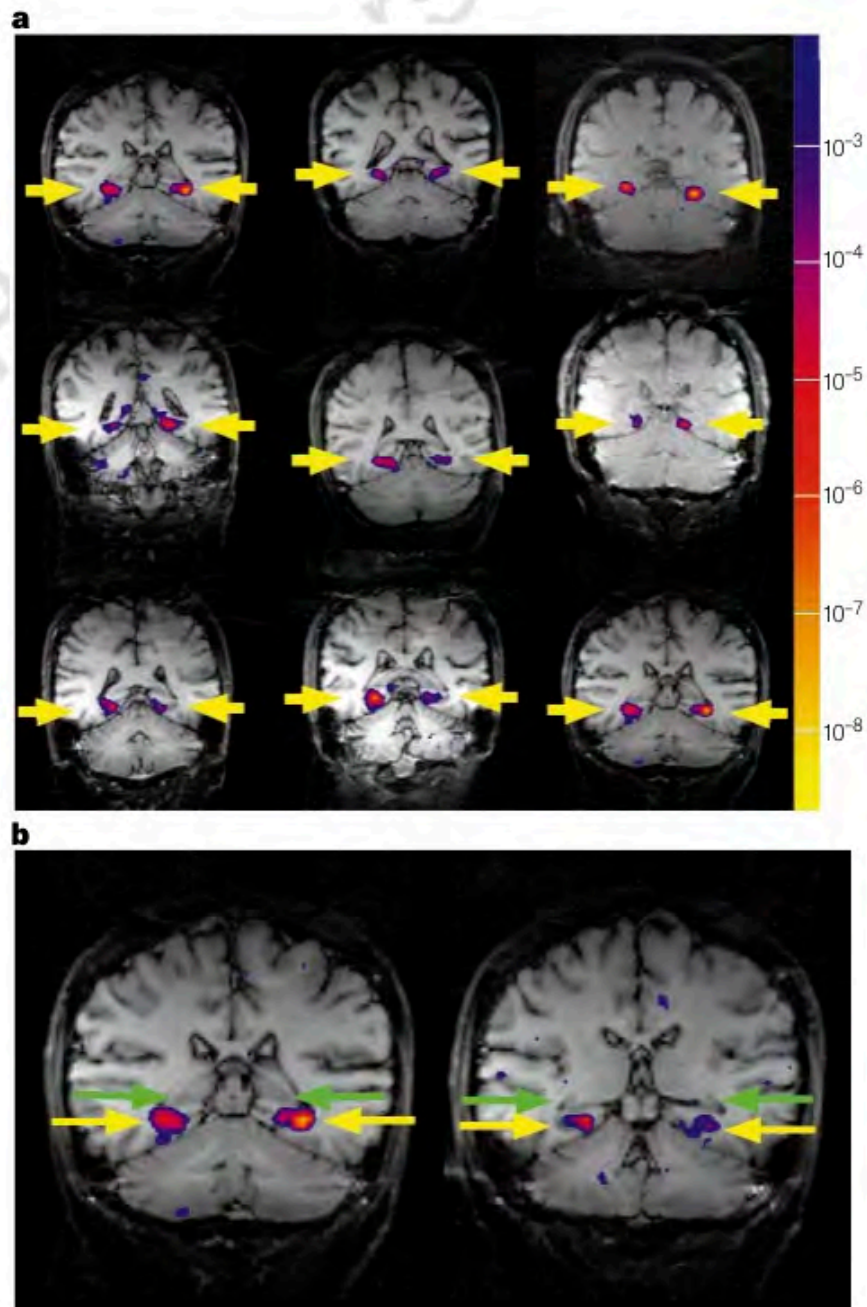
- BRAIN 2025 Report**
- BRAIN Alliance**

BRAIN Initiative Partners

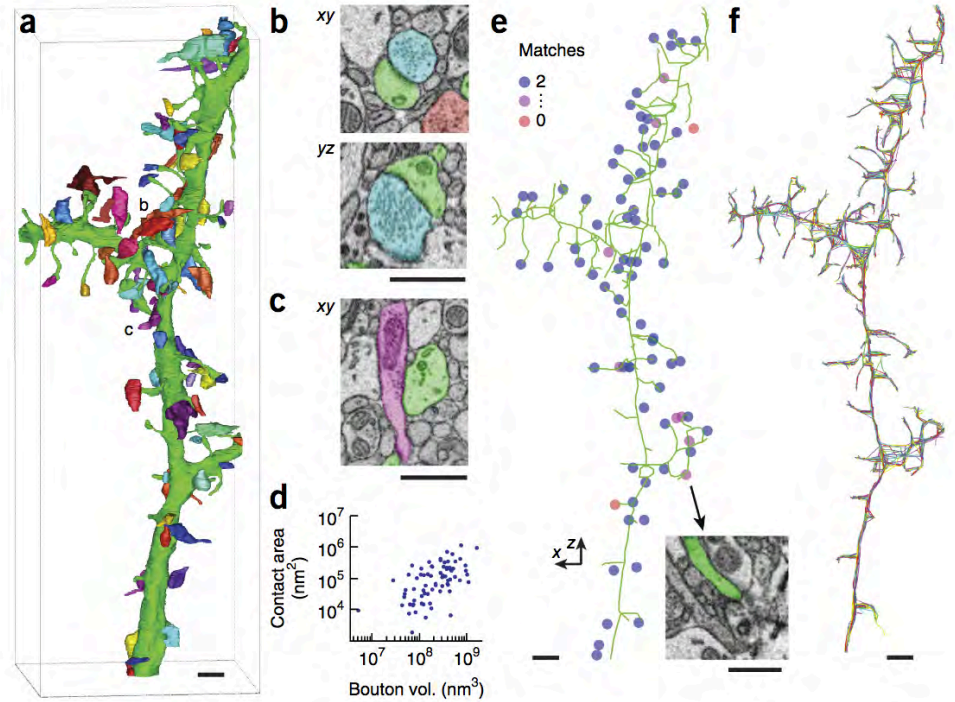
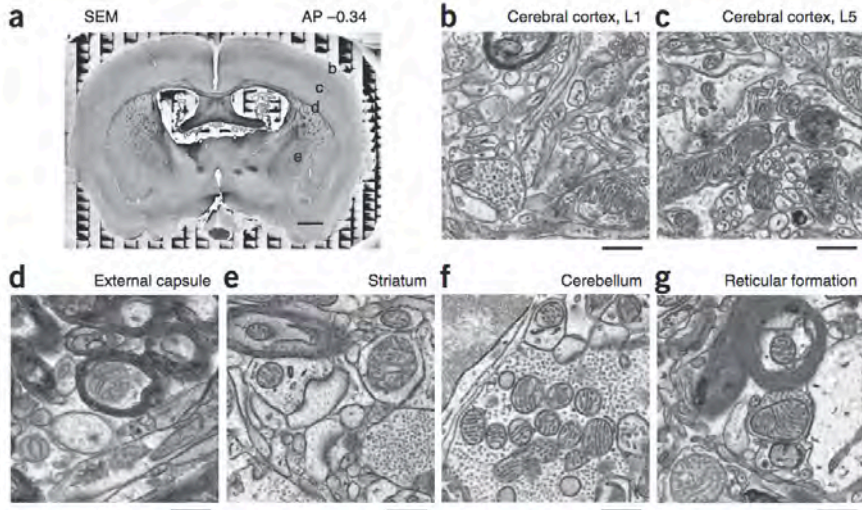
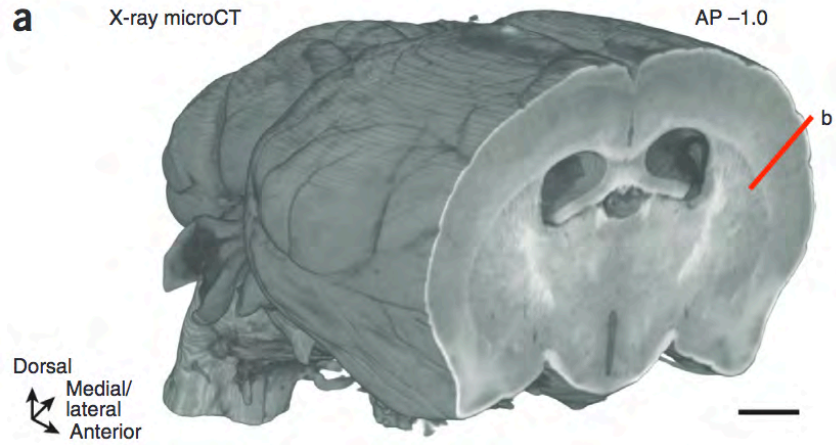
Federal

- National Science Foundation (NSF)
- Defense Advanced Research Projects Agency (DARPA)
- U.S. Food and Drug Administration (FDA)
- The Intelligence Advanced Research Projects Activity (IARPA)

Tools... (e.g., fMRI)



Epstein & Kanwisher (1998)



Tools... (e.g., Optogenetics)



OPTOGENETICS

sequence info virus preparation hardware request materials references d-lab

Brain tissue light transmission calculator
Angeled Stereotax coordinate calculator (MatLab)
Opsin and fluorophore spectra tool

Clarity Resource Site
Optogenetic courses
Fiber photometry resources

2016 Perspective
Cell
Targeting circuits

2015 Commentary
nature neuroscience
Optogenetics 10 year history

2016 Primer
Cell
Communication in the brain

2014
nature
Circuit dynamics of behavior

2015
Neuron
Closed-loop optogenetics

2014 Annual Review of Biomedical Engineering
Optical neural interfaces

2012 Analysis
nature methods
Quantitative opsin properties

2012
nature REVIEWS
Optogenetics & neural circuits in brain disease

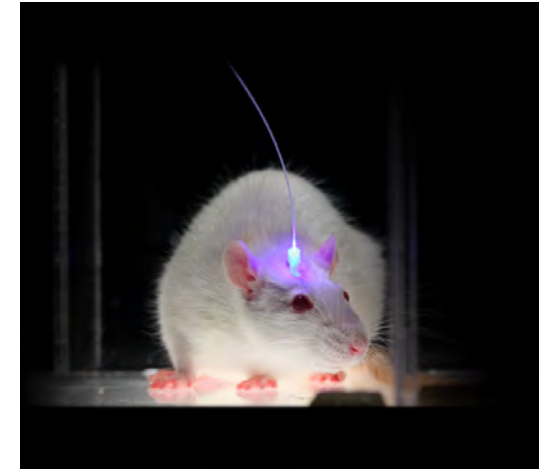
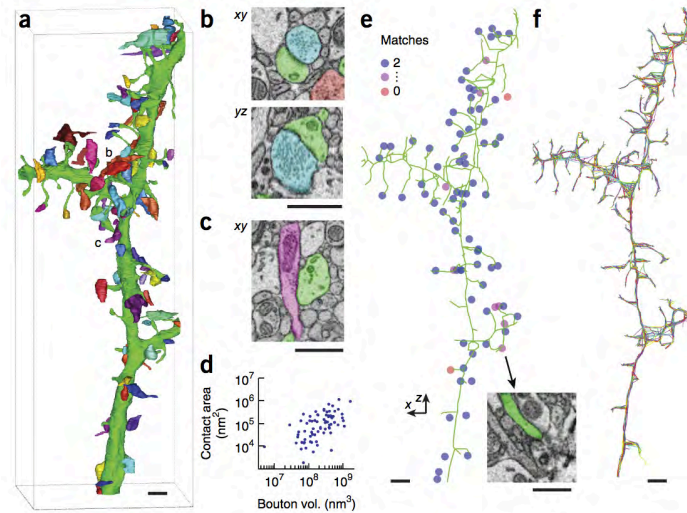
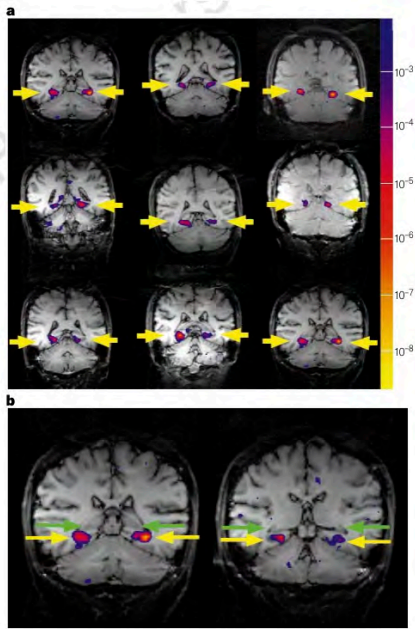
2011 Primer
Neuron
Optogenetics in neural systems

2011 Annual Review of Neuroscience
Development & application of optogenetics

2010 Method of the year
nature methods

2010
SCIENTIFIC AMERICAN
Controlling the brain with light

“Grand Challenge” (re the brain) → Role of physicists?



(pedantic aside)

Unlocking the potential of any application requires a deep understanding...

Today's Goal

Focus on a small piece of this pie to highlight a variety of key biophysical concepts/ideas

Diffusion

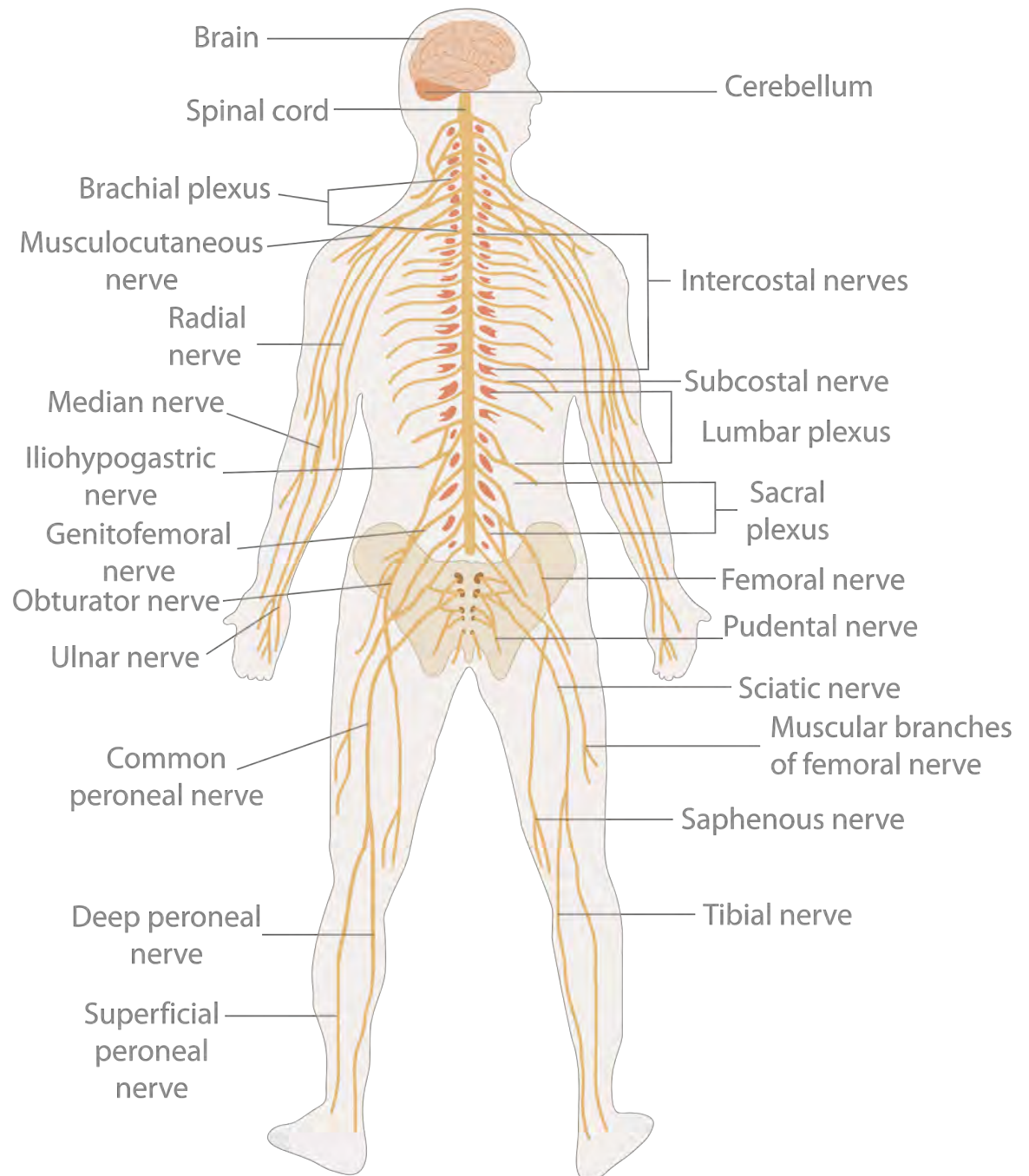
Stochastics

Model of a neuron

Micro vs Macro

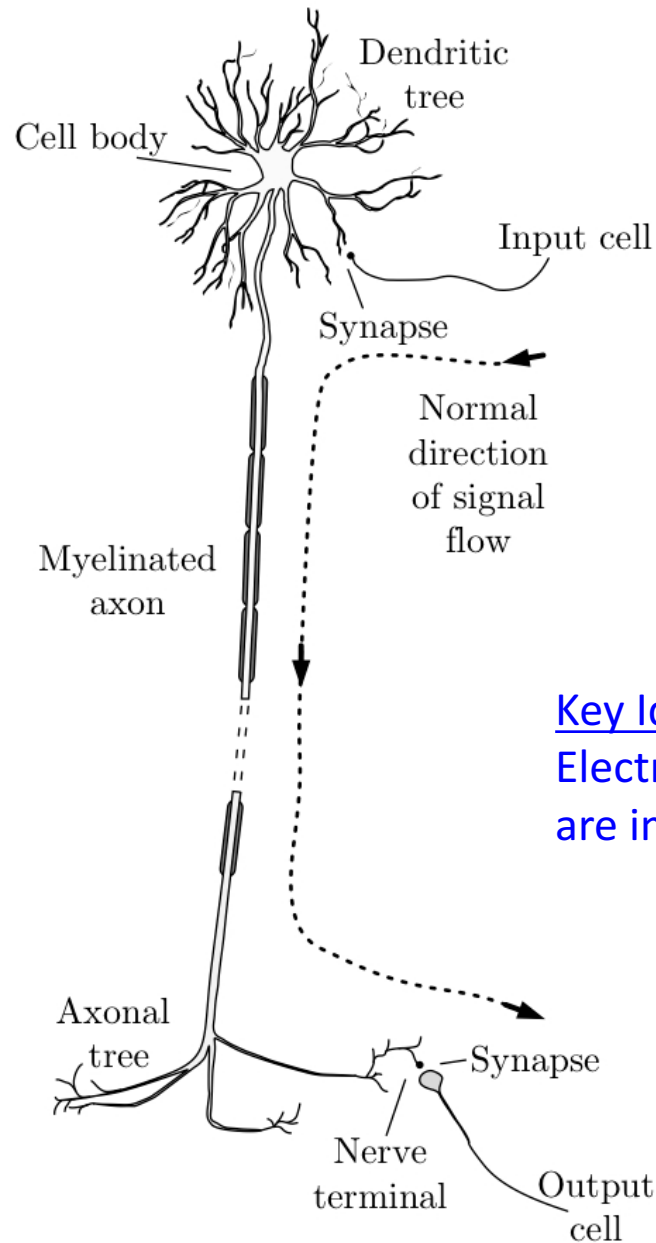
Electrodifussion

Nervous system



Neurons are key base unit of nervous system

Neurons



Neurons (“fibers”)
= Information highway

Key Idea:
Electrical properties of cells
are important

Figure 1.22

Action Potentials

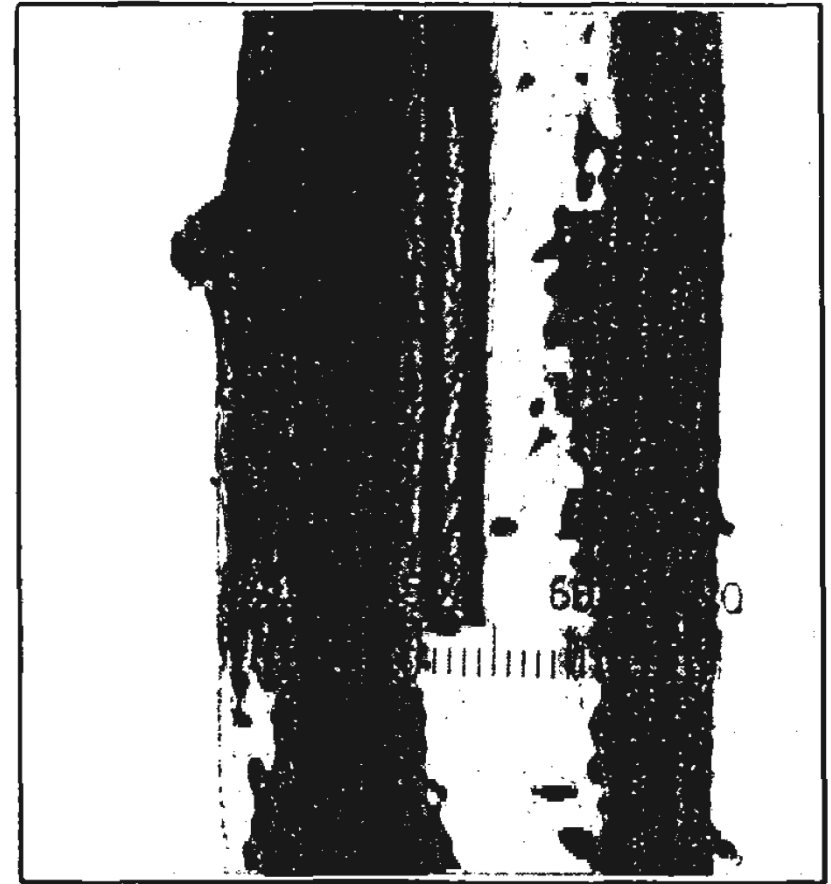
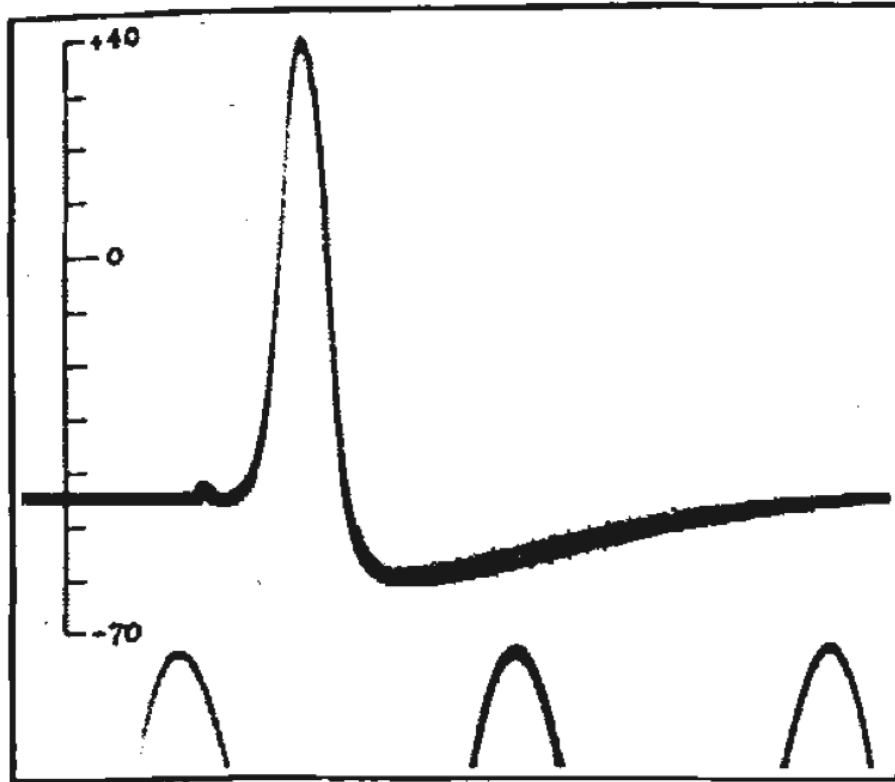


Fig. 1.
PHOTOMICROGRAPH OF ELECTRODE INSIDE GIANT
AXON. 1 SCALE DIVISION = 33 μ .

Action Potentials

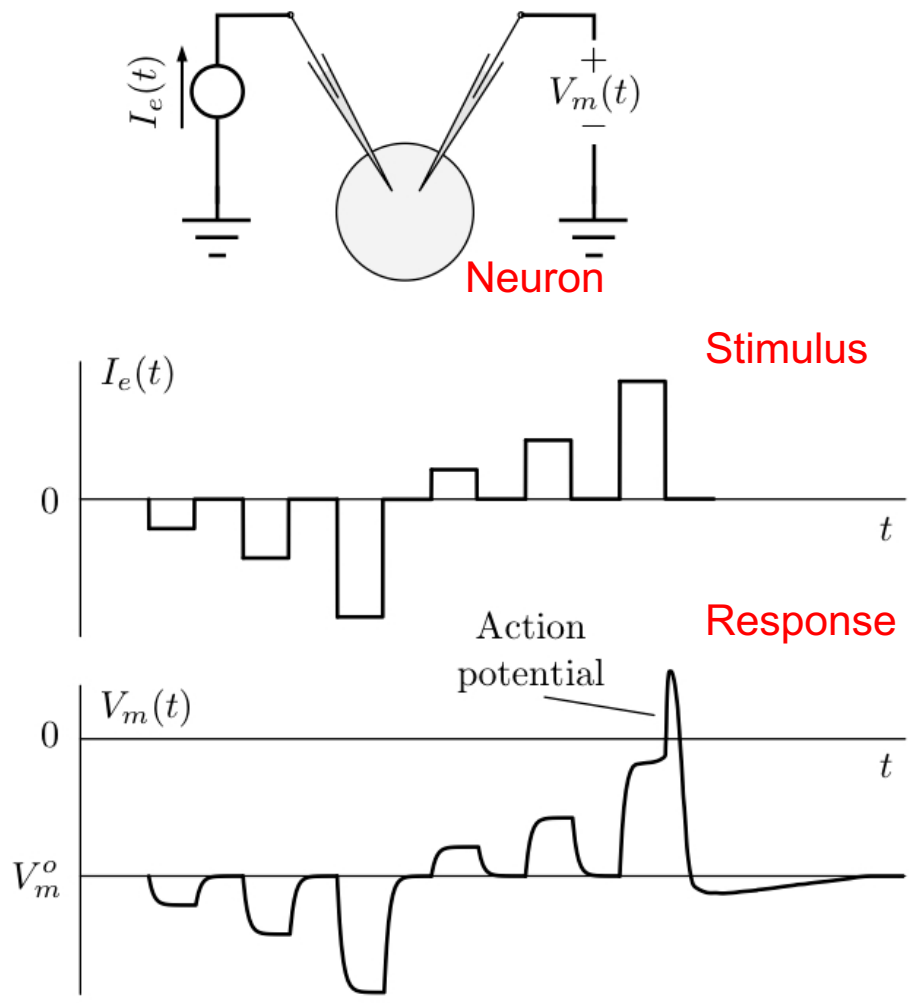


Figure 1.8

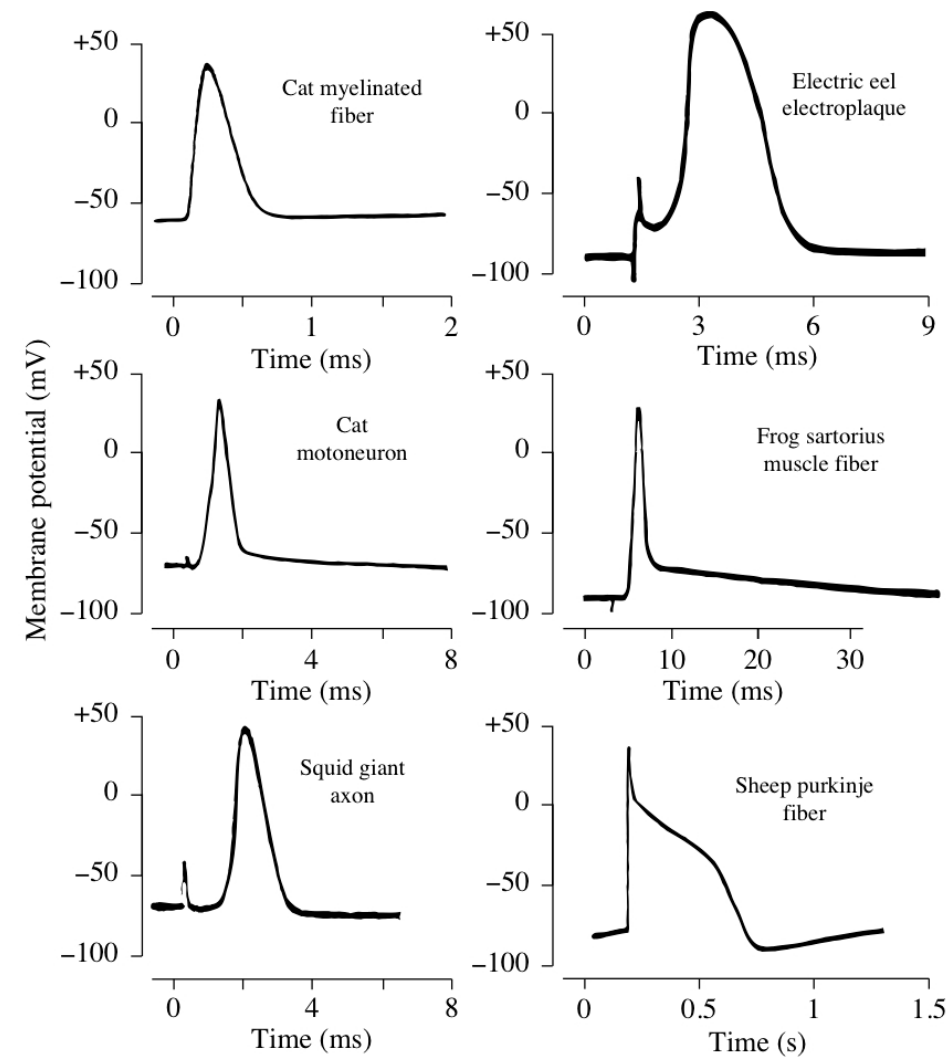


Figure 1.9

→ Neurons send info via electrical pulses (spikes) occurring **across** the cell membrane

Action Potentials

SPIKES

EXPLORING THE NEURAL CODE

“Neural code”

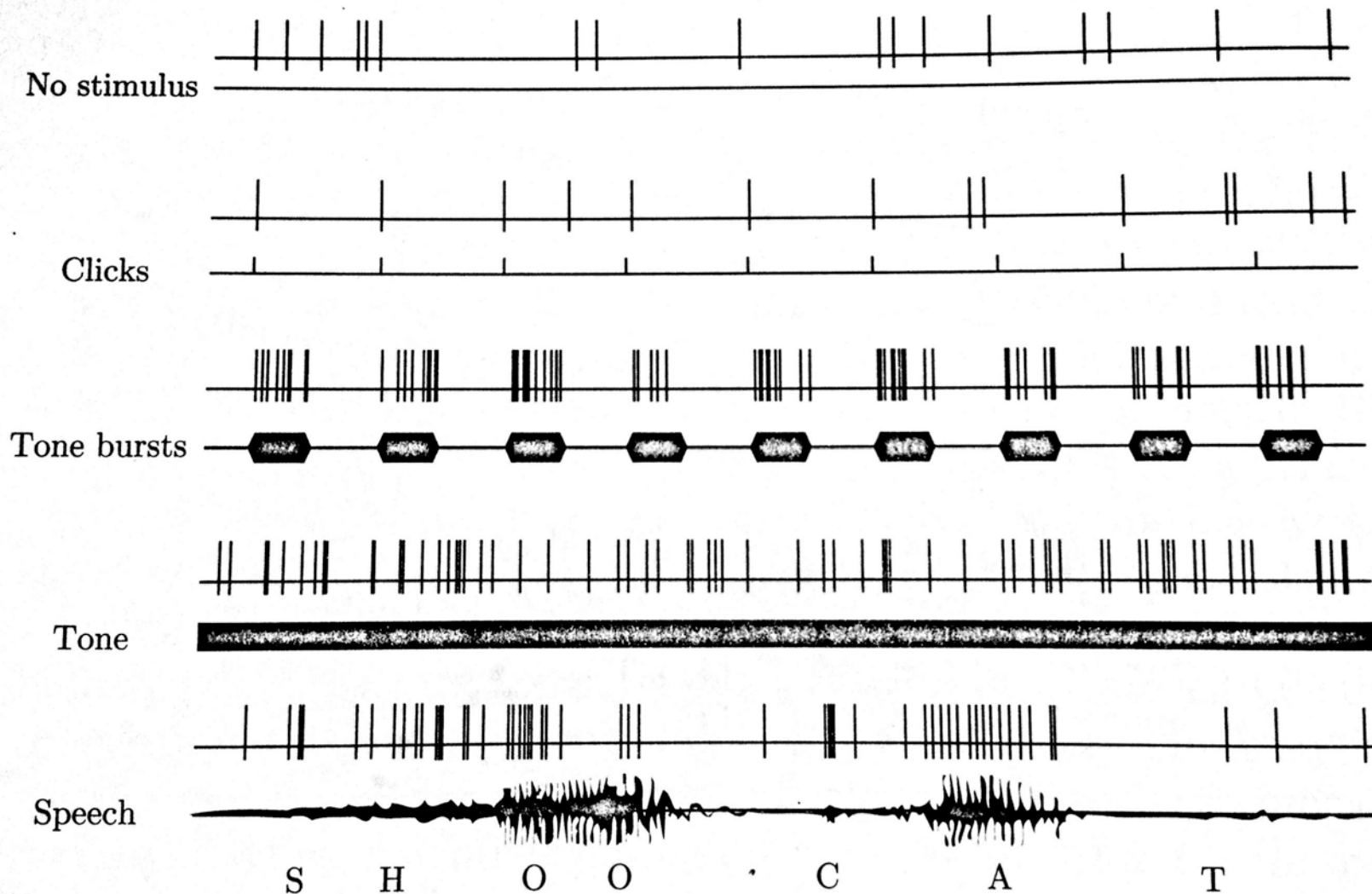
Aside

Is our central nervous system essentially “digitized”?



Aside: Neural coding of hearing

Illustrative response from a single auditory nerve fiber
(top trace; acoustic stim. is the bottom trace)



Cell Membrane

- Membrane primarily consists of a “lipid bilayer” (to separate inside from outside)
- All sorts of “stuff” embedded inside, to allow for “communication” across membrane

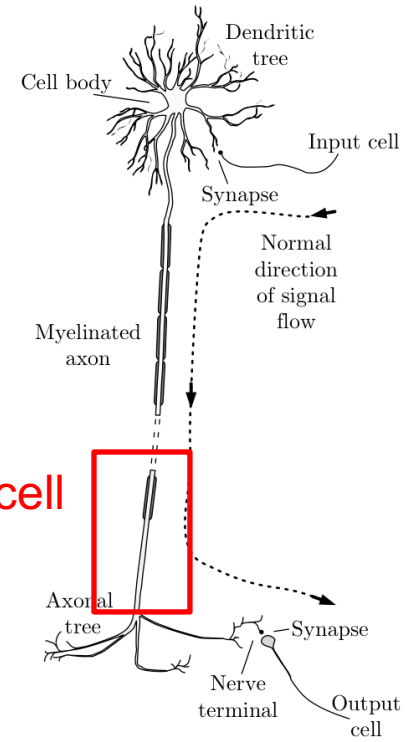


Figure 1.22

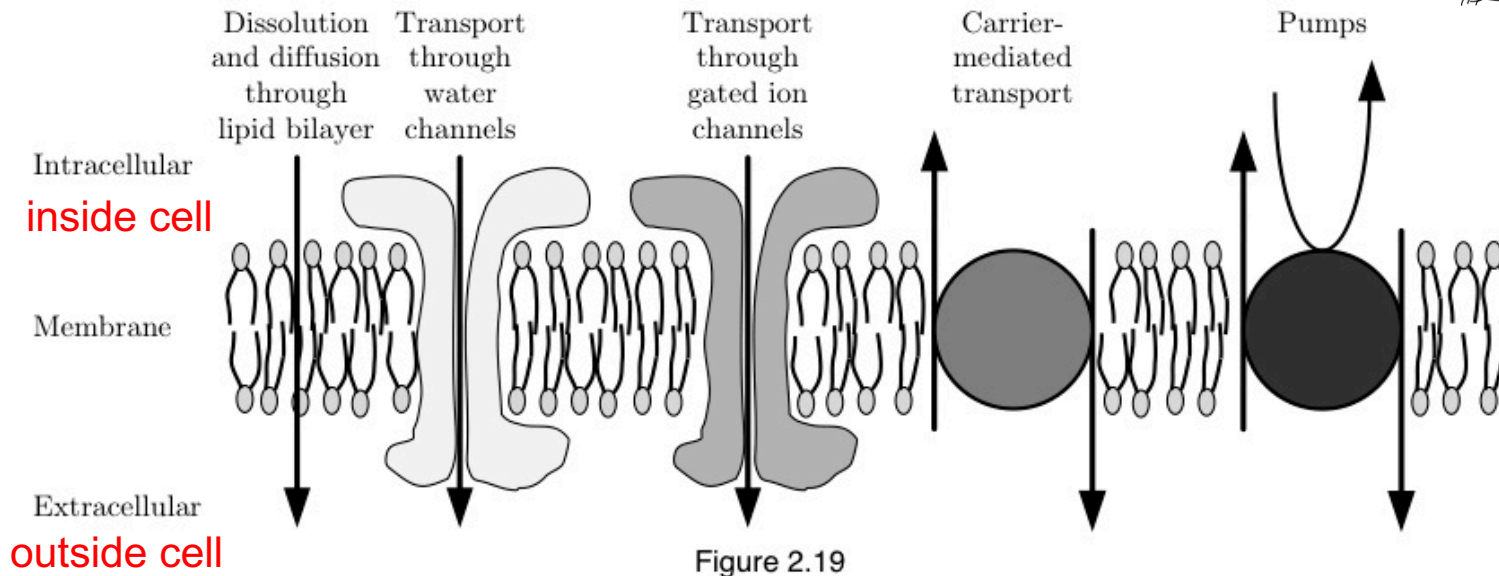


Figure 2.19

Key Idea: Membrane transport

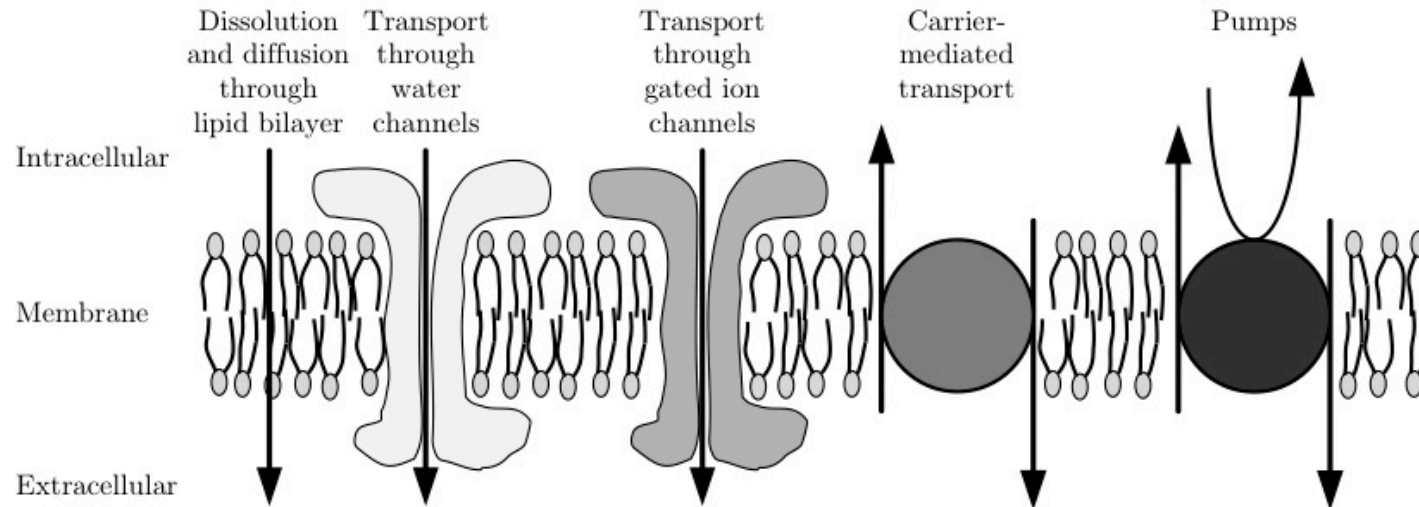


Figure 2.19

- Cell membranes separate *inside* and *outside*
- Controls what *solutes* are on either side and means to *transport* such
- Variety of transport mechanisms: carriers, ion channels, pumps, etc....

Biology is messy....

Andrew Rutenberg

“Dear Colleagues,

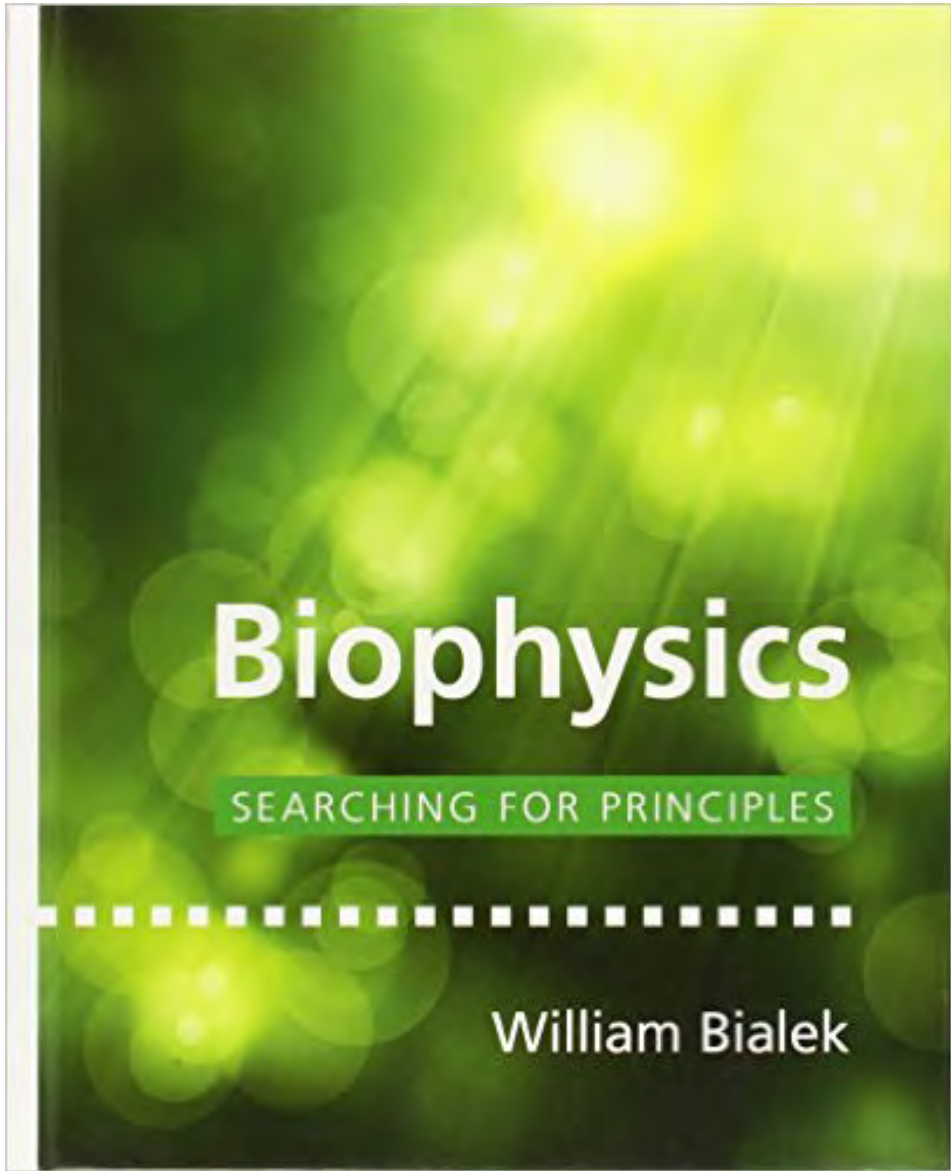
I’d like to invite you all (and/or your students) to the ‘*Stochastic Biology*’ session”

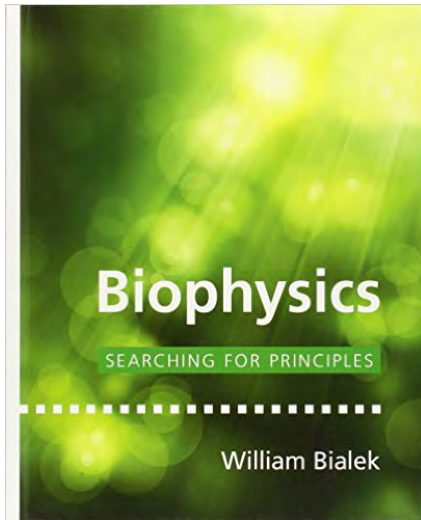
C Bergevin

“Isn't all biology stochastic?”

Andrew Rutenberg

“True, I was hoping to keep it broad but sexy for people who don’t know better.”

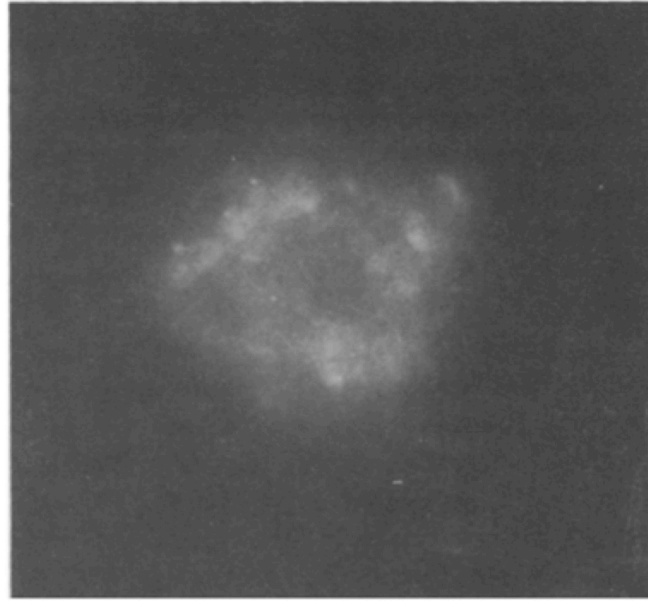
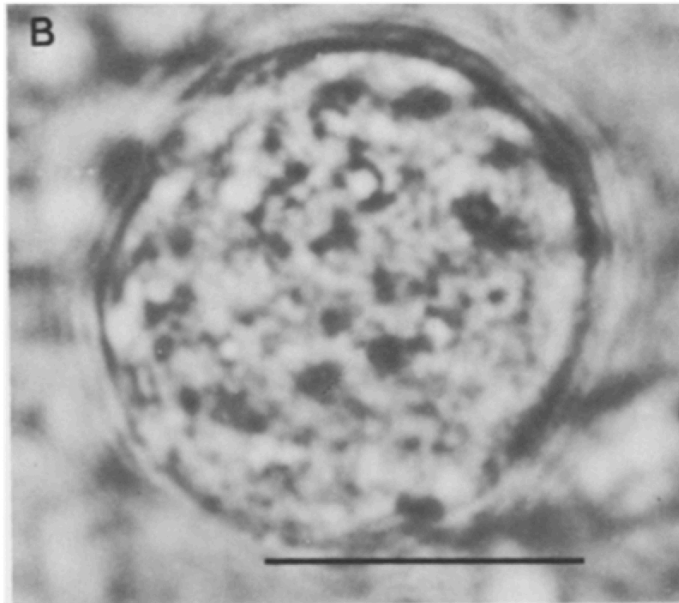
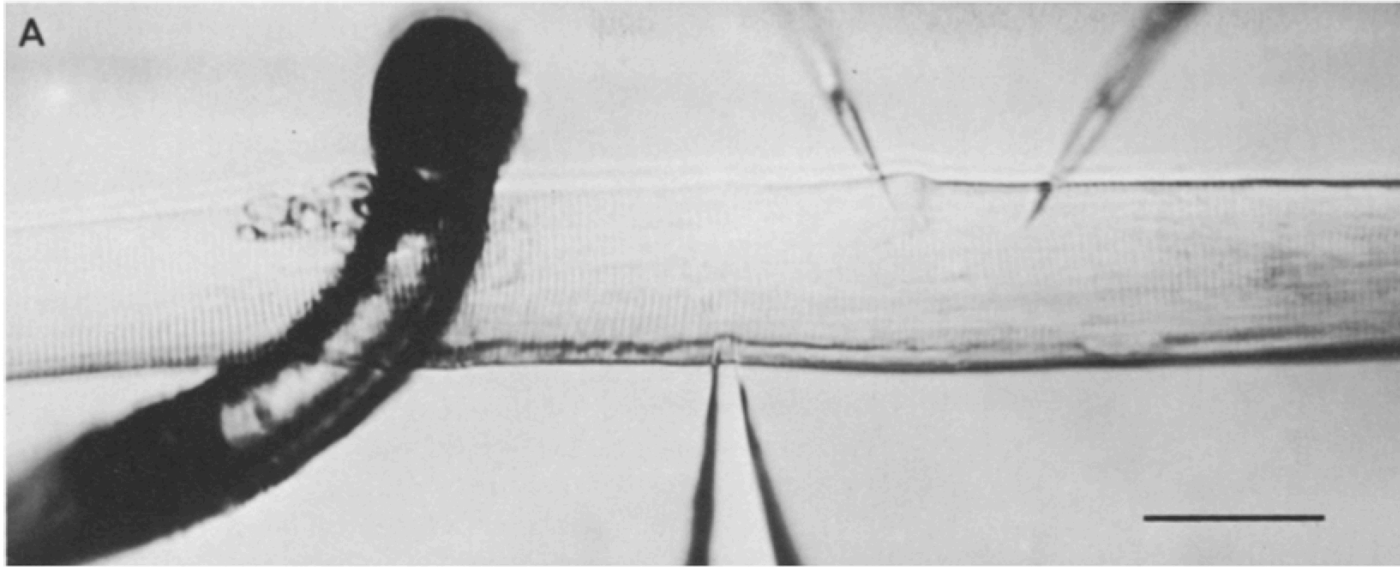




II. NOISE ISN'T NEGLIGIBLE

The great poetic images of classical physics are those of determinism and clockwork. In a clock, not only the output but also the internal mechanisms are models of precision. Strikingly, life seems very different. Interactions between molecules involve energies of just a few times the thermal energy. Biological motors, including the molecular components of our muscles, move in elementary steps that are on the nanometer scale, driven forward by energies that are larger than the thermal energies of Brownian motion, but not much larger. Crucial signals inside cells often are carried by just a handful of molecules, and these molecules inevitably arrive randomly at their targets. Human perception can be limited by noise in the detector elements of our sensory systems, and individual elements in the brain, such as the synapses that pass signals from one neuron to the next, are surprisingly noisy. How do the obviously reliable functions of life emerge from under this cloud of noise? Are there principles at work that select, out of all possible mechanisms, the ones that maximize reliability and precision in the presence of noise?

Ex. Patch clamping (re single ion channels)



Historical sidenote
This work contributed significantly to 1991 Nobel Prize to E. Neher & B. Sakmann

Ex. Patch clamping (re single ion channels)

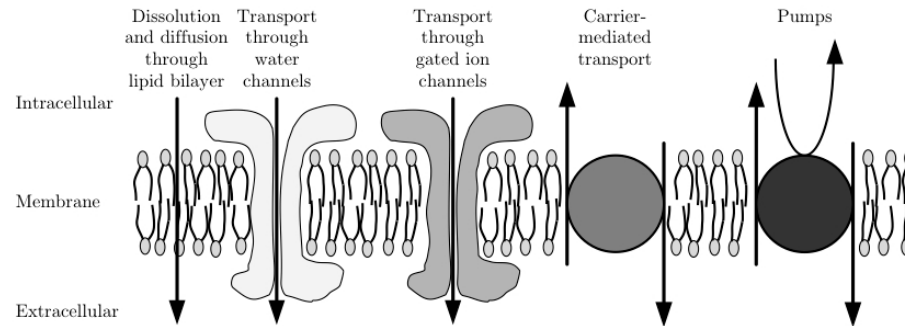
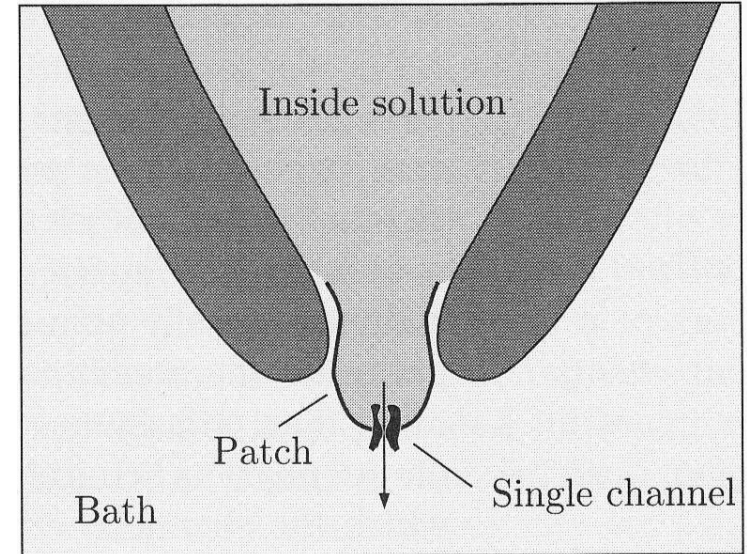


Figure 2.19

→ Single ion channel current appears 'gated' (i.e., on/off)

Ex. Patch Clamping (re single ion channels)

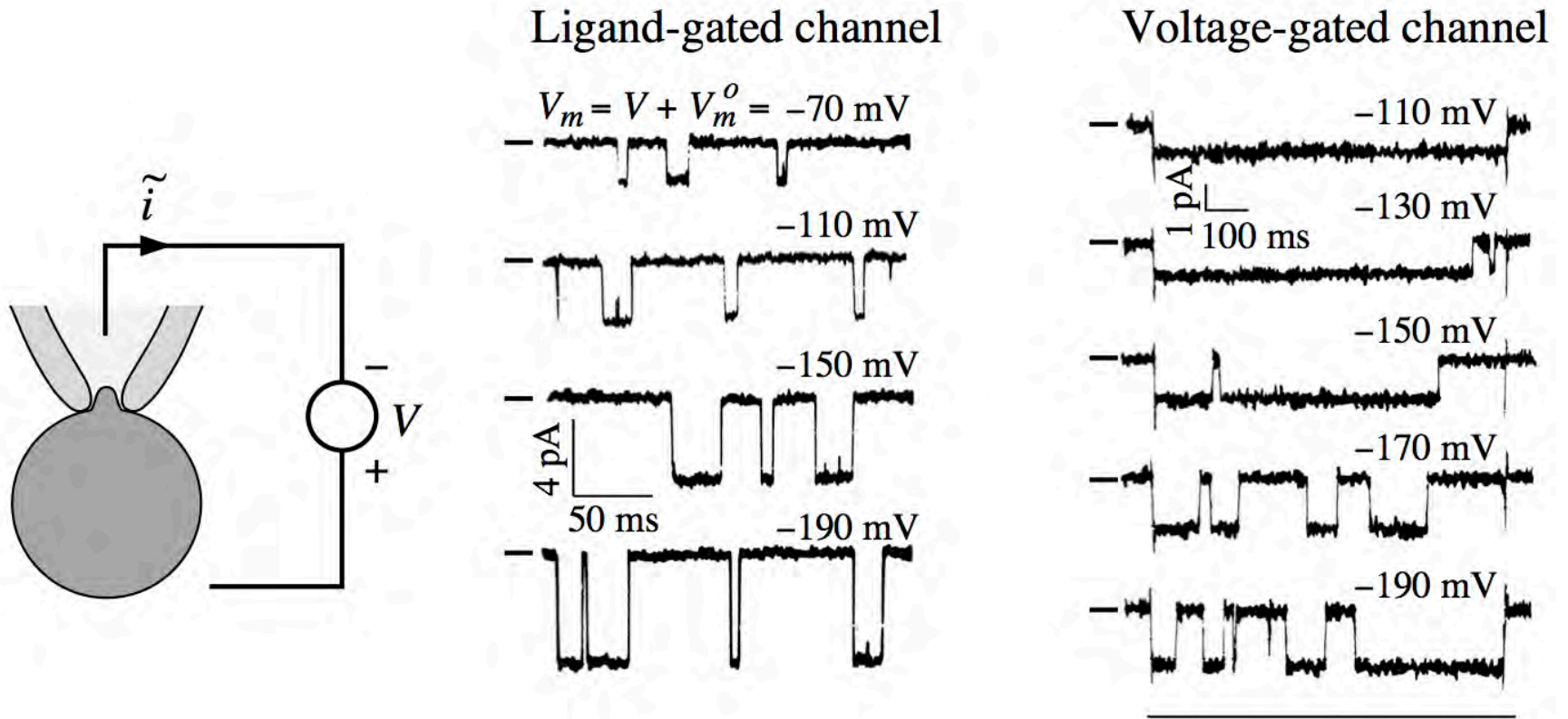


Figure 6.28

→ Single ion channel current appears 'gated' (i.e., on/off) and noisy

Key Idea: Statistical mechanics bridges “micro” & “macro”

➤ Microscopic model (+ law of large numbers) gives rise to macroscopic behavior

- Microscopic = stochastic
- Macroscopic = deterministic

➤ Useful analogy: discrete versus continuous (e.g., digital versus analog)

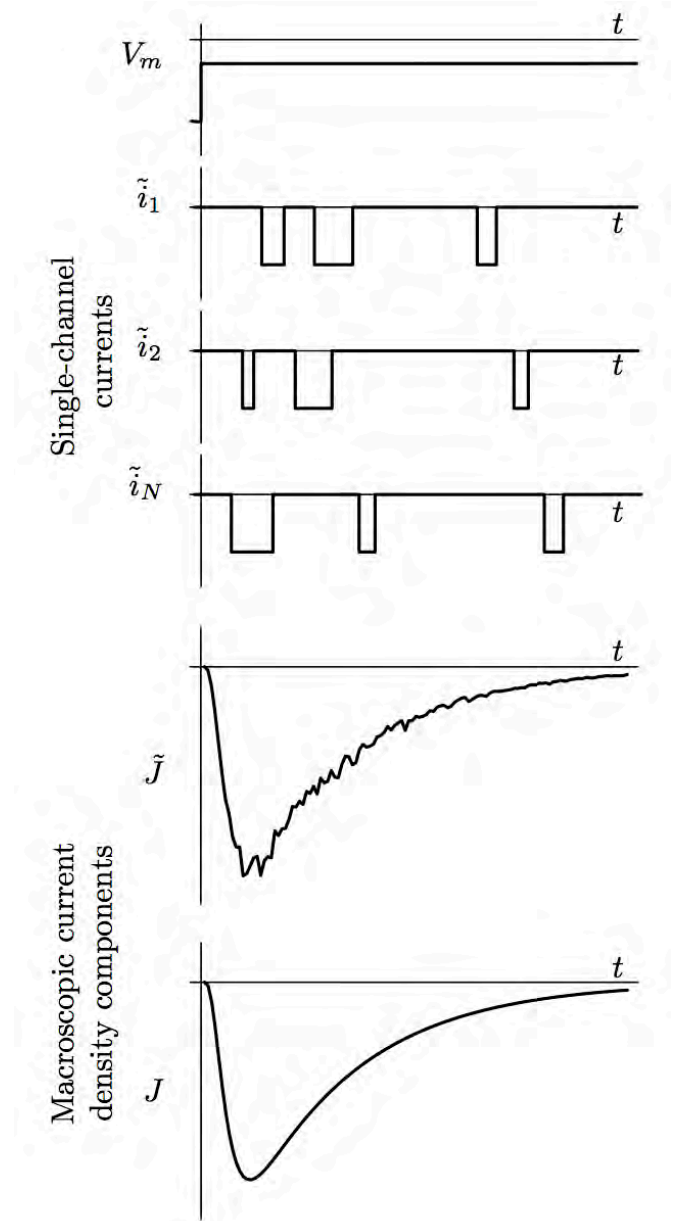


Figure 6.50 (mod)

Teaching Tangent: Blurry lines between discrete & continuous



Is this “image” a bitmap or vector-based?

Teaching Tangent

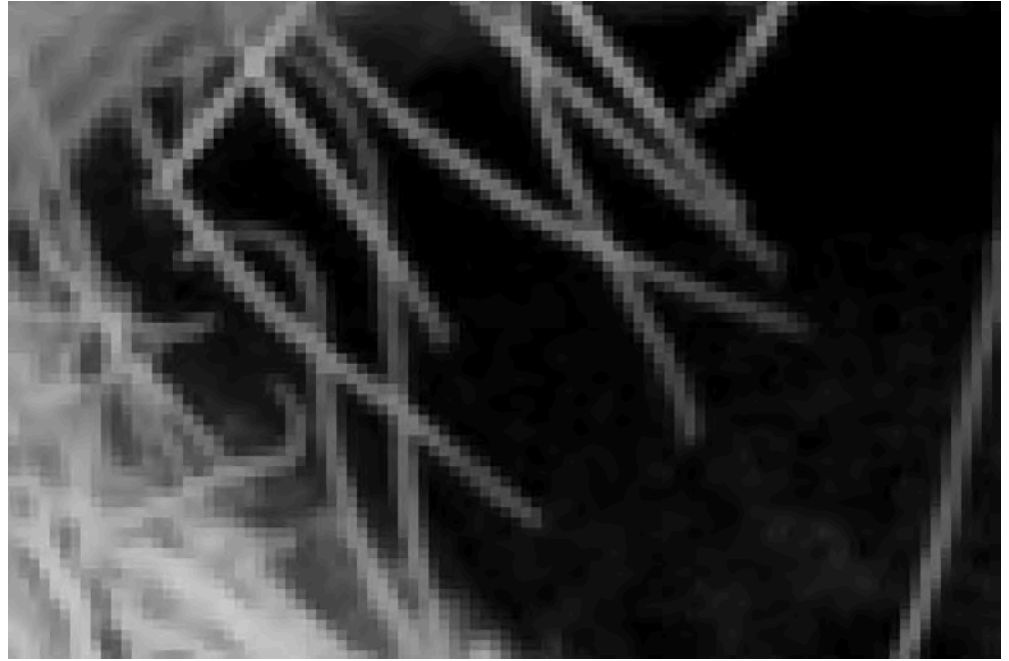
Bitmap version



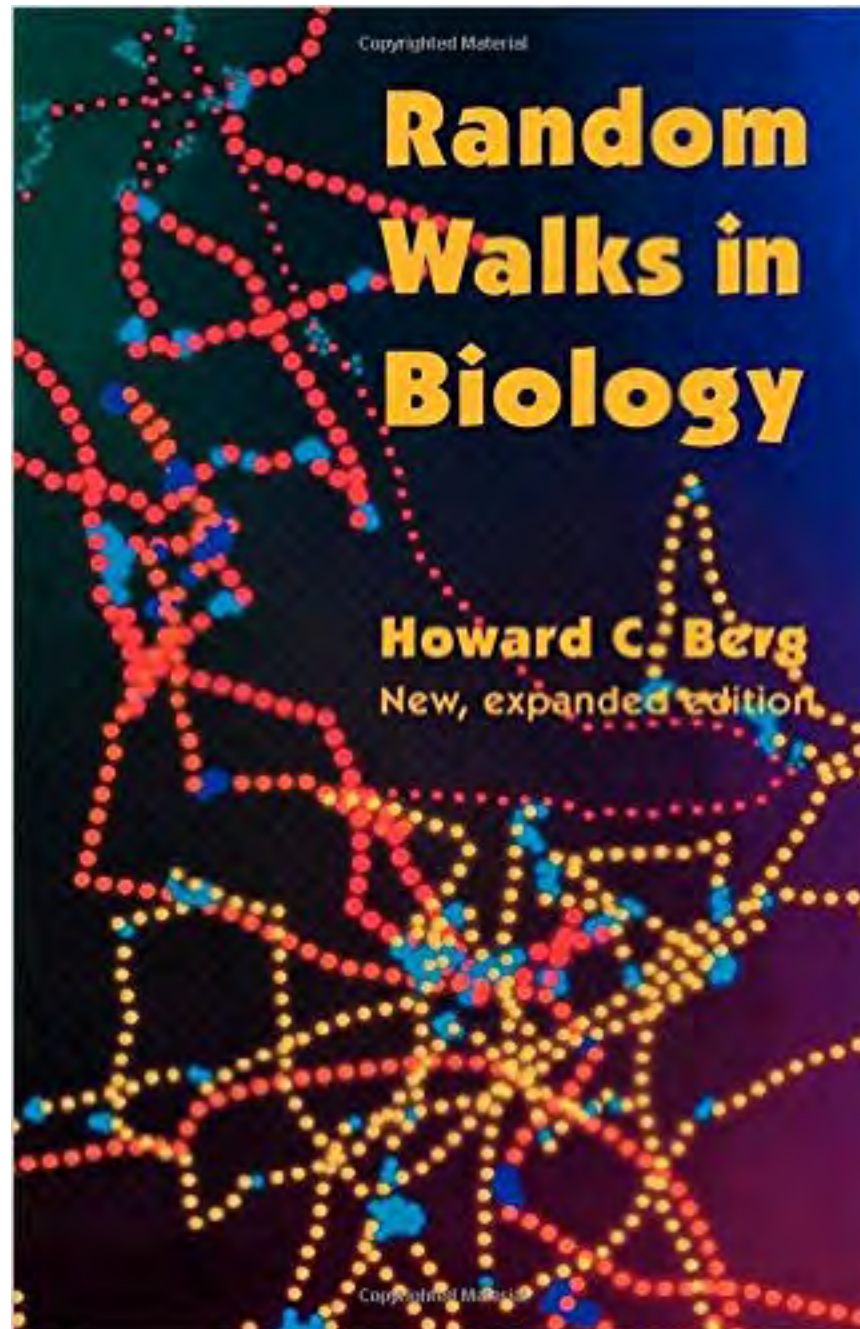
Vector version



zoom-in about corner of eye



Diffusion



Diffusion: Microscopic Theory

Diffusion is the random migration of molecules or small particles arising from motion due to thermal energy. A particle at absolute temperature T has, on the average, a kinetic energy associated with movement along each axis of $kT/2$, where k is Boltzmann's constant. Einstein showed in 1905 that this is true regardless of the size of the particle, even for particles large enough to be seen under a microscope, i.e., particles that exhibit Brownian movement. A particle of mass m and velocity v_x on the x axis has a kinetic energy $mv_x^2/2$. This quantity fluctuates, but on the average $\langle mv_x^2/2 \rangle = kT/2$, where $\langle \rangle$ denotes an average over time or over an ensemble of similar particles. From this relationship we compute the mean-square velocity,

$$\langle v_x^2 \rangle = kT/m, \quad (1.1)$$

and the root-mean-square velocity,

$$\langle v_x^2 \rangle^{1/2} = (kT/m)^{1/2}. \quad (1.2)$$

We can use Eq.1.2 to estimate the instantaneous velocity of a small particle, for example, a molecule of the protein lysozyme. Lysozyme has a molecular weight 1.4×10^4 g. This is the mass of one mole, or 6.0×10^{23} molecules; the mass of one molecule is $m = 2.3 \times 10^{-20}$ g. The value of kT at 300°K (27°C) is 4.14×10^{-14} g cm²/sec². Therefore, $\langle v_x^2 \rangle^{1/2} = 1.3 \times 10^3$ cm/sec. This is a sizeable speed. If there were no obstructions, the molecule would cross a typical classroom in about 1 second. Since the protein is not in a vacuum but is immersed in an aqueous medium, it does not go very far before it bumps into molecules of

Key Idea: Diffusion is fundamental process at play here...

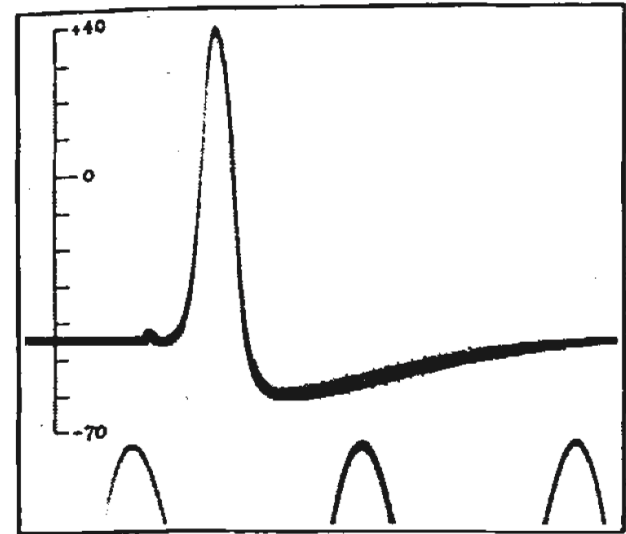
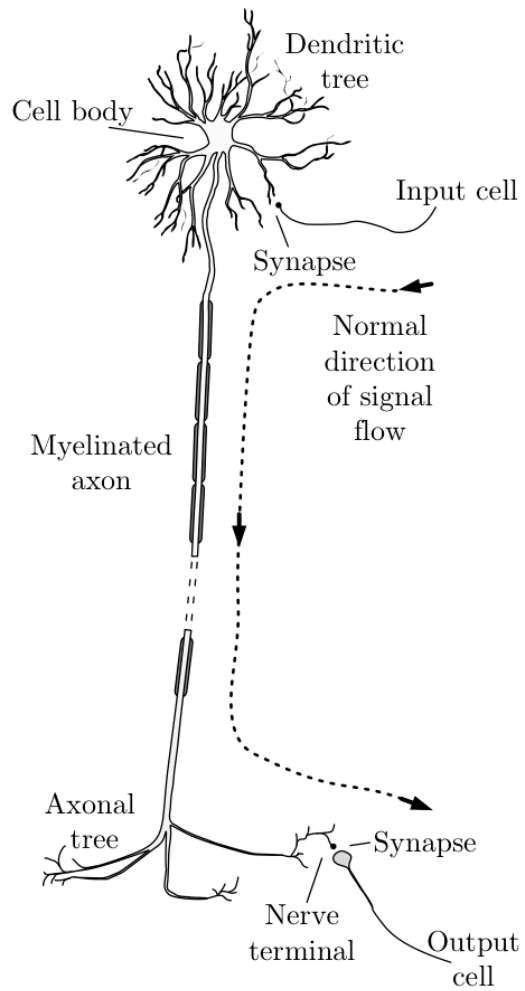
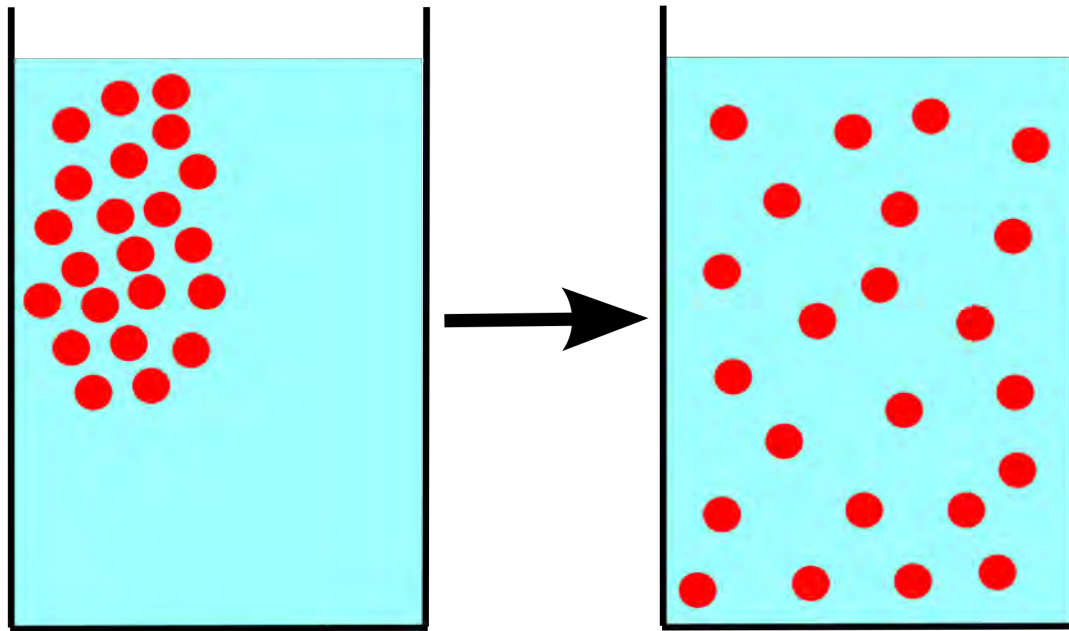


Figure 1.22

Question: What is *diffusion*?

→ Start at the *macroscopic* level...

➤ According to wikipedia....



Question: What is *diffusion*?

diffusion

[dih-**fyoo**-zhuh n]

[Examples](#)

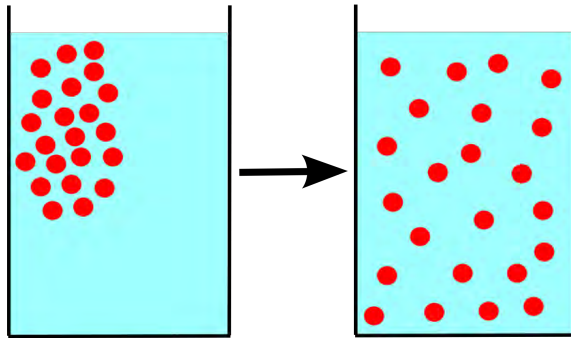
[Word Origin](#)

noun

1. act of diffusing; state of being diffused.
2. prolixity of speech or writing; discursiveness.
3. *Physics*.
 - a. Also called **migration**. an intermingling of molecules, ions, etc., resulting from random thermal agitation, as in the dispersion of a vapor in air.
 - b. a reflection or refraction of light or other electromagnetic radiation from an irregular surface or an erratic dispersion through a surface; scattering.
4. *Movies*. a soft-focus effect resulting from placing a gelatin or silk plate in front of a studio light or a camera lens, or through the use of diffusion filters.
5. *Meteorology*. the spreading of atmospheric constituents or properties by turbulent motion as well as molecular motion of the air.
6. *Anthropology, Sociology*. Also called **cultural diffusion**. the transmission of elements or features of one culture to another.



➤ According to wikipedia....

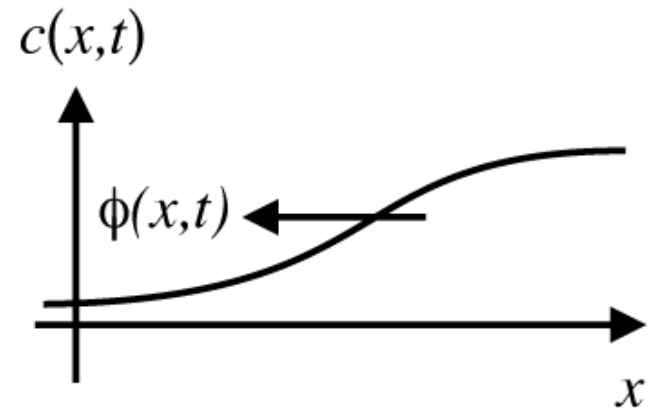
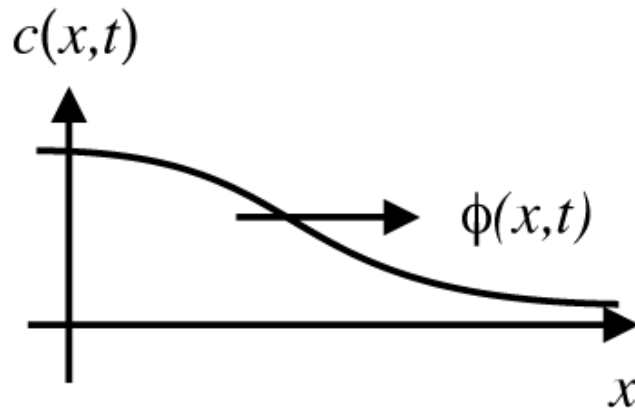


➤ According to the dictionary....

➤ Some historical perspective....

Diffusion (Macroscopic)

From Graham's observations (~1830):

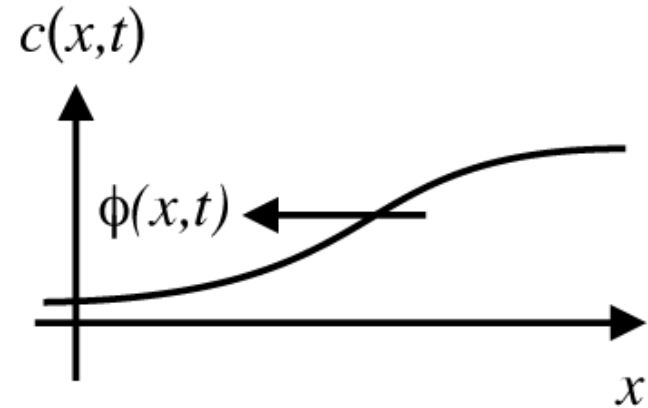
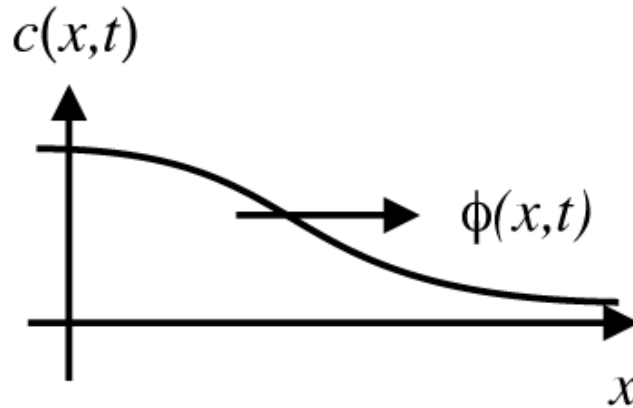


“ A few years ago, Graham published an extensive investigation on the diffusion of salts in water, in which he more especially compared the diffusibility of different salts. It appears to me a matter of regret, however, that in such an exceedingly valuable and extensive investigation, the development of a fundamental law, for the operation of diffusion in a single element of space, was neglected, and I have therefore endeavoured to supply this omission.”

- A. Fick (1855)

Diffusion (Macroscopic)

Note: These are multi-variable functions.
Will focus on 1-D case here for simplicity



$c(x,t)$

Concentration - of solute in solution [mol/m^3]

$\phi(x,t)$

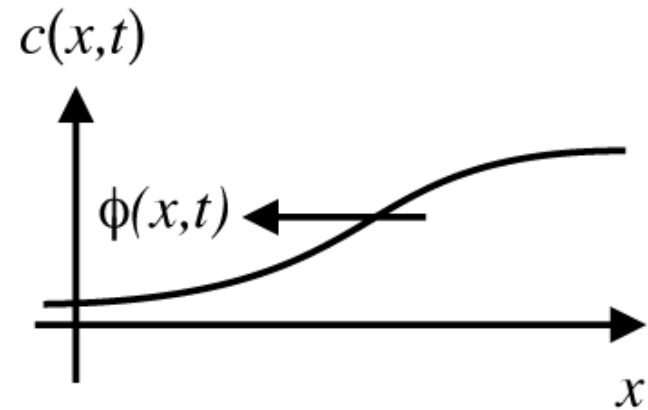
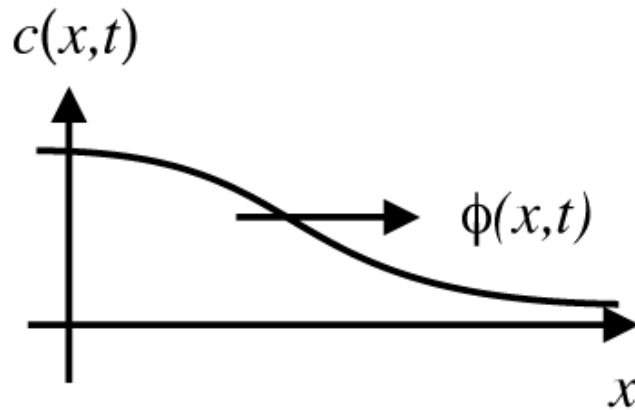
Flux - net # of moles crossing per unit time t through a unit area perpendicular to the tx -axis [$mol/m^2 \cdot s$]

Note: flux is a vector!

x, t

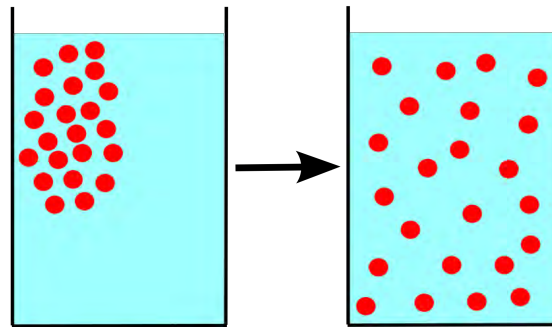
Position [m], Time [s]

Diffusion (Macroscopic)



$$\phi(x, t) \propto -\frac{\partial c(x, t)}{\partial x}$$

→ “stuff” moves DOWN a concentration gradient



Diffusion constant (D)

$$\phi(x, t) \propto -\frac{\partial c(x, t)}{\partial x} \quad \text{constant of proportionality?}$$

$$\phi(x, t) = -D \frac{\partial c(x, t)}{\partial x}$$

- Diffusion constant is always positive (i.e., $D > 0$)
- Determines time it takes solute to diffuse a given distance in a medium
- Depends upon both solute and medium (solution)
- *Stokes-Einstein relation* predicts that D is inversely proportional to solute molecular radius

Diffusion: Generalizations

Higher Dimensions:

$$\phi(x, t) = -D \frac{\partial c(x, t)}{\partial x} \longleftrightarrow \vec{\phi} = -D \nabla c$$

$$\text{where } \nabla c = \hat{x} \frac{\partial c}{\partial x} + \hat{y} \frac{\partial c}{\partial y} + \hat{z} \frac{\partial c}{\partial z} = \text{grad}(c)$$

Analogous Flux Laws:

Heat Flow (Fourier): $\phi_h = -\sigma_h \frac{\partial T}{\partial x}$ *heat flow, thermal conductivity, and temperature*

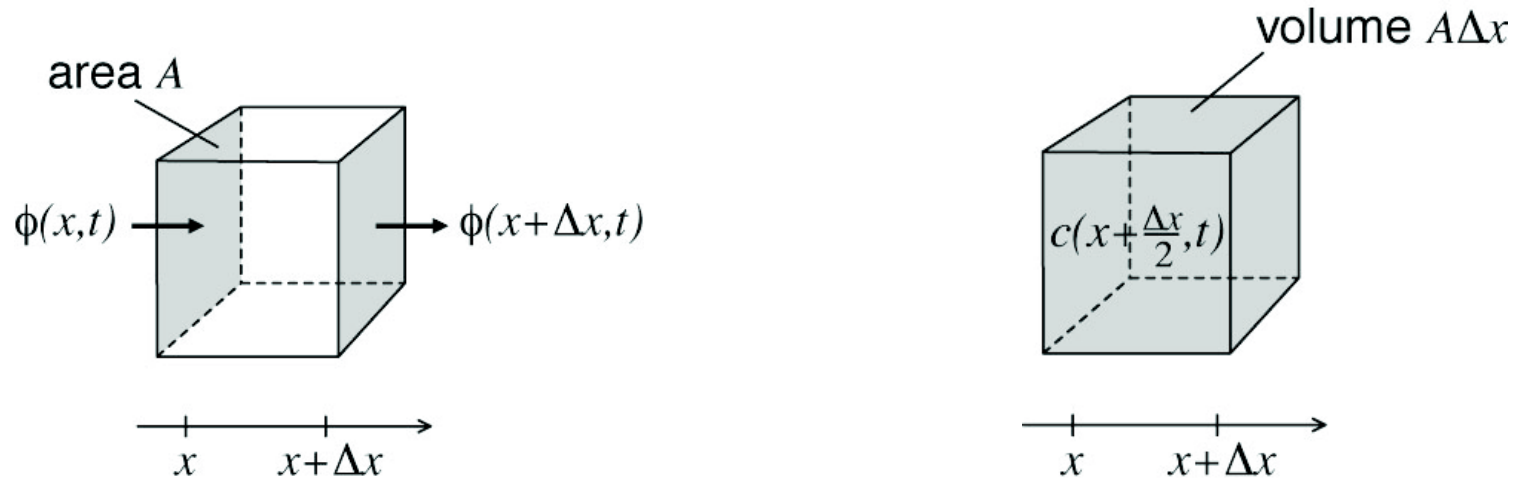
Electric Conduction (Ohm): $J = -\sigma_e \frac{\partial \psi}{\partial x}$ *current density, electrical conductivity, and electric potential*

Convection (Darcy): $\Phi_v = -\kappa \frac{\partial p}{\partial x}$ *fluid flow, hydraulic permeability, and pressure*

Diffusion (Fick): $\phi = -D \frac{\partial c}{\partial x}$

Continuity Equation (1-D)

⇒ imagine a cube (with face area A and length Δx) and a time interval Δt



solute entering from left - solute exiting from right
(during time interval $[t, t + \Delta t]$)

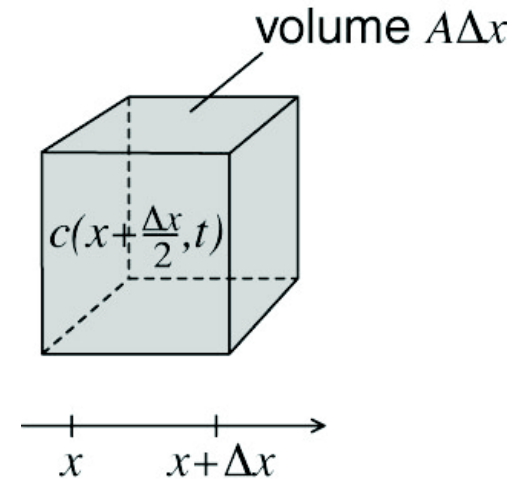
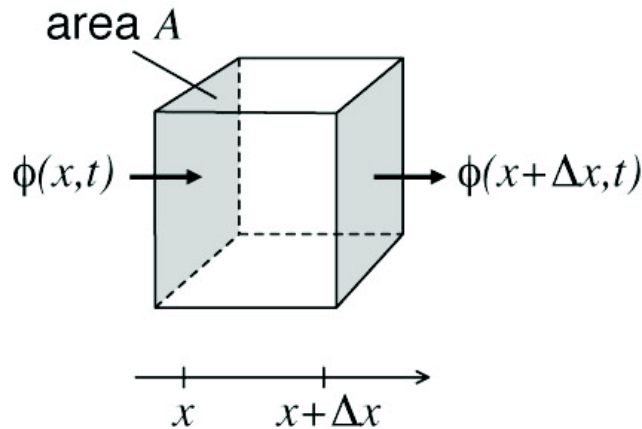
=

change in amount of solute inside cube
(during time interval $[t, t + \Delta t]$)

$$A \Delta t \phi(x, t)$$

$$A \Delta x c(x, t)$$

Continuity Equation (1-D)



solute entering from left - solute exiting from right
(during time interval $[t, t + \Delta t]$)

= change in amount of solute inside cube
(during time interval $[t, t + \Delta t]$)

$$A \Delta t \phi(x, t + \Delta t/2) - A \Delta t \phi(x + \Delta x, t + \Delta t/2)$$

amount of solute entering
on left side of cube

amount of solute leaving
on right side of cube

$$= A \Delta x c(x + \Delta x/2, t + \Delta t) - A \Delta x c(x + \Delta x/2, t)$$

amount of solute in cube at
the end of the interval

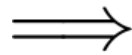
amount of solute in cube at
the start of the interval

$$\frac{\phi(x + \Delta x, t + \Delta t/2) - \phi(x, t + \Delta t/2)}{\Delta x} = \frac{c(x + \Delta x/2, t + \Delta t) - c(x + \Delta x/2, t)}{\Delta t}$$

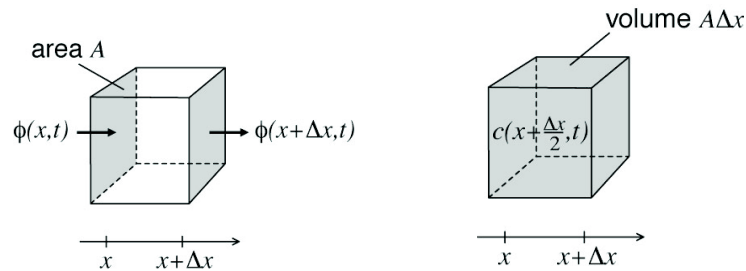
Continuity Equation (1-D)

$$-\frac{\phi(x + \Delta x, t + \Delta t/2) - \phi(x, t + \Delta t/2)}{\Delta x} = \frac{c(x + \Delta x/2, t + \Delta t) - c(x + \Delta x/2, t)}{\Delta t}$$

$$\lim_{\Delta t, \Delta x \rightarrow 0}$$



$$\frac{\partial \phi}{\partial x} = -\frac{\partial c}{\partial t}$$



\Rightarrow conservation of mass within the context of our imaginary cube yielded the *continuity equation*

Diffusion Equation

1. Fick's First Law: $\phi = -D \frac{\partial c}{\partial x}$

+

2. Continuity Equation: $\frac{\partial \phi}{\partial x} = -\frac{\partial c}{\partial t}$

$$\frac{\partial c}{\partial t} = D \frac{\partial^2 c}{\partial x^2}$$

(Fick's Second Law)

Diffusion processes

1. Equilibrium: Zero flux and concentration is independent of time

$D \neq 0 \Rightarrow$ concentration is independent of space and time

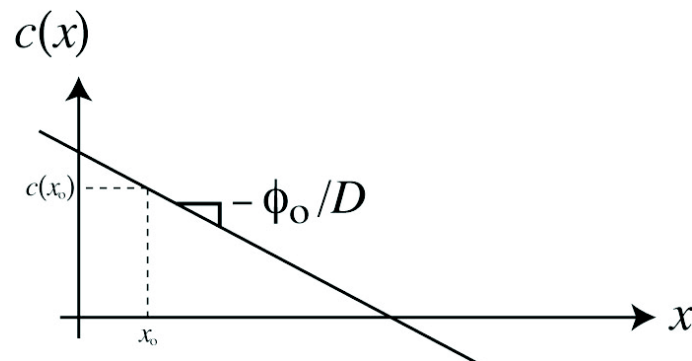
$D = 0 \Rightarrow$ non-diffusible solute is automatically at equilibrium

2. Steady-state: Flux can be non-zero, but flux and concentration are independent of time

$$\frac{\partial \phi}{\partial x} = 0 \quad \Rightarrow \quad \int \phi_o dx = \int -D dc \quad \Rightarrow \quad c(x) = c(x_o) - \frac{\phi_o}{D}(x - x_o)$$

[integrate Fick's 1st Law]

[x_o is a reference location where the concentration is known]



Diffusion processes

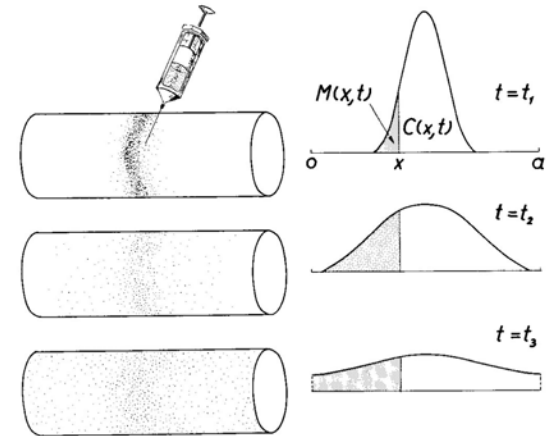
3. Impulse Response: Point-source of particles (n_o mol/cm²) at $t = 0$ and $x = 0$ [Dirac delta function $\delta(x)$]

given the initial/boundary conditions:

$$c(x, t) = n_o \delta(x) \quad \text{at } t = 0 \quad \text{where} \quad \int_{-\infty}^{\infty} \delta(x) dx = 1$$

need to solve:

$$\frac{\partial c}{\partial t} = D \frac{\partial^2 c}{\partial x^2}$$



Batschelet Fig.12.5

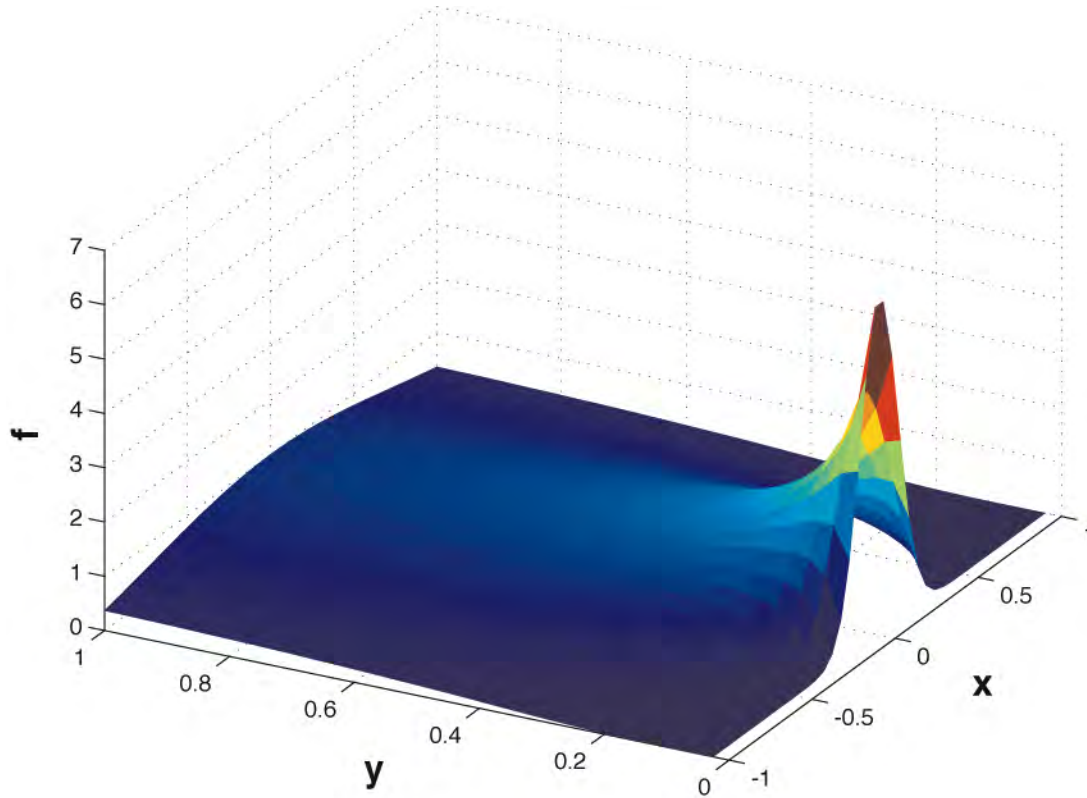
[Aside: solution can be found by a # of different methods, one being by separation of variables and using a Fourier transform]

Solution
(for $t > 0$)

$$c(x, t) = \frac{n_o}{\sqrt{4\pi Dt}} e^{-x^2/4Dt}$$

Note: Historically, this ties in directly w/ the development of “Fourier analysis”

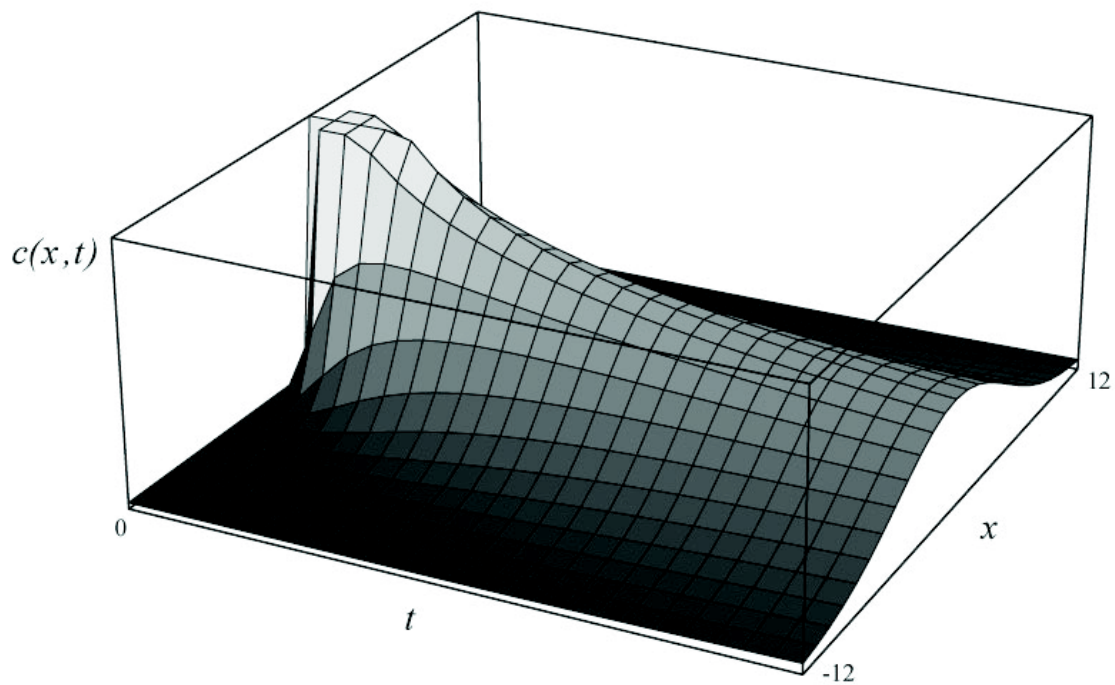
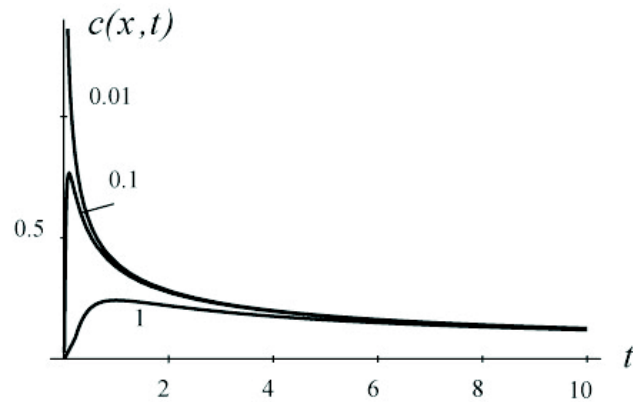
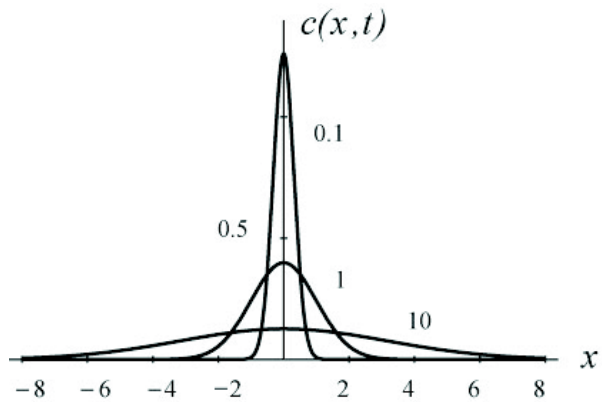
Diffusion processes



$$f(x, y) = \frac{1}{\sqrt{y}} e^{-x^2/y}$$

solution to
diffusion equation!

Diffusion processes

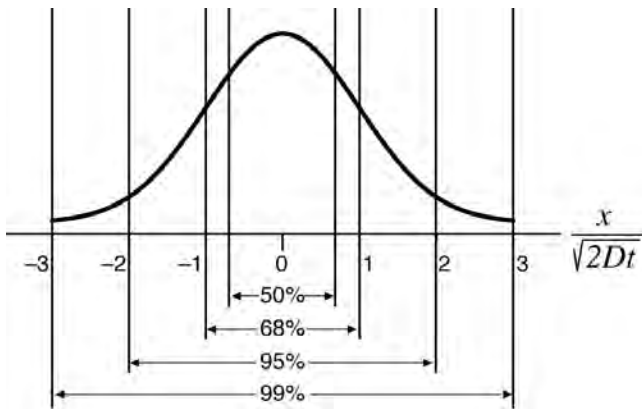


Importance of scale

$$c(x, t) = \frac{n_o}{\sqrt{4\pi Dt}} e^{-x^2/4Dt}$$

Gaussian function with zero mean and standard deviation:

$$\sigma = \sqrt{2Dt}$$



Question: How long does it take ($t_{1/2}$) for $\sim 1/2$ the solute to move at least the distance $x_{1/2}$?

$$\frac{x_{1/2}}{\sqrt{2Dt_{1/2}}} \approx \frac{2}{3} \implies t_{1/2} \approx \frac{x_{1/2}^2}{D}$$

For small solutes
(e.g. K^+ at body temperature) $D \approx 10^{-5} \frac{\text{cm}^2}{\text{s}}$

	$x_{1/2}$	$t_{1/2}$
membrane sized	10 nm	$\frac{1}{10} \mu\text{sec}$
cell sized	10 μm	$\frac{1}{10}$ sec
dime sized	10 mm	10^5 sec \approx 1 day

Tangent: Why is a cell “cell-sized”?

- Cells are typically 1-100 μm or so in size. Why?

What determines cell size?

Wallace F Marshall^{*1}, Kevin D Young², Matthew Swaffer³, Elizabeth Wood³, Paul Nurse^{3,4,5}, Akatsuki Kimura⁶, Joseph Frankel⁷, John Wallingford⁸, Virginia Walbot⁹, Xian Qu¹⁰ and Adrienne HK Roeder¹¹

Marshall *et al.* *BMC Biology* 2012, **10**:101
<http://www.biomedcentral.com/1741-7007/10/101>

- Non-trivial question and likely a # of factors (e.g., optimizing volume to surface area), but....

- ... limits stemming from diffusion are likely central

	$x_{1/2}$	$t_{1/2}$
membrane sized	10 nm	$\frac{1}{10}$ μsec
cell sized	10 μm	$\frac{1}{10}$ sec
dime sized	10 mm	10^5 sec \approx 1 day

Membrane Diffusion: History 101

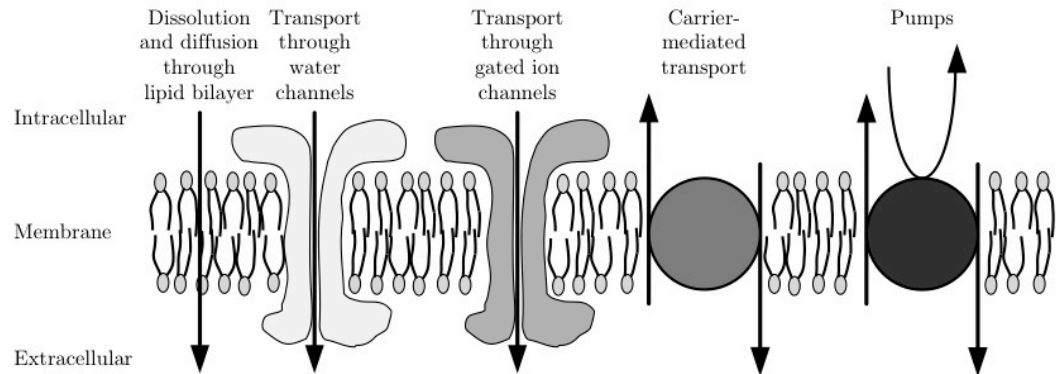


Figure 2.19

Diffusion through Cell Membranes

Charles Ernest Overton (late 1800s): first systematic studies

- qualitative:
 - put cell in bath with solute
 - wait, rinse, squeeze
 - analyze to see how much got in (+ = some; +++ = a lot)
- 100's of solutes, dozens of cell types
- surprising results: previously cell membranes had been thought to be impermeant to essentially everything but water

Overton's Rules:

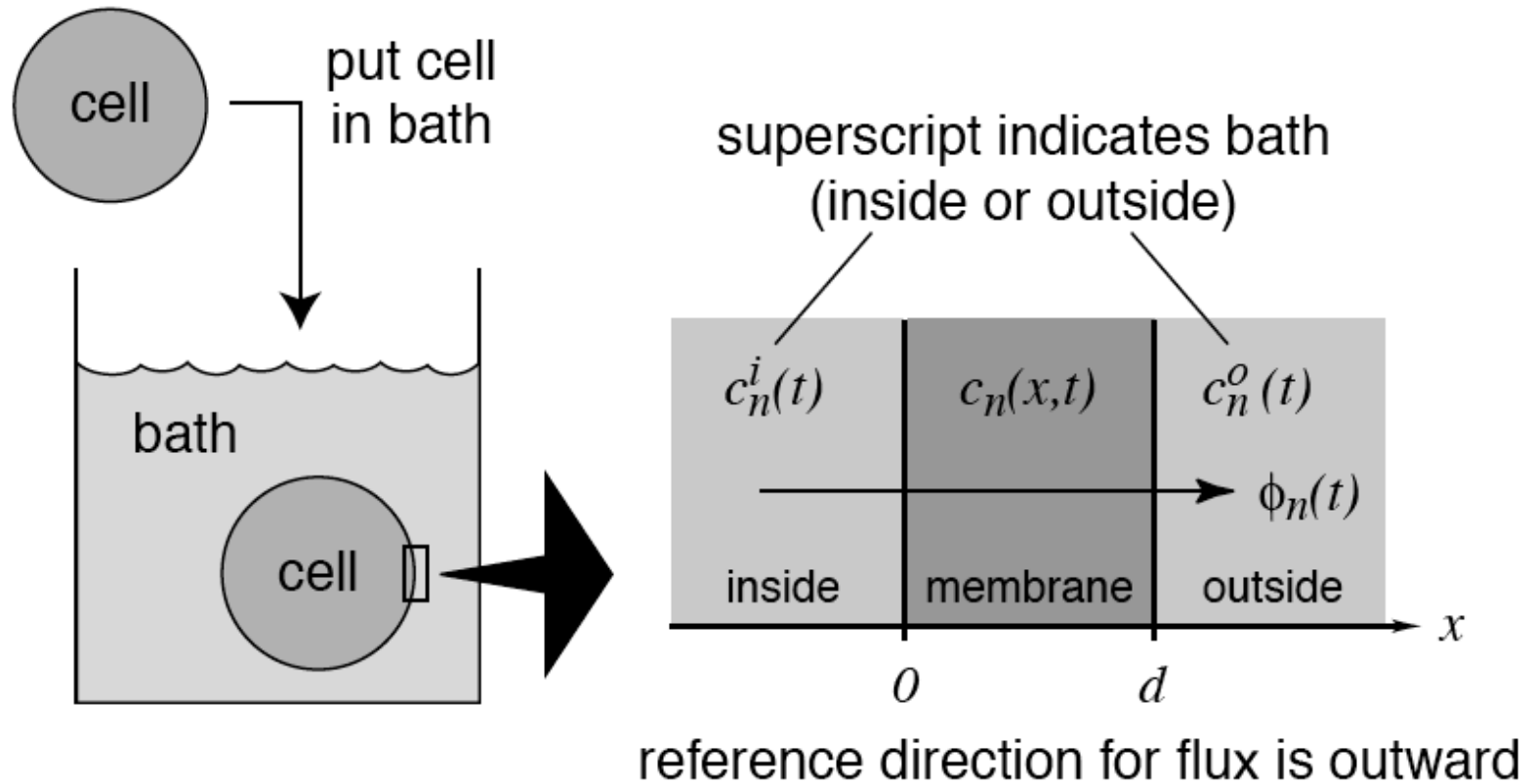
- cell membranes are semi-permeable
- relative permeabilities of plant and animals cells are similar
- permeabilities correlate with solubility of solute in organic solvents
 - membrane is lipid (specifically cholesterol and phospholipids)
- certain cells concentrate some solutes → active transport
- potency of anesthetics correlated with lipid solubility
 - Meyer-Overton theory of narcosis
- muscles don't contract in sodium-free media

Diffusion through Cell Membranes

Paul Runar Collander (1920-1950): first quantitative studies

- large cells (cylindrical algae cells, 1 mm diameter, 1 cm long)
- bathe cell in solute for time t_1 , squeeze out cytoplasm, analyze
- repeat with new cell and new time t_2
- plot intracellular quantity versus time
- fit with exponential function of time (two-compartment theory)
- infer permeability from time constant

Membrane Diffusion: Two-Compartment Geometry

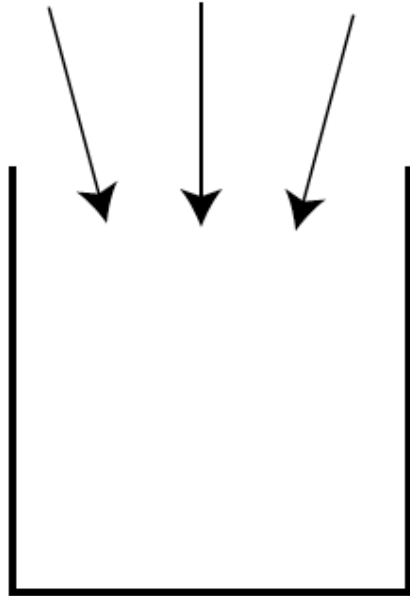


Solute "dissolves" into membrane & diffuses across
(and then dissolves back out)

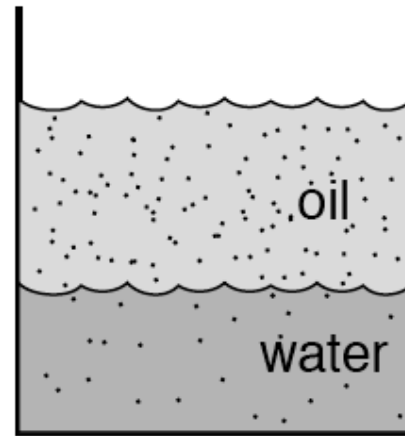
Membrane Diffusion: Partition coefficient

Step 1: Dissolve

solute oil water



shake
then
wait



c_n^{oil}

c_n^{water}

Equilibrium characterized by relative solubilities
of solute n in oil and water

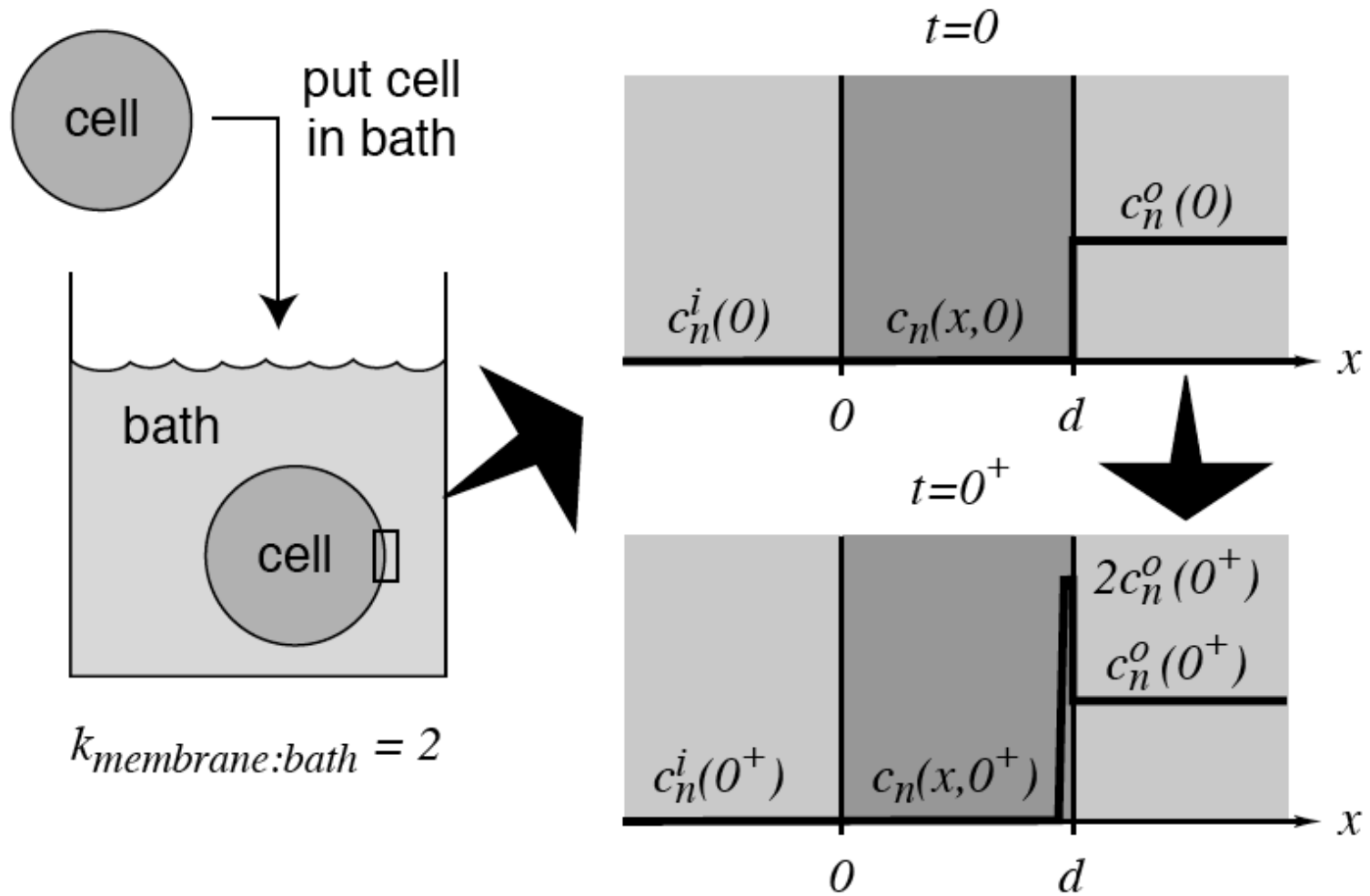
$$\text{partition coefficient } k_{oil:water} = \frac{c_n^{oil}}{c_n^{water}}$$

Historic sidenote

Measuring the PC was a key approach to figuring out the chemical composition of the cell membrane (i.e., phospholipids)

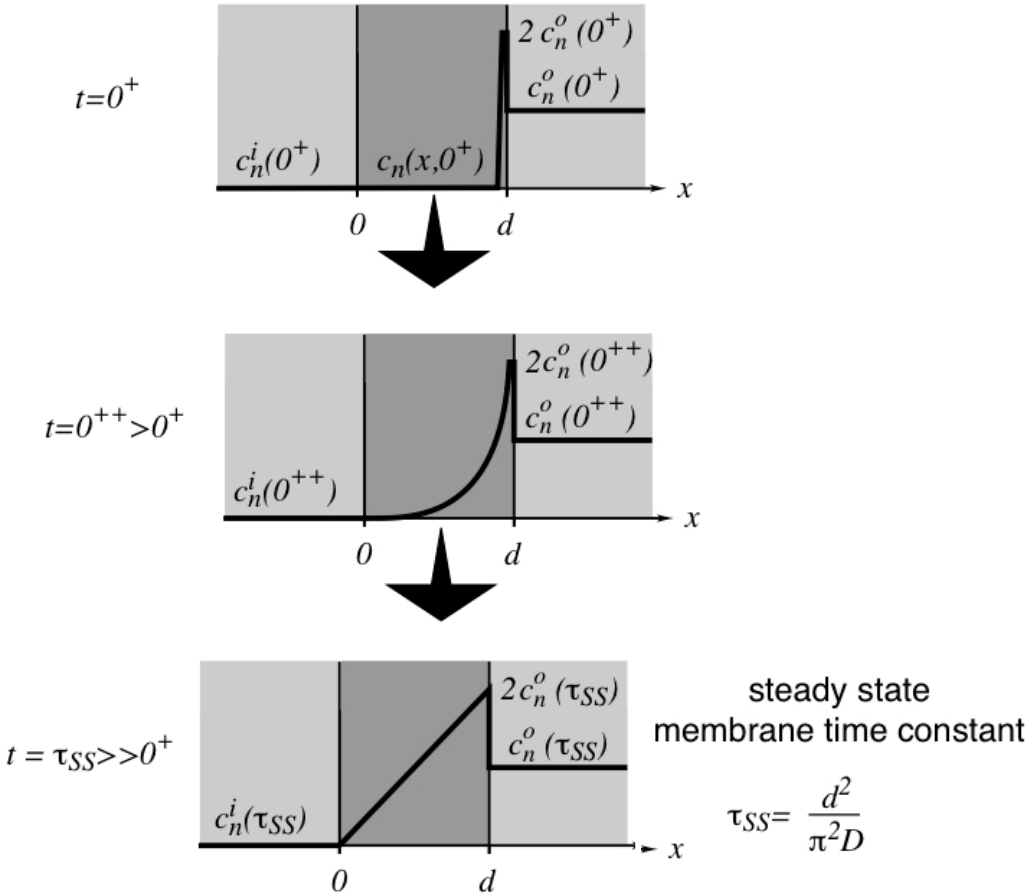
Membrane Diffusion: Dissolve

Assume Dissolving is fast relative to diffusing



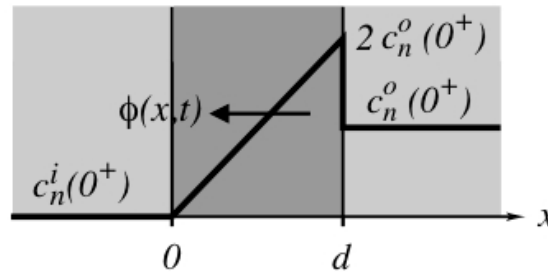
Membrane Diffusion

Step 2: Solute diffuses through membrane



Key Idea: Membrane Permeability

Step 3: Solute enters the cell



$$c_n(x,t) = c_n(0,t) + \frac{x}{d}(c_n(d,t) - c_n(0,t))$$

$$= k_n c_n^i(t) + \frac{k_n x}{d}(c_n^o(t) - c_n^i(t))$$

$$k_n = k_{\text{membrane:bath}}$$

$$= k_{\text{membrane:cytoplasm}}$$

Fick's law: $\phi_n(t) = -D_n \frac{\partial c_n(x,t)}{\partial x}$

$$= -D_n \frac{c_n(d,t) - c_n(0,t)}{d}$$

$$= \frac{D_n k_n}{d} (c_n^i(t) - c_n^o(t))$$

$$\phi_n(t) = P_n (c_n^i(t) - c_n^o(t)) ; P_n = \frac{D_n k_n}{d}$$

Fick's law for membranes

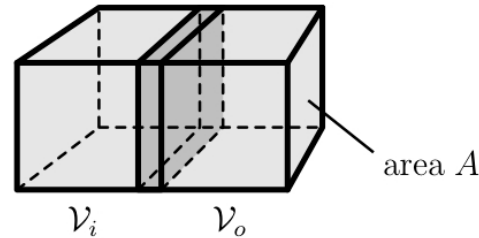
P_n = permeability of membrane to solute n

Membrane permeability

$$P_n = \frac{D_n k_n}{d}$$

Membrane Diffusion

Step 4: Concentration in cell changes: two-compartment diffusion



Assume

- \mathcal{V}_i and \mathcal{V}_o constant
- well-stirred baths: $c_n^i(t)$, $c_n^o(t)$
- solute is conserved and membrane is thin: $c_n^i(t)\mathcal{V}_i + c_n^o(t)\mathcal{V}_o = N_n$
- membrane always in steady state: $\phi_n(t) = P_n(c_n^i(t) - c_n^o(t))$

By continuity,

$$A\phi_n(t) = -\frac{d}{dt}(c_n^i(t)\mathcal{V}_i) = \frac{d}{dt}(c_n^o(t)\mathcal{V}_o)$$

$$\frac{d}{dt}c_n^i(t) = -\frac{AP_n}{\mathcal{V}_i}(c_n^i(t) - c_n^o(t)) = -\frac{AP_n}{\mathcal{V}_i}\left(c_n^i(t) - \frac{1}{\mathcal{V}_o}N_n + c_n^i(t)\frac{\mathcal{V}_i}{\mathcal{V}_o}\right)$$

$$\frac{d}{dt}c_n^i(t) + AP_n\left(\frac{1}{\mathcal{V}_i} + \frac{1}{\mathcal{V}_o}\right)c_n^i(t) = \frac{AP_nN_n}{\mathcal{V}_i\mathcal{V}_o}$$

First-order linear differential equation with constant coefficients, therefore

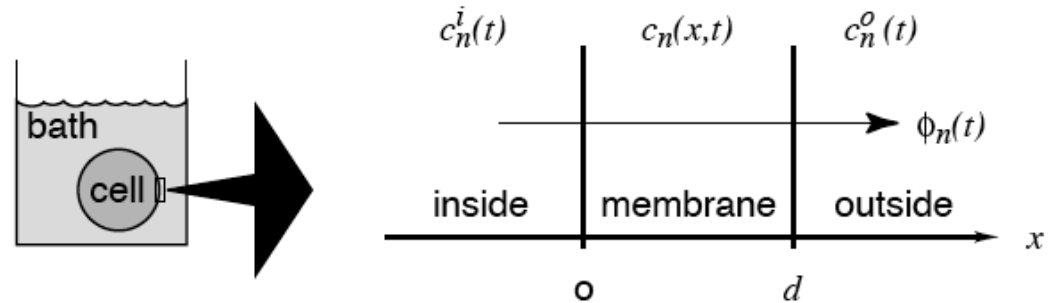
$$c_n^i(t) = c_n^i(\infty) + [c_n^i(0) - c_n^i(\infty)]e^{-t/\tau_{EQ}}$$

$$c_n^i(\infty) = \frac{N_n}{\mathcal{V}_i + \mathcal{V}_o}$$

$$\tau_{EQ} = \frac{1}{AP_n\left(\frac{1}{\mathcal{V}_i} + \frac{1}{\mathcal{V}_o}\right)}$$

Membrane Diffusion: Summary

Membrane diffusion



Dissolve and diffuse model

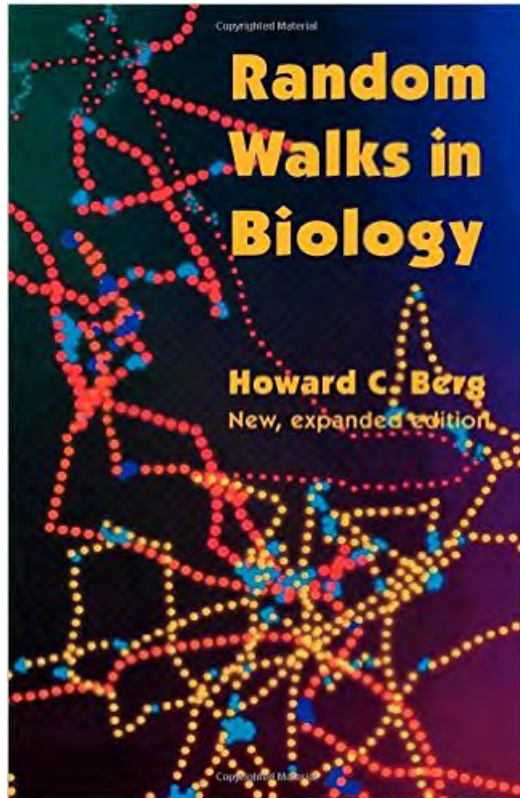
- solute outside cell dissolves into cell membrane
- solute diffuses through membrane
- solute dissolves into cytoplasm

Membrane time constant $t_{SS} = \frac{d^2}{\pi^2 D_n}$

Fick's law for membranes: $\phi_n(t) = P_n (c_n^i(t) - c_n^o(t))$; $P_n = \frac{D_n k_n}{d}$

Two-compartment diffusion

Cell time constant $t_{EQ} = \frac{1}{AP_n \left(\frac{1}{V_o} + \frac{1}{V_i} \right)}$



→ Shift back to the *microscopic* level...

Chapter 1

Diffusion: Microscopic Theory

Diffusion is the random migration of molecules or small particles arising from motion due to thermal energy. A particle at absolute temperature T has, on the average, a kinetic energy associated with movement along each axis of $kT/2$, where k is Boltzmann's constant. Einstein showed in 1905 that this is true regardless of the size of the particle, even for particles large enough to be seen under a microscope, i.e., particles that exhibit Brownian movement. A particle of mass m and velocity v_x on the x axis has a kinetic energy $mv_x^2/2$. This quantity fluctuates, but on the average $\langle mv_x^2/2 \rangle = kT/2$, where $\langle \rangle$ denotes an average over time or over an ensemble of similar particles. From this relationship we compute the mean-square velocity,

$$\langle v_x^2 \rangle = kT/m, \quad (1.1)$$

and the root-mean-square velocity,

$$\langle v_x^2 \rangle^{1/2} = (kT/m)^{1/2}. \quad (1.2)$$

We can use Eq. 1.2 to estimate the instantaneous velocity of a small particle, for example, a molecule of the protein lysozyme. Lysozyme has a molecular weight 1.4×10^4 g. This is the mass of one mole, or 6.0×10^{23} molecules; the mass of one molecule is $m = 2.3 \times 10^{-20}$ g. The value of kT at 300°K (27°C) is 4.14×10^{-14} g cm²/sec². Therefore, $\langle v_x^2 \rangle^{1/2} = 1.3 \times 10^3$ cm/sec. This is a sizeable speed. If there were no obstructions, the molecule would cross a typical classroom in about 1 second. Since the protein is not in a vacuum but is immersed in an aqueous medium, it does not go very far before it bumps into molecules of

Diffusion (Microscopic)

Chapter 1

Diffusion: Microscopic Theory

Diffusion is the random migration of molecules or small particles arising from motion due to thermal energy. A particle at absolute temperature T has, on the average, a kinetic energy associated with movement along each axis of $kT/2$, where k is Boltzmann's constant. Einstein showed in 1905 that this is true regardless of the size of the particle, even for particles large enough to be seen under a microscope, i.e., particles that exhibit Brownian movement. A particle of mass m and velocity v_x on the x axis has a kinetic energy $mv_x^2/2$. This quantity fluctuates, but on the average $\langle mv_x^2/2 \rangle = kT/2$, where $\langle \rangle$ denotes an average over time or over an ensemble of similar particles. From this relationship we compute the mean-square velocity,

$$\langle v_x^2 \rangle = kT/m, \quad (1.1)$$

and the root-mean-square velocity,

$$\langle v_x^2 \rangle^{1/2} = (kT/m)^{1/2}. \quad (1.2)$$

We can use Eq. 1.2 to estimate the instantaneous velocity of a small particle, for example, a molecule of the protein lysozyme. Lysozyme has a molecular weight 1.4×10^4 g. This is the mass of one mole, or 6.0×10^{23} molecules; the mass of one molecule is $m = 2.3 \times 10^{-20}$ g. The value of kT at 300°K (27°C) is 4.14×10^{-14} g cm^2/sec^2 . Therefore, $\langle v_x^2 \rangle^{1/2} = 1.3 \times 10^3$ cm/sec. This is a sizeable speed. If there were no obstructions, the molecule would cross a typical classroom in about 1 second. Since the protein is not in a vacuum but is immersed in an aqueous medium, it does not go very far before it bumps into molecules of

Some (remarkably deep) ideas right off the bat:

- Random walkers
- Temperature, Boltzmann's constant
- Einstein and 1905
- Mean-squared velocity, "ensemble"
- "Brownian movement"
- "Microscopic theory" (ch.2 is "Macroscopic theory")

➔ A kernel of a deep idea is here, the distinction between "lots of little things" versus "big things"

[statistical mechanics being the thread tying things together]

5. *Über die von der molekularkinetischen Theorie der Wärme geforderte Bewegung von in ruhenden Flüssigkeiten suspendierten Teilchen;*
von A. Einstein.

In dieser Arbeit soll gezeigt werden, daß nach der molekularkinetischen Theorie der Wärme in Flüssigkeiten suspendierte Körper von mikroskopisch sichtbarer Größe infolge der Molekularbewegung der Wärme Bewegungen von solcher Größe ausführen müssen, daß diese Bewegungen leicht mit dem Mikroskop nachgewiesen werden können. Es ist möglich, daß die hier zu behandelnden Bewegungen mit der sogenannten „Brownschen Molekularbewegung“ identisch sind; die mir erreichbaren Angaben über letztere sind jedoch so ungenau, daß ich mir hierüber kein Urteil bilden konnte.

Wenn sich die hier zu behandelnde Bewegung samt den für sie zu erwartenden Gesetzmäßigkeiten wirklich beobachten läßt, so ist die klassische Thermodynamik schon für mikroskopisch unterscheidbare Räume nicht mehr als genau gültig anzusehen und es ist dann eine exakte Bestimmung der wahren Atomgröße möglich. Erwies sich umgekehrt die Voraussage dieser Bewegung als unzutreffend, so wäre damit ein schwerwiegendes Argument gegen die molekularkinetische Auffassung der Wärme gegeben.

§ 1. Über den suspendierten Teilchen zuzuschreibenden osmotischen Druck.

Im Teilvolumen V^* einer Flüssigkeit vom Gesamtvolumen V seien z -Gramm-Moleküle eines Nichtelektrolyten gelöst. Ist das Volumen V^* durch eine für das Lösungsmittel, nicht aber für die gelöste Substanz durchlässige Wand vom reinen Lösungs-

INVESTIGATIONS ON THE THEORY OF ,THE BROWNIAN MOVEMENT

BY

ALBERT EINSTEIN, PH.D.



- One of Einstein's *Annus Mirabilis* papers from 1905 (the other two are on special relativity and the photoelectric effect)

- Solidified the foundations of statistical mechanics and characterized the conditions for most living things on this planet (i.e., cell-sized entities)

Random walks

Consider that:

- the drunkard (randomly) stumbles about
- the drunkard may have some sense of where (s)he is going

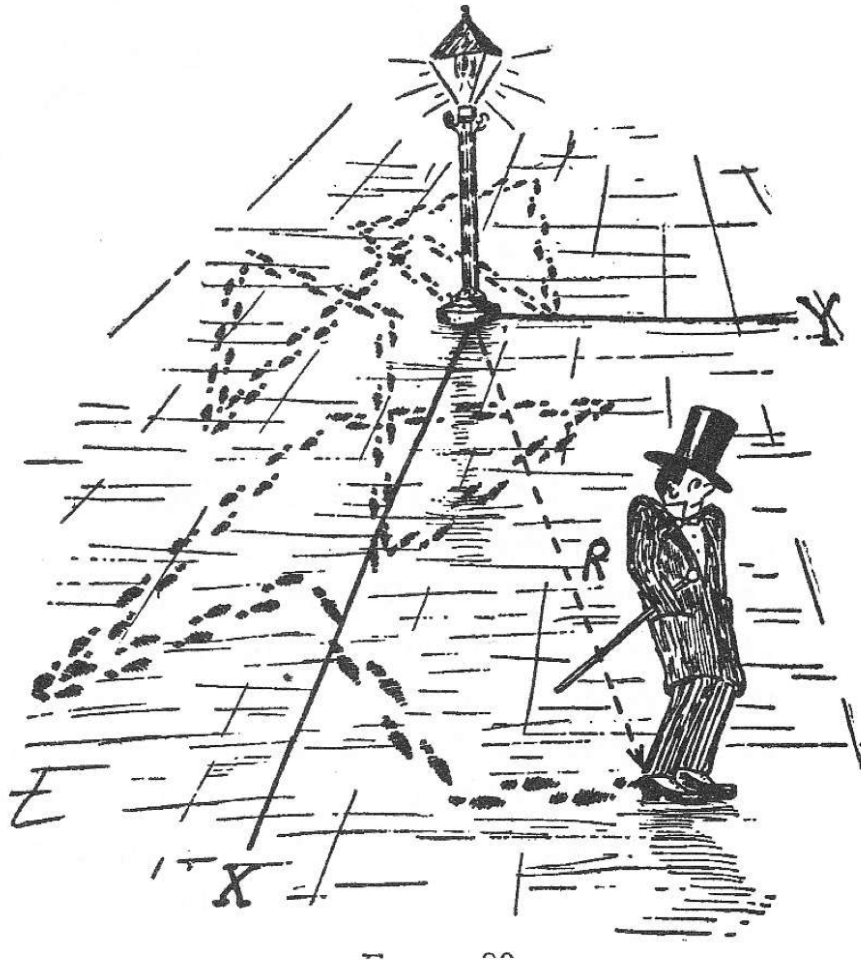


Figure 4.1: (Metaphor.) A random (or “drunkard’s”) walk. [Cartoon by George Gamow, from Gamow, 1961.]

Random walks

Random (2-D) walker (i.e., no bias)

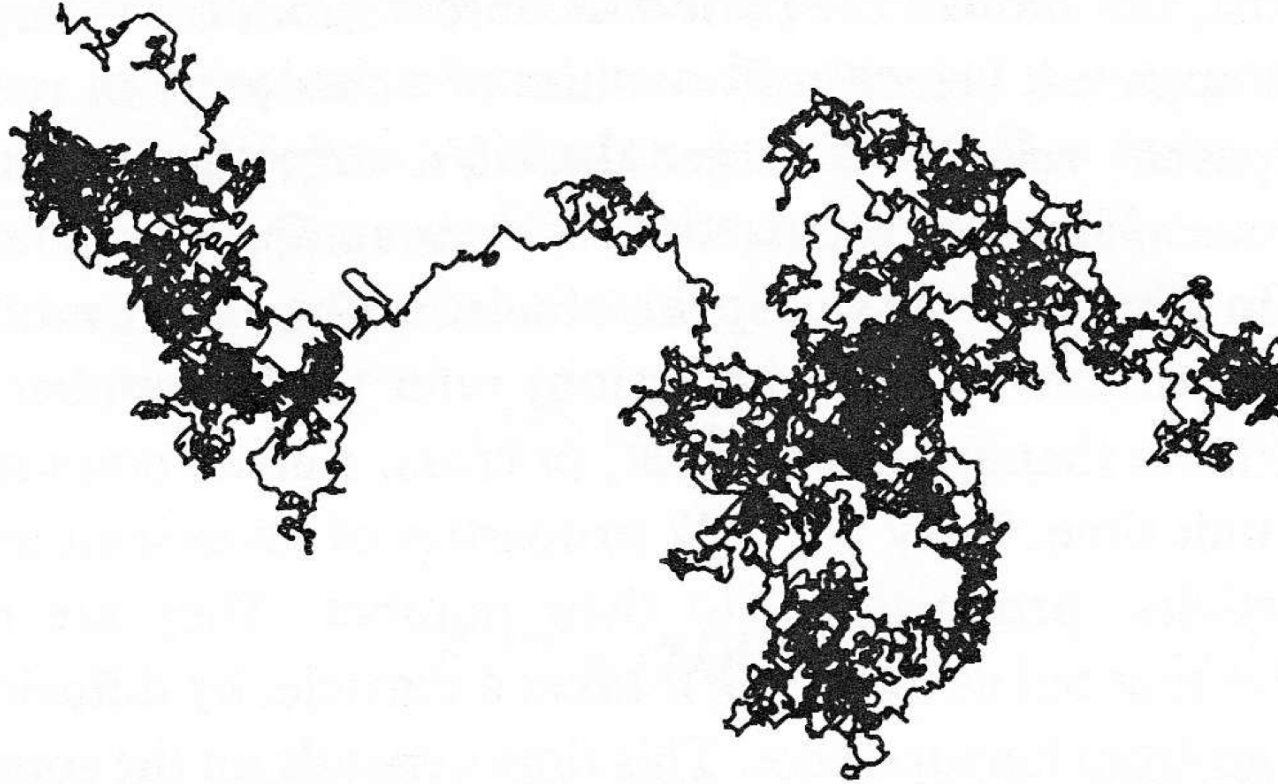
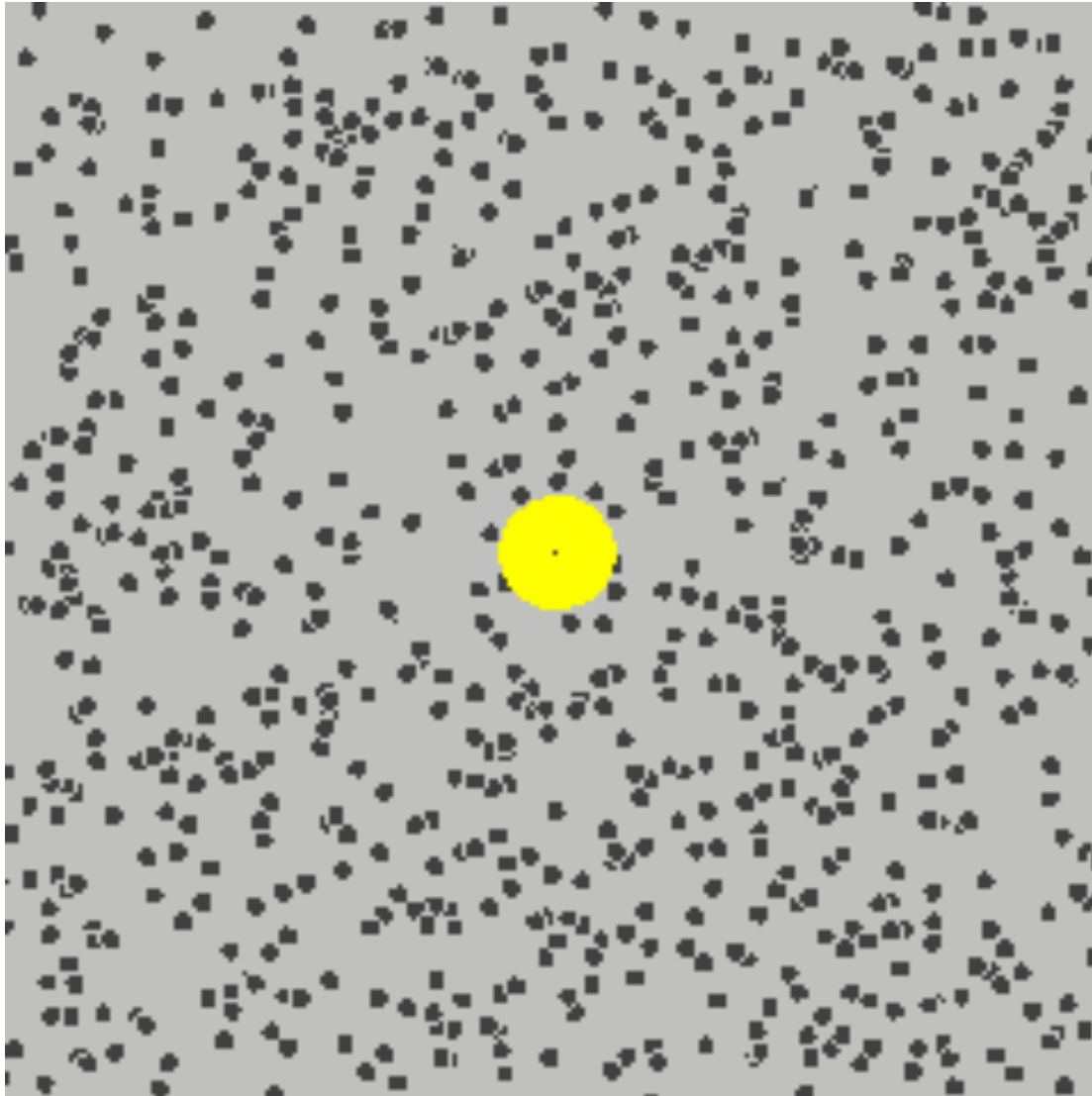


Fig. 1.4. An x, y plot of a two-dimensional random walk of $n = 18,050$ steps. The computer pen started at the upper left corner of the track and worked its way to the upper right edge of the track. It repeatedly traversed regions that are completely black. It moved, as the crow flies, 196 step lengths. The expected root-mean-square displacement is $(2n)^{1/2} = 190$ step lengths.

Brownian Motion

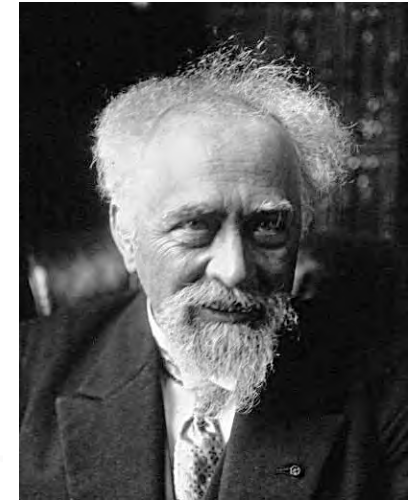
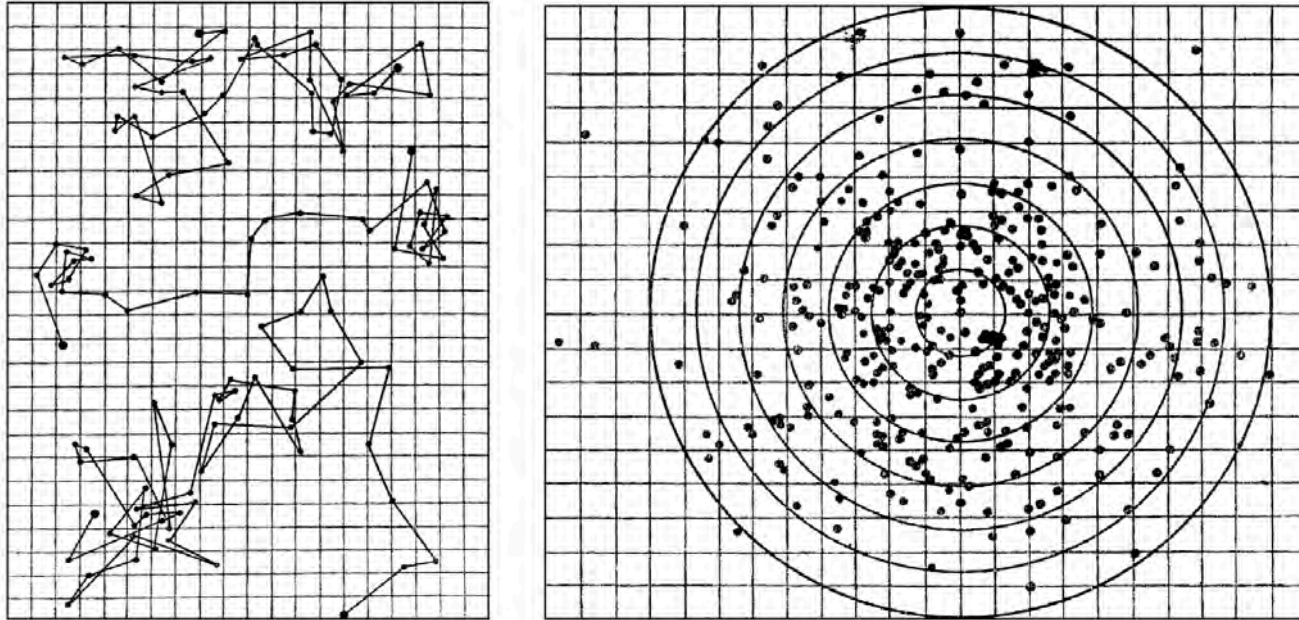
Random motion of large object (yellow circle) due to interaction with many little objects (black circles)



Aside: A bit more history re Brownian motion

8

R. Metzler, J. Klafter / *Physics Reports* 339 (2000) 1–77



Jean Baptiste Perrin (1870-1942)

Fig. 2. Recorded random walk trajectories by Jean Baptiste Perrin [72]. Left part: three designs obtained by tracing a small grain of putty (*mastic*, used for varnish) at intervals of 30 s. One of the patterns contains 50 single points. Right part: the starting point of each motion event is shifted to the origin. The figure illustrates the pdf of the travelled distance r to be in the interval $(r, r + dr)$, according to $(2\pi\xi^2)^{-1} \exp(-r^2/[2\xi^2])2\pi r dr$, in two dimensions, with the length variance ξ^2 . These figures constitute part of the measurement of Perrin, Dabrowski and Chaudesaigues leading to the determination of the Avogadro number. The result given by Perrin is 70.5×10^{22} . The remarkable *œuvre* of Perrin discusses all possibilities of obtaining the Avogadro number known at that time. Concerning the trajectories displayed in the left part of this figure, Perrin makes an interesting statement: “Si, en effet, on faisait des pointés de seconde en seconde, chacun de ces segments rectilignes se trouverait remplacé par un contour polygonal de 30 côtés relativement aussi compliqué que le dessin ici reproduit, et ainsi de suite”. [If, veritably, one took the position from second to second, each of these rectilinear segments would be replaced by a polygonal contour of 30 edges, each itself being as complicated as the reproduced design, and so forth.] This already anticipates Lévy’s cognisance of the self-similar nature, see footnote 9, as well as of the non-differentiability recognised by N. Wiener.

What Brown saw and you can too

Philip Pearle^{a)} and Brian Collett
Department of Physics, Hamilton College, Clinton, New York 13323

Kenneth Bart
Department of Biology, Hamilton College, Clinton, New York 13323

David Bilderback, Dara Newman, and Scott Samuels
Division of Biological Sciences, The University of Montana, Montana 59812

(Received 11 September 2009; accepted 14 July 2010)

A discussion of Robert Brown's original observations of particles ejected by pollen of the plant *Clarkia pulchella* undergoing what is now called Brownian motion is given. We consider the nature of those particles and how he misinterpreted the Airy disk of the smallest particles to be universal organic building blocks. Relevant qualitative and quantitative investigations with a modern microscope and with a "homemade" single lens microscope similar to Brown's are presented.

© 2010 American Association of Physics Teachers.

[DOI: 10.1119/1.3475685]

Am. J. Phys. **78** (12), December 2010

the plant
he nature
universal
modern
resented.

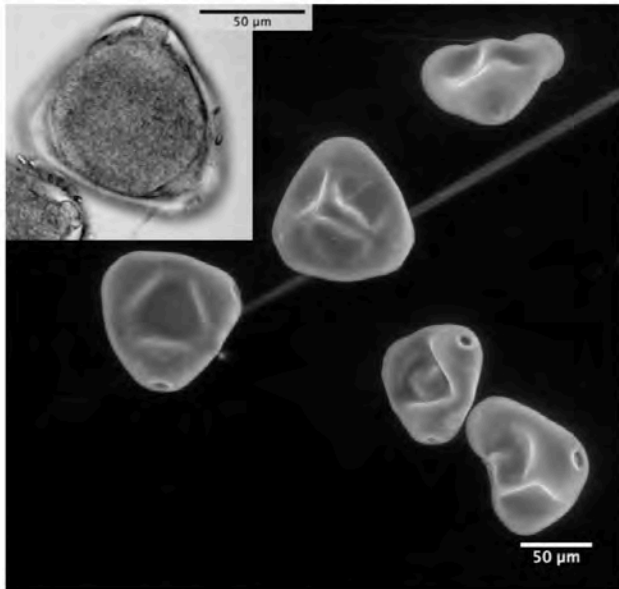


Fig. 1. *Clarkia pulchella* pollen imaged by a microscope (inset) and by an electron microscope.

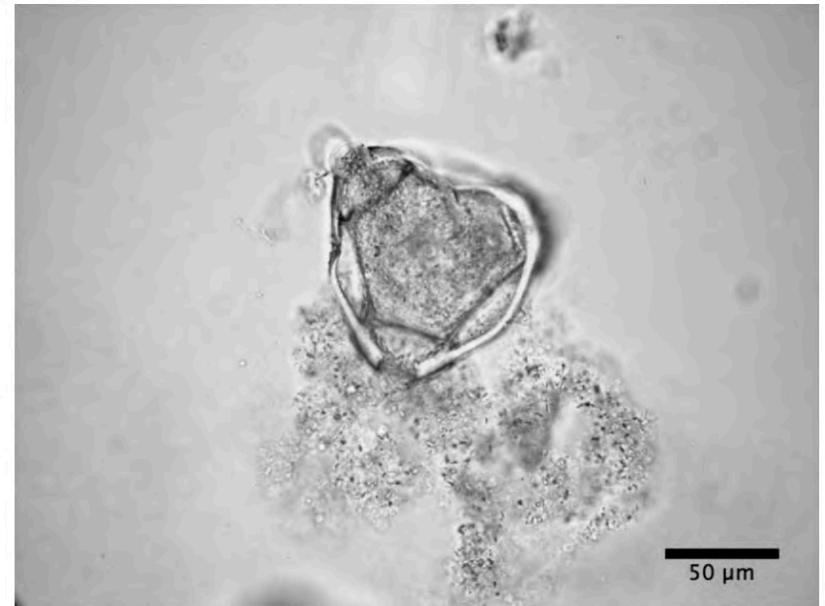
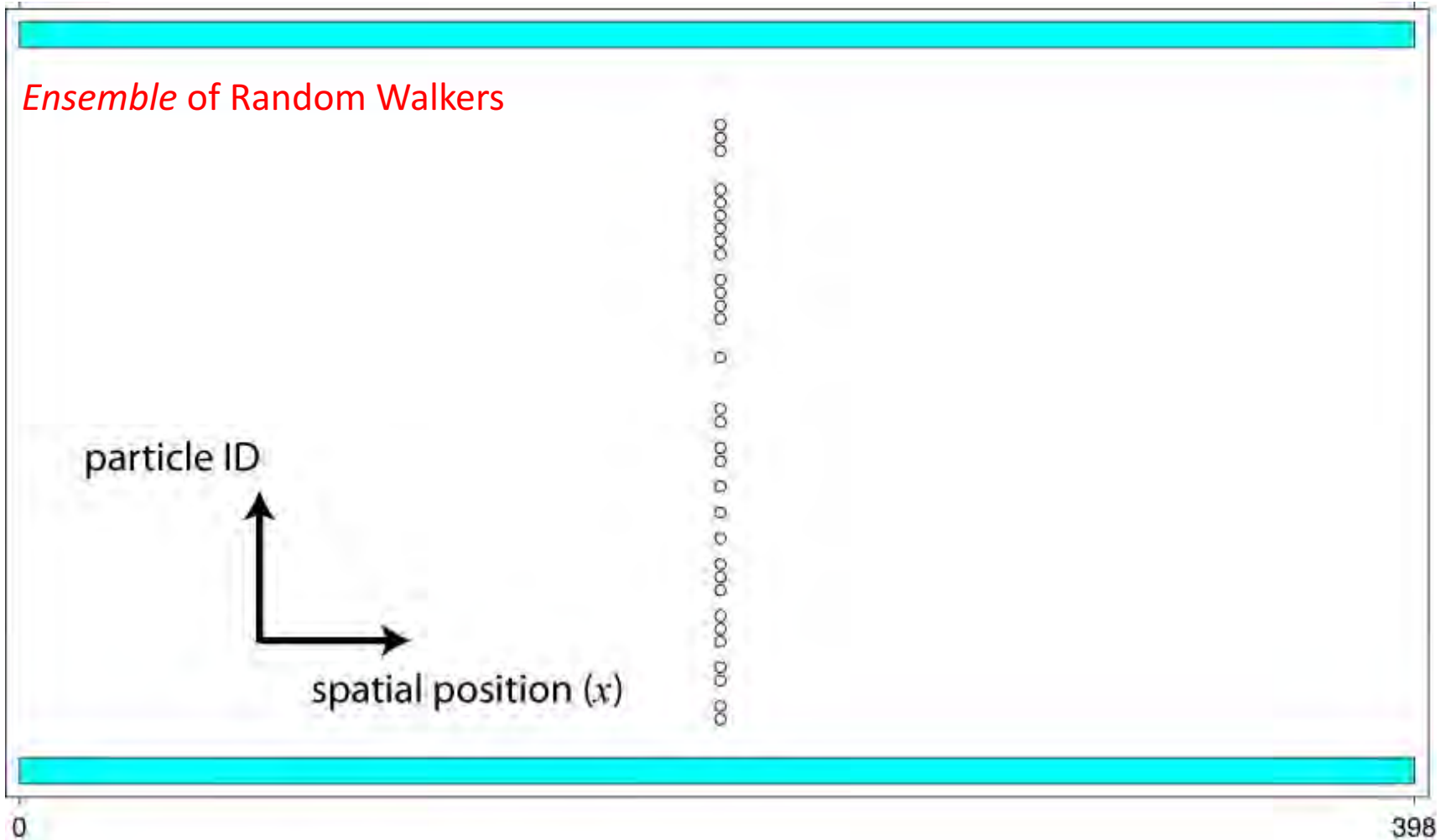


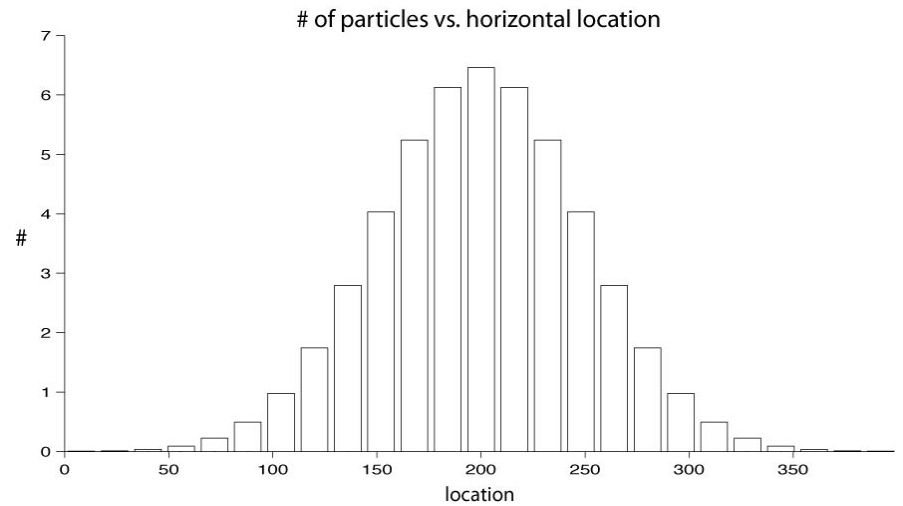
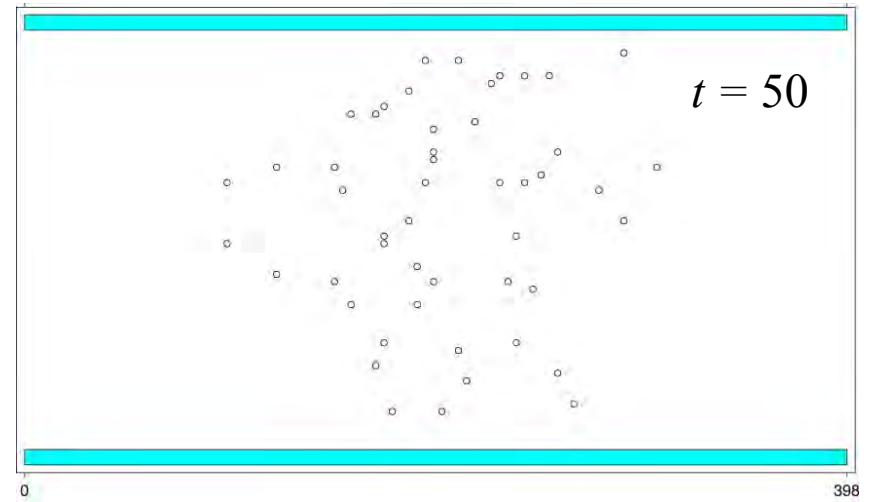
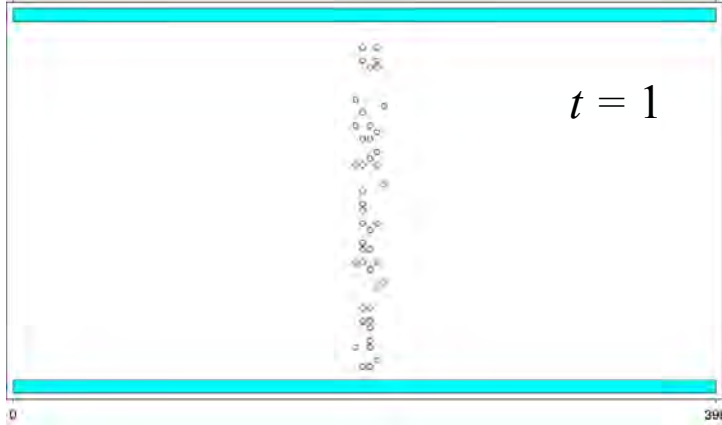
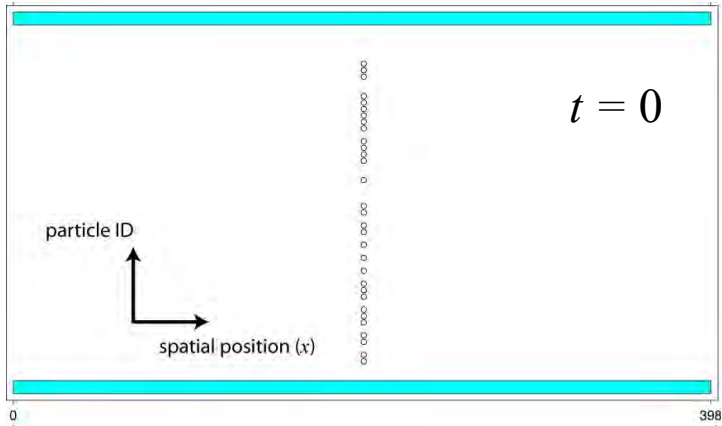
Fig. 2. Bursting *Clarkia pulchella* pollen.

Diffusion (Microscopic)

- Brownian motion \Rightarrow 'Random Walker' (1-D)



Diffusion: Microscopic



→ On average, they don't go anywhere... but they do "spread out" with time

Diffusion (Microscopic)

➤ Random walking (in 1-D for simplicity)

- independent of one another
- equal probability either way

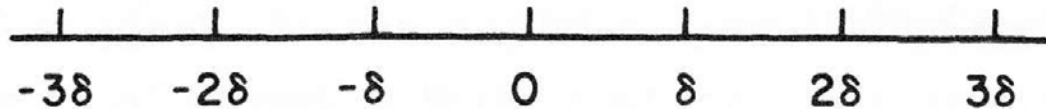


Fig. 1.2. Particles executing a one-dimensional random walk start at the origin, 0, and move in steps of length δ , occupying positions $0, \pm\delta, \pm2\delta, \pm3\delta, \dots$

Position of i 'th walker
after n 'th step:

$$x_i(n) = x_i(n - 1) \pm \delta.$$

Mean displacement:

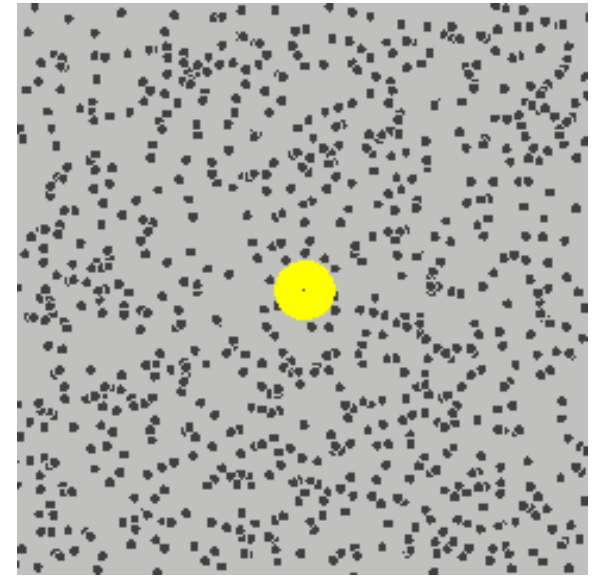
$$\langle x(n) \rangle = \frac{1}{N} \sum_{i=1}^N x_i(n)$$

$$\begin{aligned} \langle x(n) \rangle &= \frac{1}{N} \sum_{i=1}^N [x_i(n - 1) \pm \delta] \\ &= \frac{1}{N} \sum_{i=1}^N x_i(n - 1) = \langle x(n - 1) \rangle \end{aligned}$$

→ On average, they don't go anywhere(!)

Key Idea (REVISTED): Stat. mech. bridges “micro” & “macro”

- So lots of “really small things” can push around “small things”



- ... and lots of “small things” can “spread out”

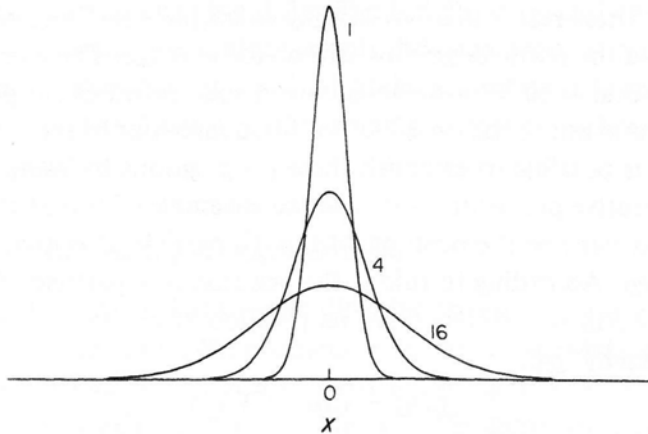
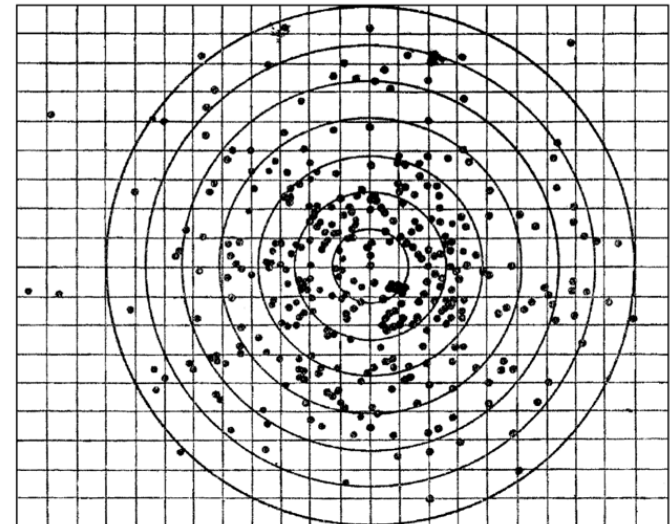


Fig. 1.3. The probability of finding particles at different points x at times $t = 1, 4$, and 16 . The particles start out at position $x = 0$ at time $t = 0$. The standard deviations (root-mean-square widths) of the distributions increase with the square-root of the time. Their peak heights decrease with the square-root of the time. See Eq. 1.22.

Two sides of the same coin:
micro- & macro-scopic, which
collectively amount to “diffusion”



Aside: Mean-Squared Distance (MSD)

- If we consider an 'ensemble' of random walkers, each starting at the origin and independent of one another, computationally it's easy for us to keep track of the *average net movement* (Mean Squared Distance, MSD)

$$\langle x^2 \rangle = D t$$

$\langle x^2 \rangle$ - Mean-squared distance

D - 'diffusion' constant

t - time allowed before 'checking' $\langle x^2 \rangle$

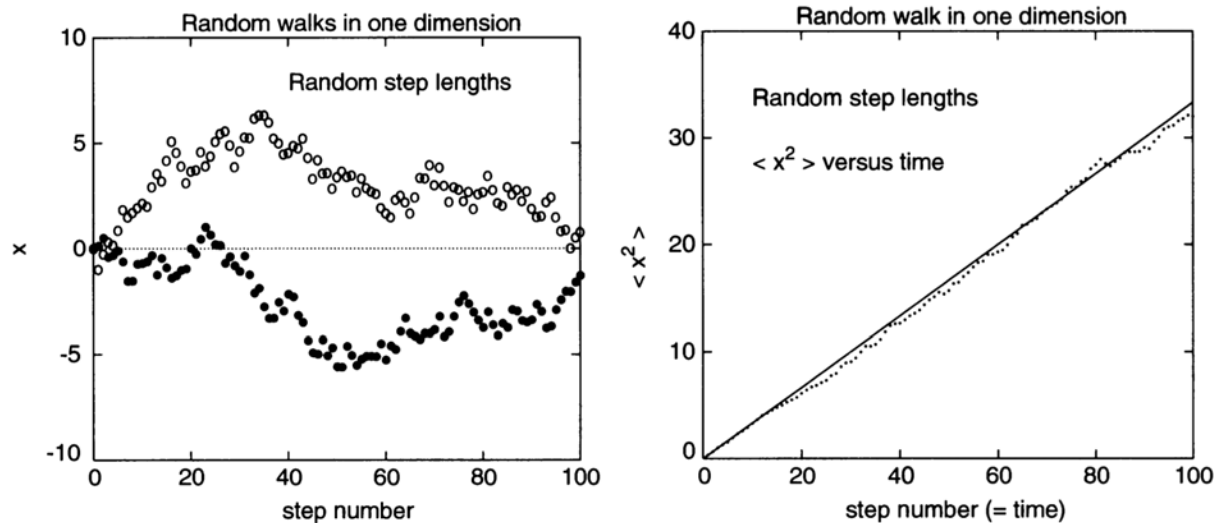


Figure 7.10: Left: x versus step number (that is, time) for two random walks in one dimension. Here the steps were of random lengths in the range -1 to 1 . Right: $\langle x^2 \rangle$ as a function of time for a collection of these one-dimensional random walks. The results for 500 walks were averaged.

- So while each individual walker is random, the basic idea is that in an *ensemble average*, a repeatable/consistent trend emerges

Aside: Mean-Squared Distance (MSD)

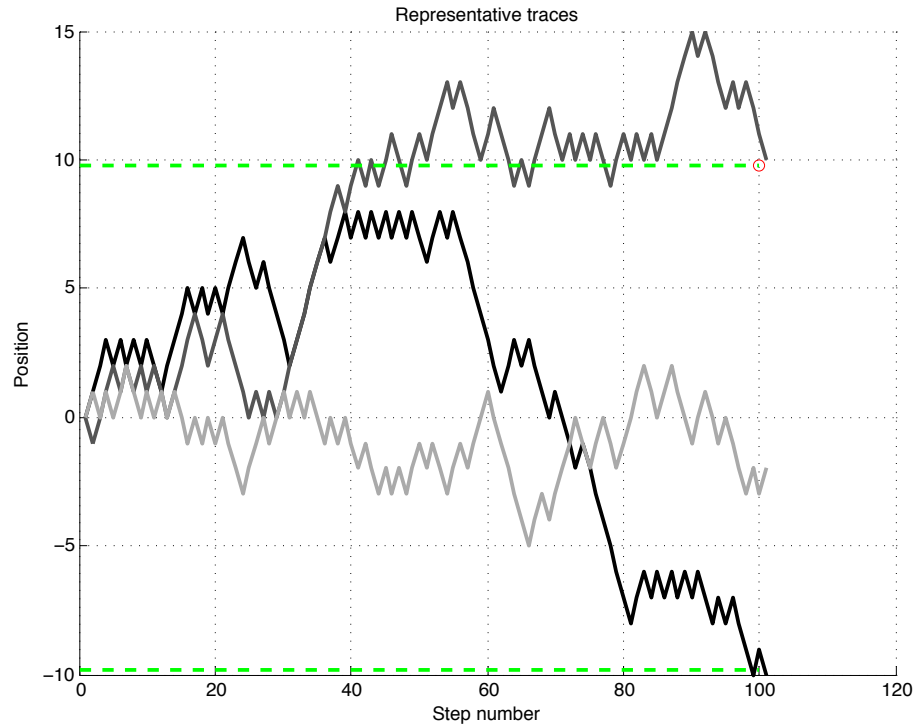
```

% ### EXrandomWalk1D.m ###      11.15.14
clear;
% -----
N= 200;      % Total # of (independent) walkers (each starts at x=0)
M= 100;      % Total # of steps for each walker
K= 3;        % # of walkers to show individual traces for [3]
bias= 0.5;   % number between [0,1] to indicate bias for left vs right (0.5= equal prob.)
% -----
% +++
step_number= zeros(1,M);      %
x2ave= zeros(1,M);           % allocate array to stored (sequentially averaged) MSD
step_number_array= [1:1:M];   %
% +++
%
% NOTE: the loop is set up in such a way to average x2ave across walkers
for r= 1:N
    x=0;      % initialize position for r'th walker
    position(r,1)= 0;
    % loop to go through M steps for r'th walker
    for nn=1:M;
        % conditional determines whether step is to the left or right
        if (rand<bias), x=x+1;
        else x=x-1; end;
        x2ave(nn)=x2ave(nn)+x^2;      % store squared displacement (handles averaging across r)
        position(r,nn+1)= x;         % store displacement for each walker and step
    end;
end;
x2ave= x2ave/N;      % Divide by number of walkers
% plot MSD
figure(1);
plot(step_number_array, x2ave, 'k'); hold on;
title('MSD for 1-D random walk');
xlabel('Step number'); ylabel('Mean-Squared Distance (x^2)');
% plot a subset of individual traces
figure(2); clf; hold on; grid on;
for nn=1:K
    shade= 1-(nn-1)/K;
    plot(position(nn,:), 'Color',[1 1 1]-shade);
end
xlabel('Step number'); ylabel('Position'); title('Representative traces');
plot([0 M],[1 1]*sqrt(x2ave(end)), 'g--', 'LineWidth',2) % include MSD bounds at step M
plot([0 M],[-1 -1]*sqrt(x2ave(end)), 'g--', 'LineWidth',2)
plot(M,sqrt(mean(position(:,end).^2)), 'ro');      % reality check (another way to compute final MSD)
disp(['Final mean (non-squared) distance = ',num2str(mean(position(:,end)))]);

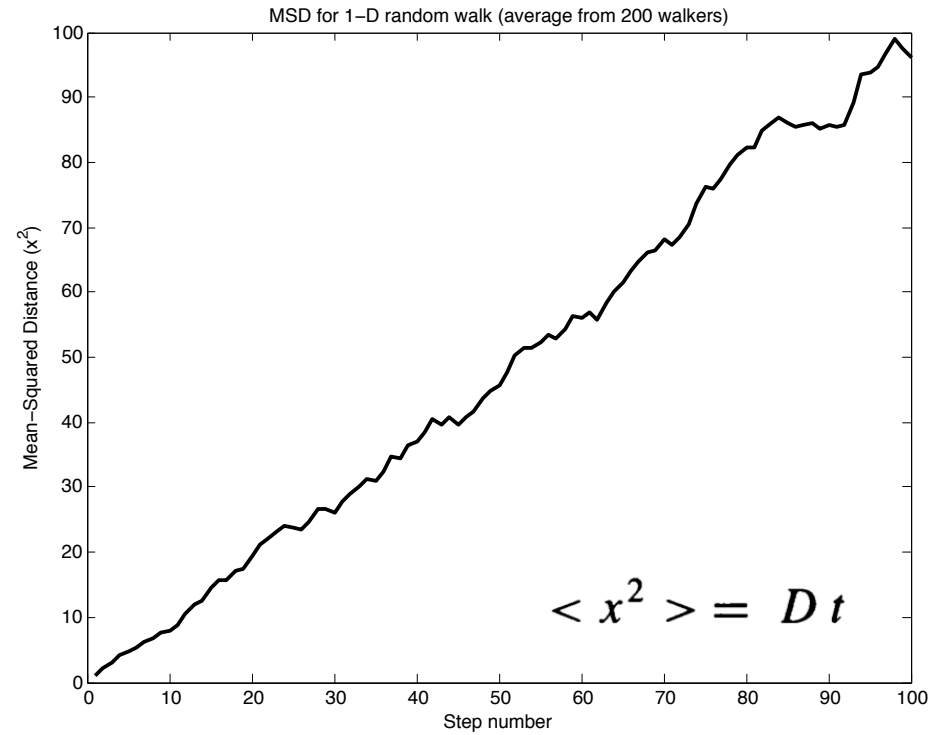
```

- Ensemble of N (independent) walkers
- Each takes M total steps, each step either left or right
- Note that the `for` loop averages as it goes

Aside: Mean-Squared Distance (MSD)



Representative traces from three different (independent) walkers



Mean-squared distance traveled by a large ensemble of walkers

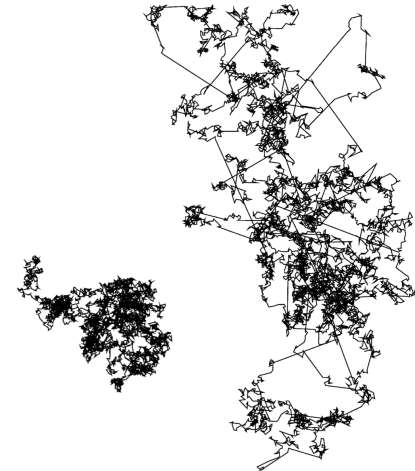
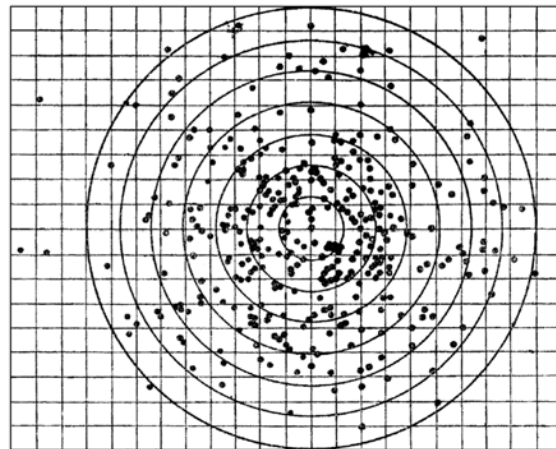
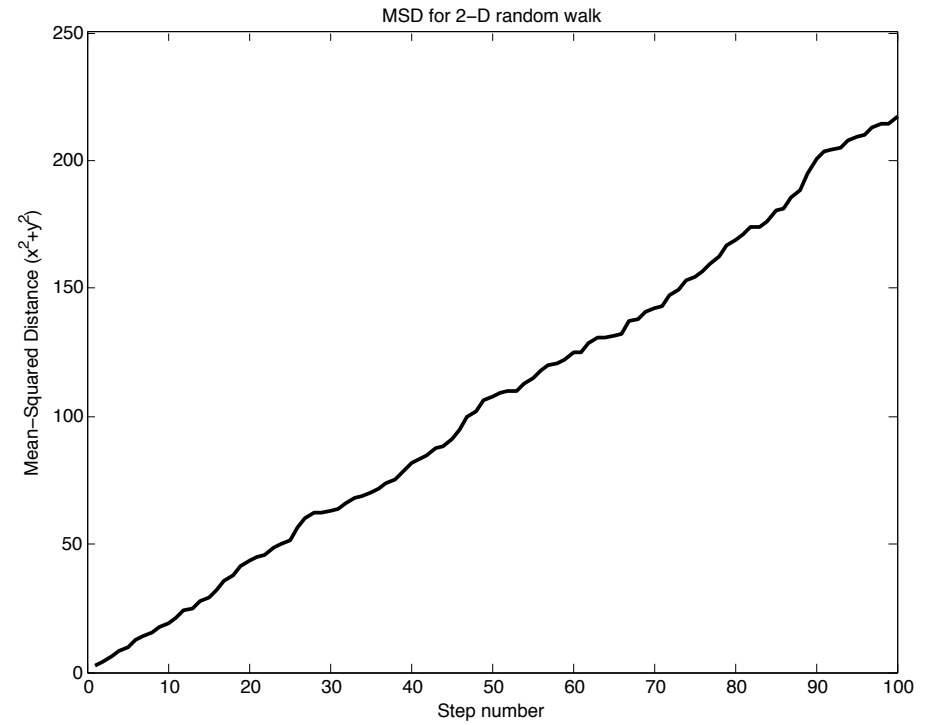
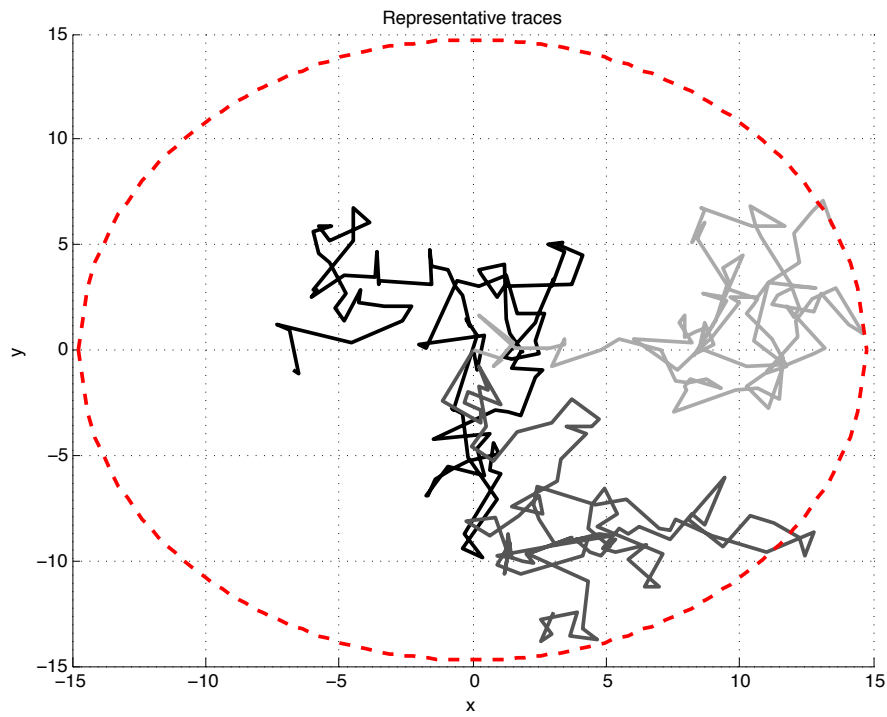
```

% ### EXrandomWalk2D.m ###
% o Method 1 - simply equal probability one step up/down (U/D) and left/right (L/R)
% o Method 2 - U/D and L/R steps are sampled from a uniform distribution over [-1,1]
% o Method 3 - U/D and L/R steps are sampled from a Gaussian distribution
clear;
% -----
N= 200;      % Total # of (independent) walkers (each starts at x=0)
M= 100;      % Total # of steps for each walker
K= 3;        % # of walkers to show individual traces for [3]
method= 3;   % see comments above
% -----
% +++
step_number= zeros(1,M);      %
posAvg= zeros(1,M);           % allocate array to stored (sequentially averaged) MSD
step_number_array= [1:1:M];   %
% +++
for r= 1:N
    x=0; y=0; % initialize positions for r'th walker
    positionX(r,1)= 0; positionY(r,1)= 0;
    % loop to go through M steps for r'th walker
    for nn=1:M;
        if method==1
            if (rand<0.5), x=x+1; % conditional for left or right
            else x=x-1; end;
            if (rand<0.5), y=y+1; % conditional for up or down
            else y=y-1; end;
        elseif method==2
            x= x+2*rand(1)-1; y= y+2*rand(1)-1;
        elseif method==3
            x= x+randn(1); y= y+randn(1);
        end
        posAvg(nn)= posAvg(nn)+ (x^2+y^2); % store squared displacement (handles averging across r)
        positionX(r,nn+1)= x; % store displacements for each walker and step
        positionY(r,nn+1)= y;
    end;
end;
posAvg= posAvg/N; % Divide by number of walkers
% plot MSD
figure(1);
plot(step_number_array,posAvg, 'k'); hold on;
title('MSD for 2-D random walk');
xlabel('Step number'); ylabel('Mean-Squared Distance (x^2+y^2)');
% plot a subset of individual traces
figure(2); clf; hold on; grid on;
for nn=1:K
    shade= 1-(nn-1)/K;
    plot(positionX(nn,:),positionY(nn,:), 'Color',[1 1 1]-shade);
end
xlabel('x'); ylabel('y'); title('Representative traces');
% also plot MSD (which is a circular arc in this case)
rBND= sqrt(posAvg(end)); % radius MSD
xBND= linspace(-rBND,rBND,100); yBND= sqrt(rBND^2-xBND.^2);
plot(xBND,yBND,'r--','LineWidth',2); plot(xBND,-yBND,'r--','LineWidth',2);

```

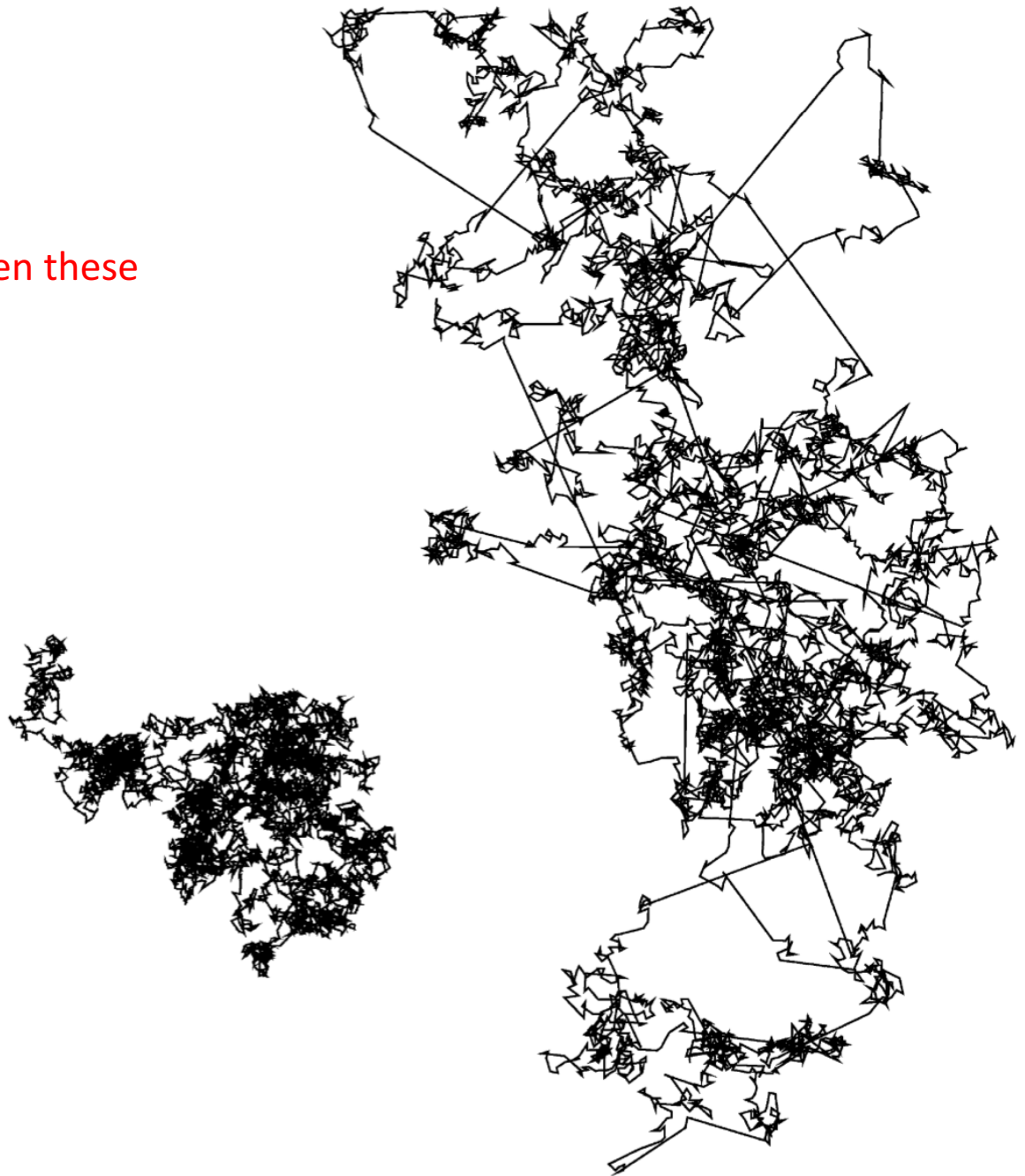
- Same basic idea as 1-D code, but allows for more flexibility

Aside: Mean-Squared Distance (MSD)



Quiz

What is different between these two “random” walkers?



Brownian Motion??

Note: This is a 3-D plot!
(try crossing your eyes)

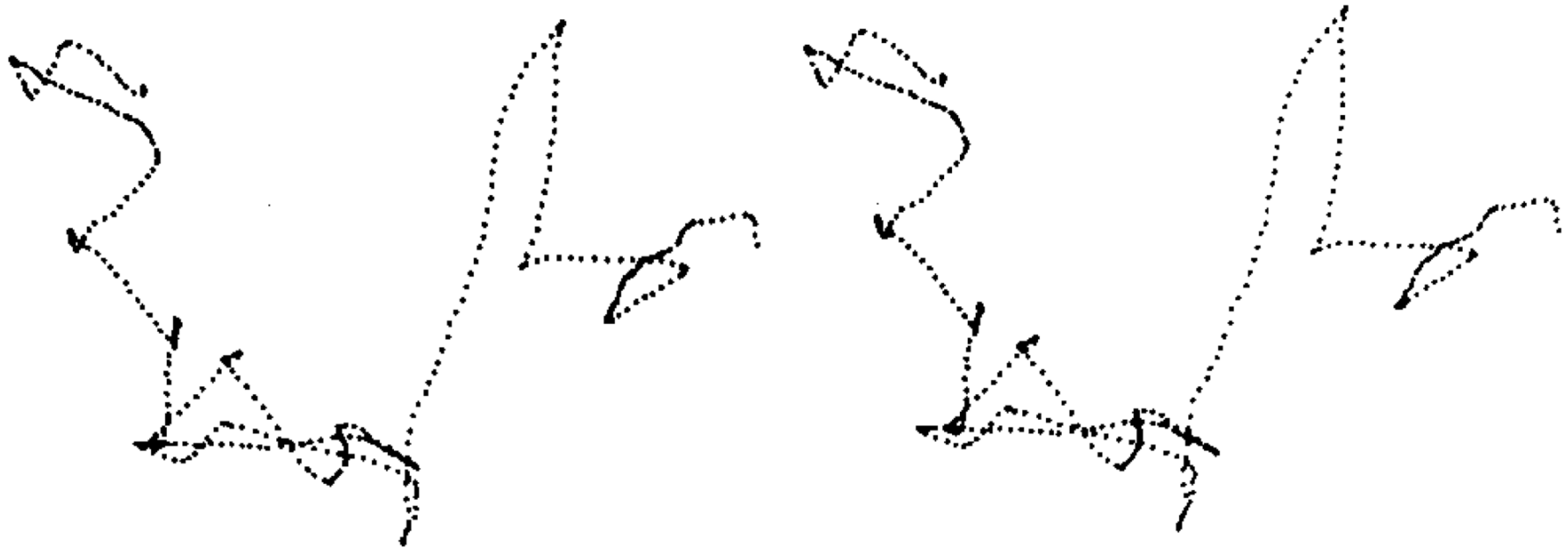


FIGURE 3. MOVEMENT. This stereo plot shows about 30 s in the life of one *Escherichia coli* K-12 bacterium swimming in an isotropic homogenous medium.¹⁸ The track spans about 0.1 mm, left to right. The plot shows 26 runs and tumbles, the longest run (nearly vertical) lasting 3.6 s. The mean speed is about 21 $\mu\text{m/s}$. To see this plot in three dimensions, look at the left image with your left eye and the right image with your right eye, and relax your eye muscles so that the two images overlap. A stereoscope (pair of lenses) helps.

Key Idea: Passive versus Active

- Passive: movement is subject to the medium you are in moving you around (e.g., diffusion)
- Active: you move yourself around (e.g., swimming)



MOTILE BEHAVIOR OF BACTERIA

JANUARY 2000 PHYSICS TODAY

E. coli, a self-replicating object only a thousandth of a millimeter in size, can swim 35 diameters a second, taste simple chemicals in its environment, and decide whether life is getting better or worse.

Howard C. Berg

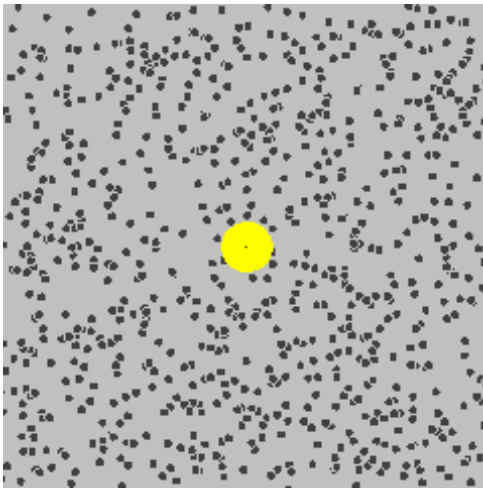
Anomalous Diffusion

Question:

So how can we tell the difference between passive and active?

Answer:

How “normal” is your diffusion?



$$\langle x^2 \rangle = D t$$

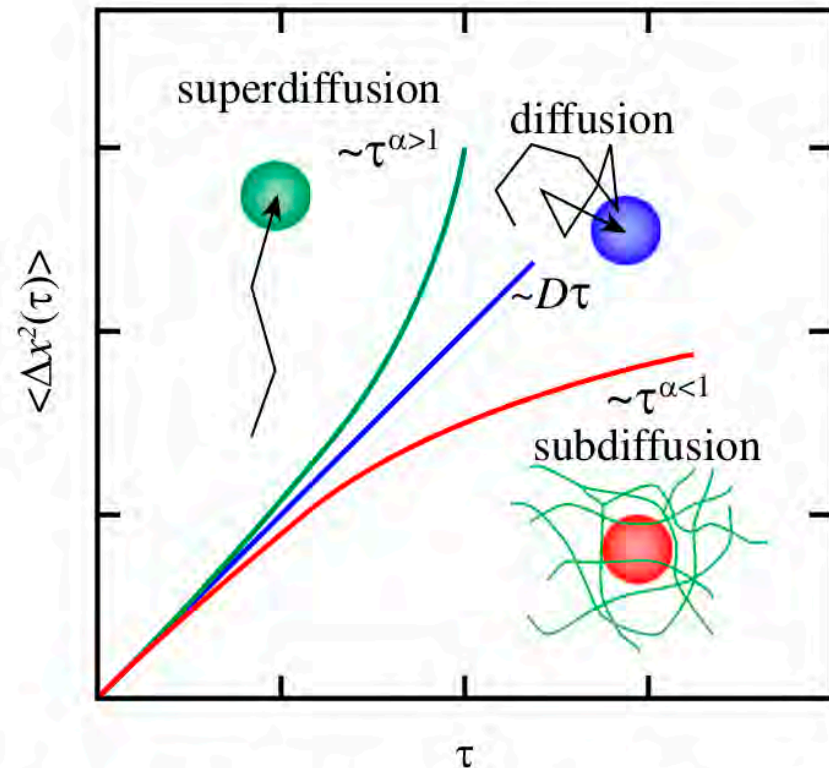


Fig. 1. Thermal diffusion (blue line) of a particle in a liquid is characterized by an MSD given by $\langle \Delta x^2(\tau) \rangle = 2D\tau$, where the displacement $\Delta x(\tau) = x(t+\tau) - x(t)$ along one axis is measured over a time interval τ . In equilibrium, this linear dependence on τ is only expected for motion in simple liquids. In viscoelastic materials, such as polymer solutions, subdiffusive motion (red) is expected in equilibrium. By contrast, superdiffusive motion (green) often indicates partially or fully directed motion (e.g., for transport along a substrate) (11).

Aside: Reaction-Diffusion (or *How the leopard got its spots*)

- Chiefly just described diffusion as “flow” thus far...

Diffusion equation

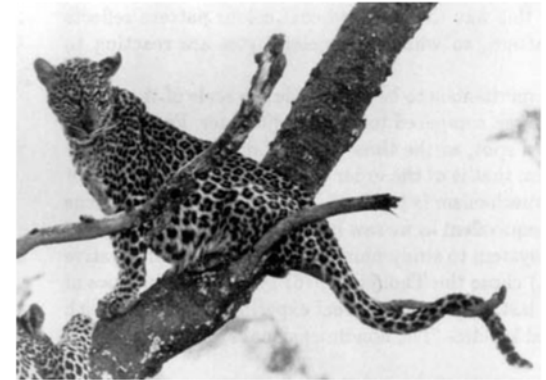
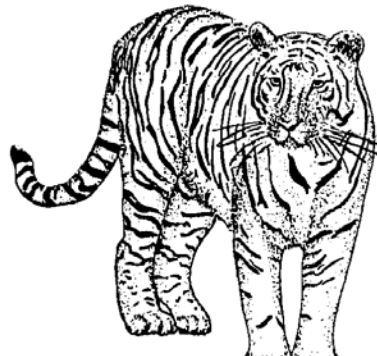
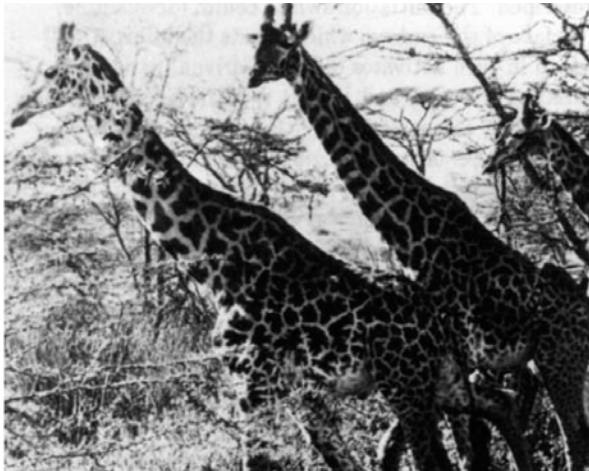
$$\frac{\partial c}{\partial t} = D \frac{\partial^2 c}{\partial x^2}$$

- But addition of a “reaction” term forms a key approach to pattern formation
(this stems from Alan Turing’s famous 1952 paper *The Chemical Basis of Morphogenesis*)

Reaction-Diffusion equation

$$\frac{\partial \mathbf{c}}{\partial t} = \mathbf{f}(\mathbf{c}) + D \nabla^2 \mathbf{c},$$

$\mathbf{f}(\mathbf{c})$ describes “reaction kinetics”

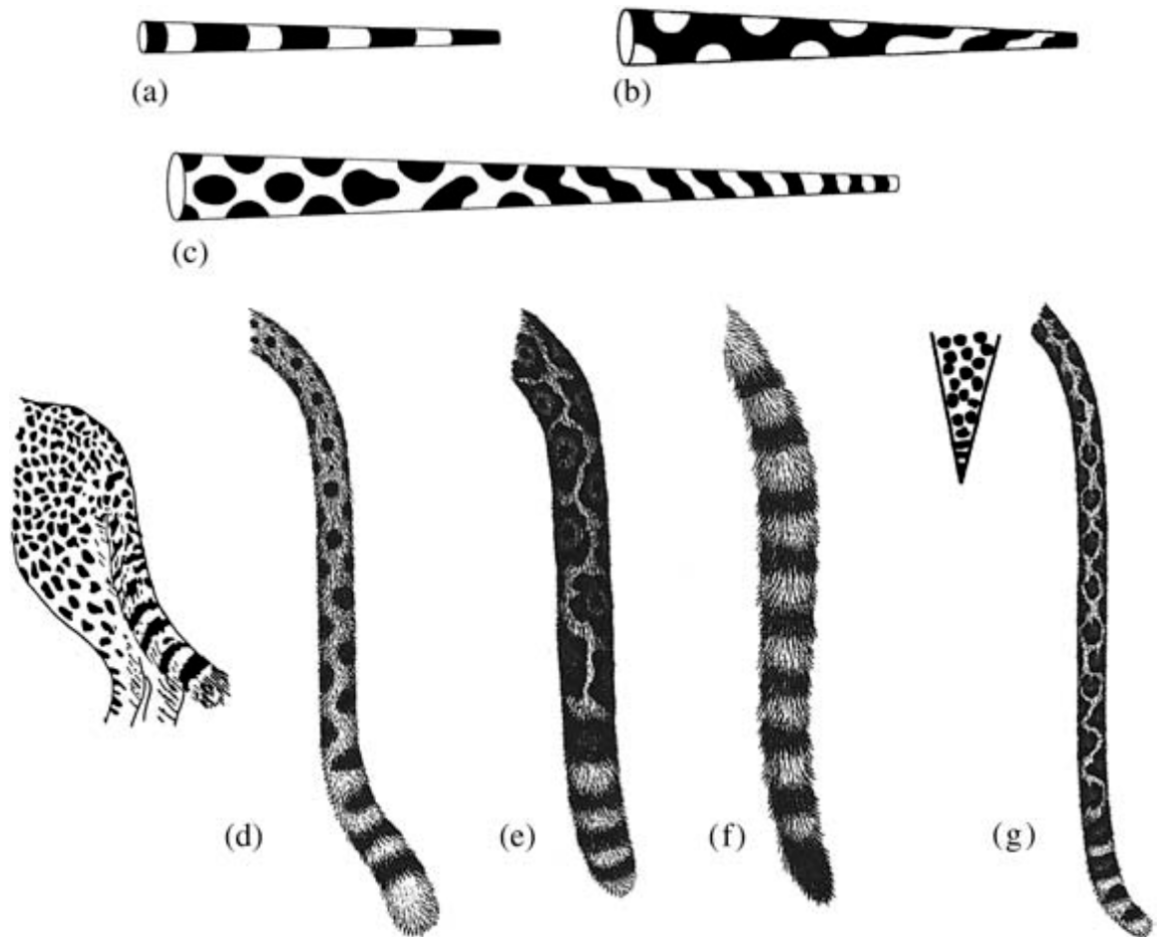


Aside: Reaction-Diffusion (or How the leopard got its spots)

$$\frac{\partial u}{\partial t} = \gamma f(u, v) + \nabla^2 u, \quad \frac{\partial v}{\partial t} = \gamma g(u, v) + d \nabla^2 v$$

$$f(u, v) = a - u - h(u, v), \quad g(u, v) = \alpha(b - v) - h(u, v)$$

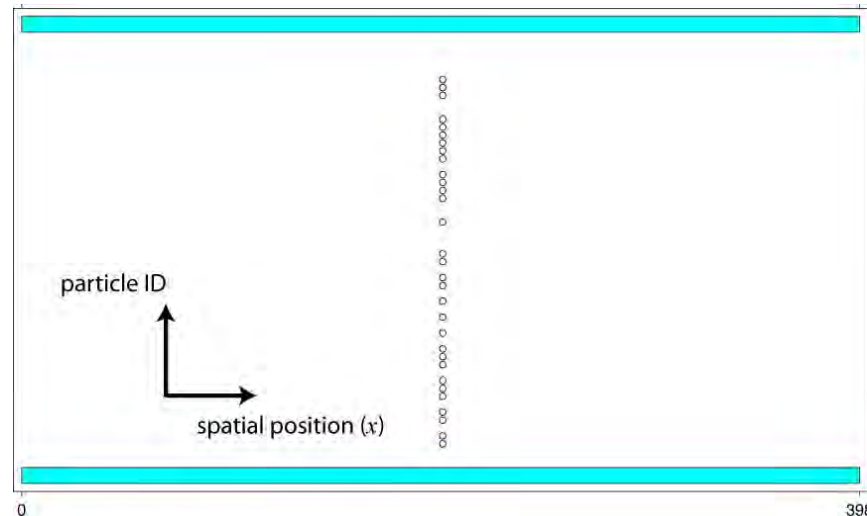
$$h(u, v) = \frac{\rho uv}{1 + u + Ku^2}$$



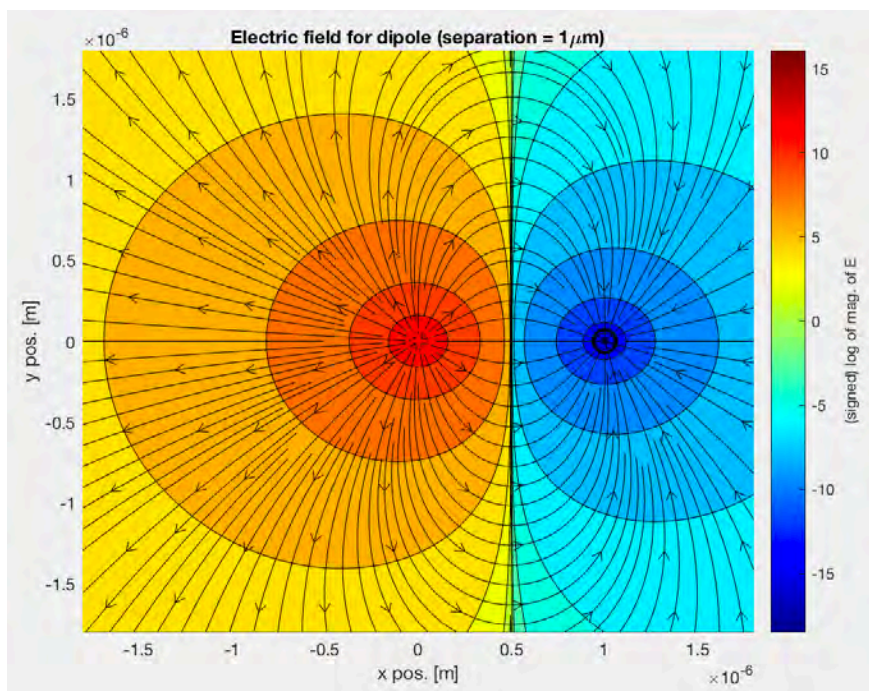
Key Idea: Charged random walkers?

- Up until this point, we have considered our walkers to not be interacting

$$x_i(n) = x_i(n - 1) \pm \delta.$$

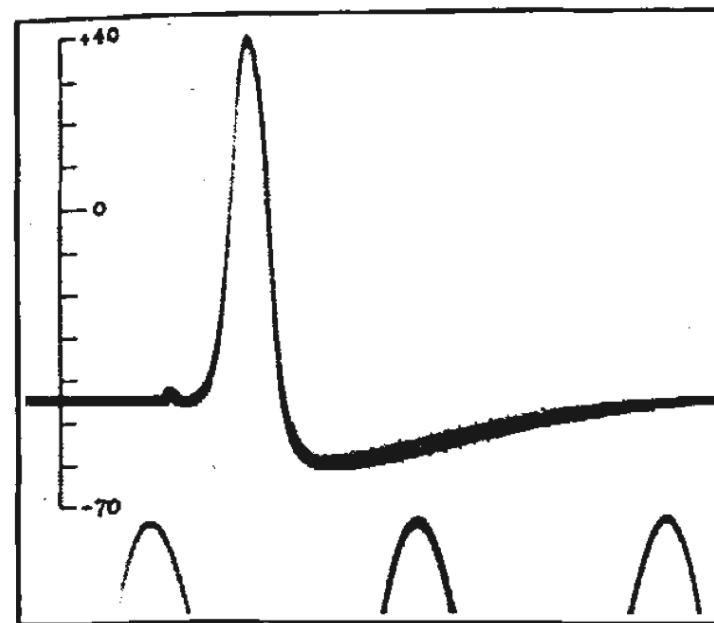


→ But what if they were (electrically) charged?



Recall from earlier

(and think about what the axes are here!)



Electrical properties of cells

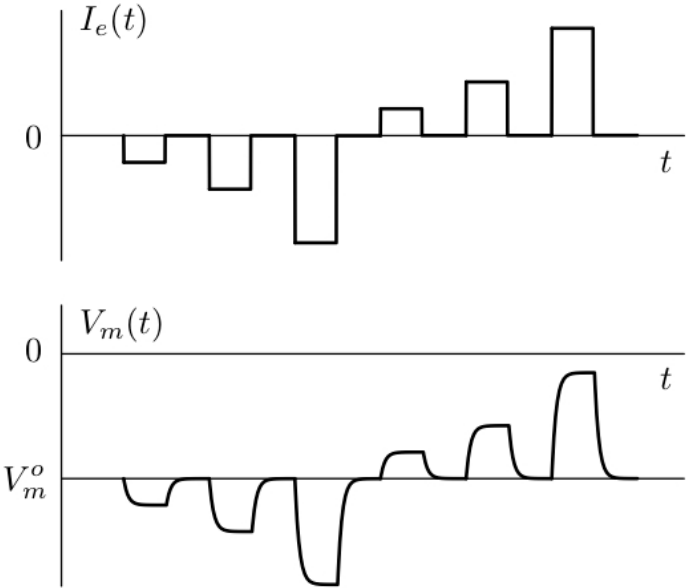
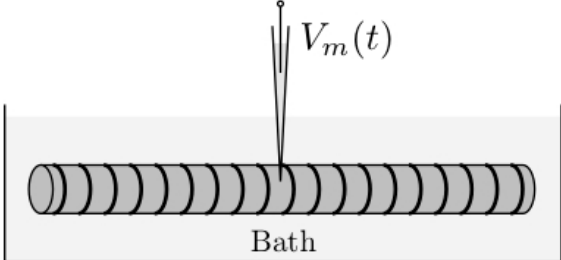
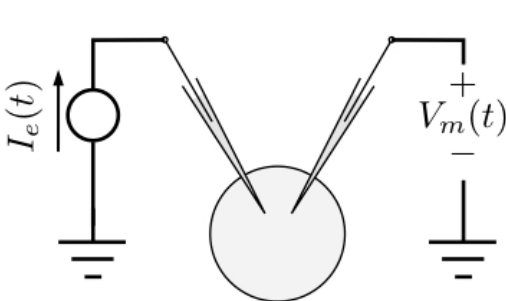


Figure 1.1

Graded potentials (note RC time constant!)

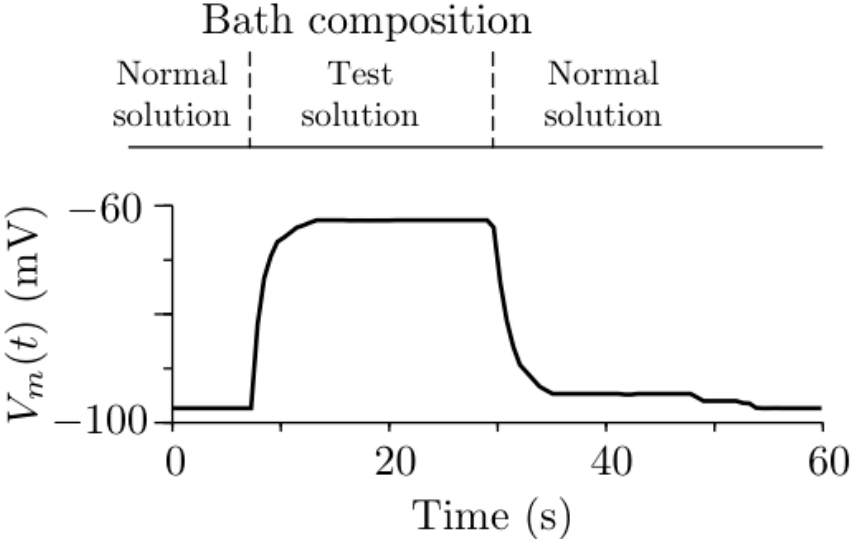


Figure 1.2

Extracellular solution can have a big effect

Aside: Electrical responses in sensory systems

Photoreceptors (re vision)

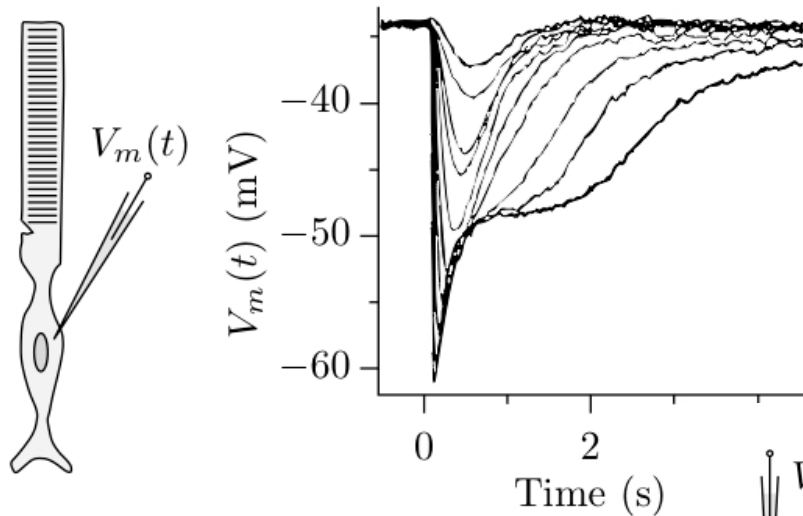
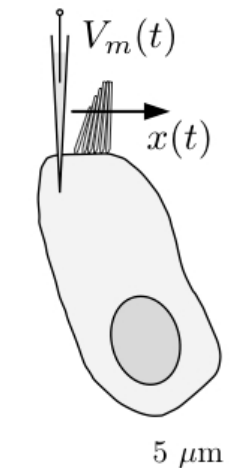


Figure 1.3



Hair cells
(re hearing)

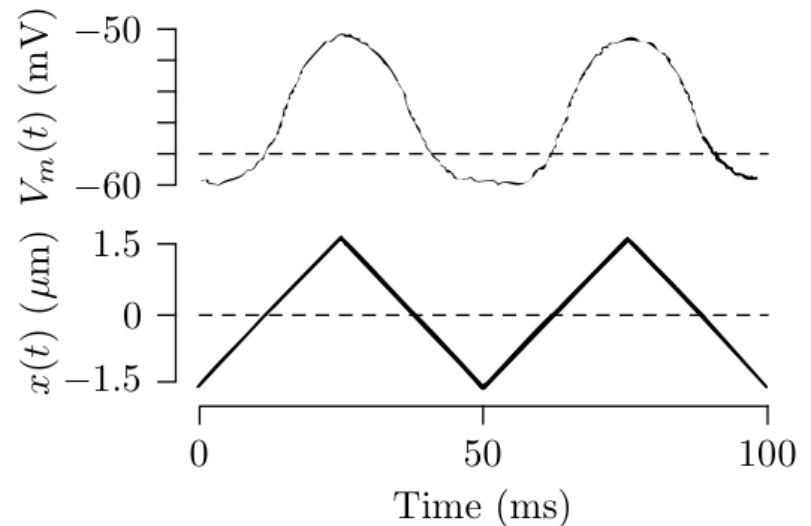


Figure 1.5

Similar qualitative behavior for mechano- (touch) and chemo-receptors (taste, smell)

Looking Ahead: Electrodiffusion Equations

Nernst-Planck Equation

$$J_n(x, t) = -z_n F D_n \frac{\partial c_n(x, t)}{\partial x} - u_n z_n^2 F^2 c_n(x, t) \frac{\partial \psi(x, t)}{\partial x}$$

Continuity

$$\frac{\partial J_n(x, t)}{\partial x} = -z_n F \frac{\partial c_n(x, t)}{\partial t}$$

Poisson's Equation

$$\frac{\partial^2 \psi(x, t)}{\partial x^2} = -\frac{1}{\epsilon} \sum_n z_n F c_n(x, t)$$

→ Now we can proceed to briefly derive these eqns.

Electrodiffusion: New Variables

Note: We will assume circuit theory is sufficient by ignoring electromagnetic dynamics (e.g., no relevant magnetic terms or electromagnetic radiation)

Z_n - charge # (or “valence charge”) (e.g., +1, -1, +2, 0, etc...) [re $1 e = 1.602 \times 10^{-19} \text{ C}$]

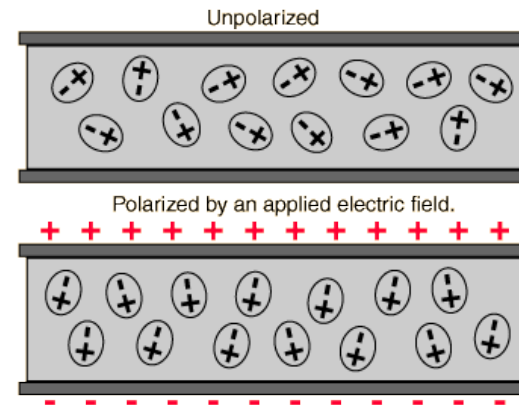
F - Faraday's constant [$9.65 \times 10^4 \text{ C/mol}$]

J_n - current density [A/cm^2]

ψ - electrical potential [V]

ϵ - permittivity [F/m]

u_n - mechanical mobility [s/kg]



<http://en.wikipedia.org/wiki/Permittivity>

from Einstein
relation

Aside: Mobility & Stokes-Einstein Relation

u_n - mechanical mobility [s/kg]

from Einstein
relation

➤ Force (f_p) required to move a sphere of radius a through a viscous medium of viscosity η with a velocity of v is

$$f_p = 6\pi a\eta v$$

Stoke's Law
(eqn.3.22)

➤ Particle mobility, u_p , is defined as the ratio of the particle velocity to the force on the particle

$$u_p \equiv \frac{v}{f_p} = \frac{1}{6\pi a\eta}$$

Similar to
(reciprocal of)
impedance

➤ Relating to the diffusion constant (Annus Mirabilis):

$$D = u_p kT = u N_A kT = uRT$$

$$D_n = u_n RT$$

1. u_n is the molar mechanical mobility of ion n . In some fields (e.g., solid-state physics), it is customary to use the *molar electrical mobility*, \hat{u}_n , where $\hat{u}_n = |z_n| F u_n$. \hat{u}_n has units of (cm/s)/(V/cm). In terms of the molar electrical mobility, the Einstein relation is $D_n = (RT\hat{u}_n)/(|z_n|F)$.

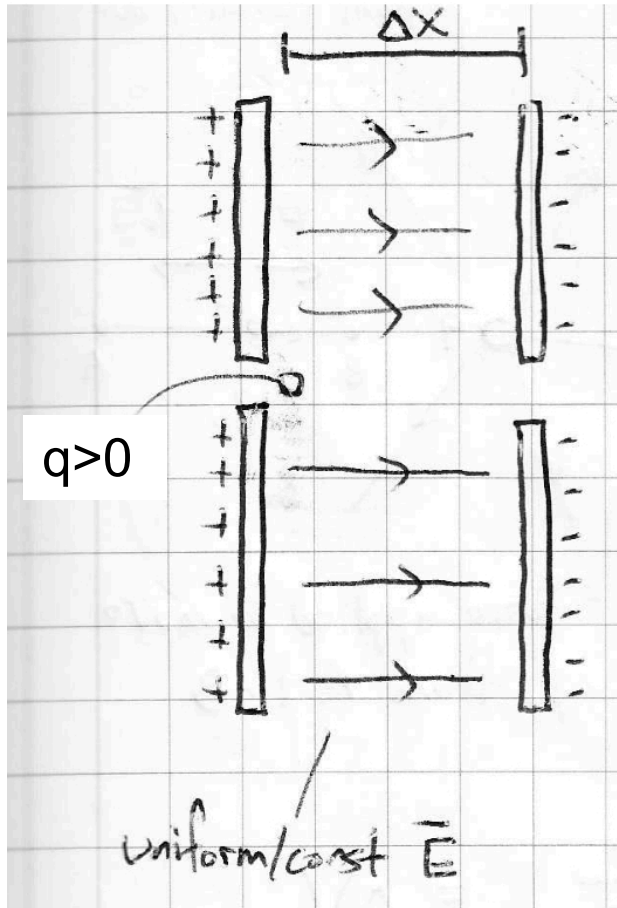
Electrodiffusion: Nernst-Planck Equation

current
density

$$J_n(x, t) = \underbrace{-z_n F D_n \frac{\partial c_n(x, t)}{\partial x}}_{\text{diffusion}} - \underbrace{u_n z_n^2 F^2 c_n(x, t) \frac{\partial \psi(x, t)}{\partial x}}_{\text{electric drift}}$$

→ Essentially a charged version of Fick's first law, but now with an additional term due to electric forces (the *drift* term on the right)

Aside: Electric Drift



→ Consider a charge q placed between two uniformly/oppositely charged plates

- uniform E field between
- force exerted on charge (Coulomb's law)

$$\mathbf{F} = q\mathbf{E}$$

- E depends upon spatial gradient of the potential

$$E = -\frac{\partial\psi}{\partial x}$$

Think in terms of energy

(e.g., where does it come from? conserved?)

$$J_n(x, t) = -z_n F D_n \frac{\partial c_n(x, t)}{\partial x} - u_n z_n^2 F^2 c_n(x, t) \frac{\partial \psi(x, t)}{\partial x}$$

Electrodiffusion: Continuity Equation

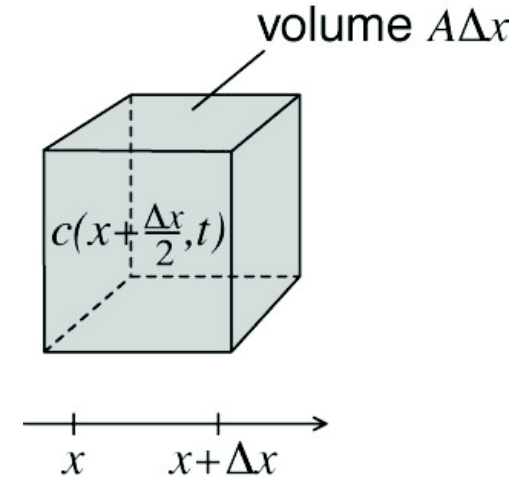
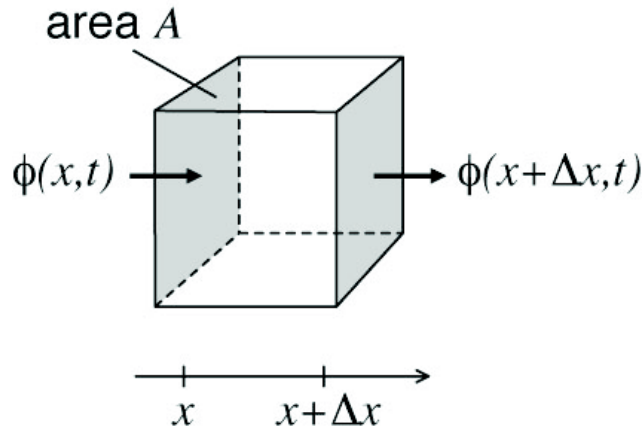
$$\frac{\partial J_n(x, t)}{\partial x} = -z_n F \frac{\partial c_n(x, t)}{\partial t}$$

spatial change in
current density

temporal change in
charge density

→ Just like our derivation for regular diffusion, this essentially tells us about the conservation of charge

Aside: Continuity Equation (REVISTED)



solute entering from left - solute exiting from right
(during time interval $[t, t + \Delta t]$)

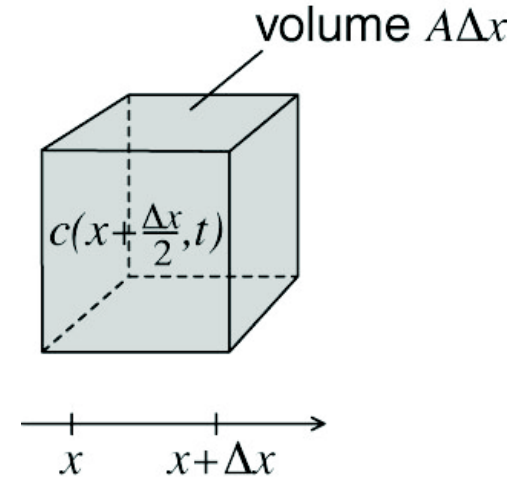
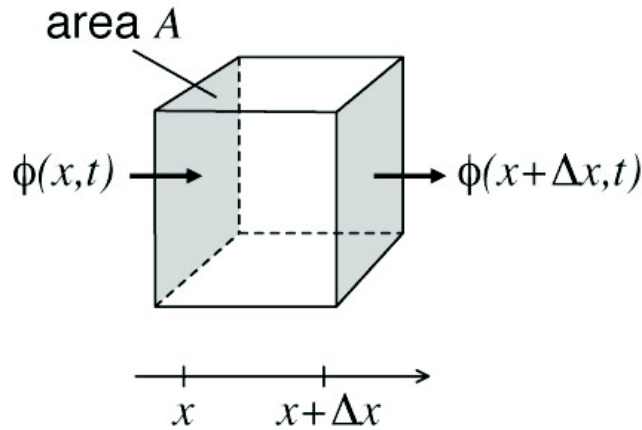
= change in amount of solute inside cube
(during time interval $[t, t + \Delta t]$)

$$A \Delta t \phi(x, t + \Delta t/2) - A \Delta t \phi(x + \Delta x, t + \Delta t/2) = A \Delta x c(x + \Delta x/2, t + \Delta t) - A \Delta x c(x + \Delta x/2, t)$$

$$\frac{\phi(x + \Delta x, t + \Delta t/2) - \phi(x, t + \Delta t/2)}{\Delta x} = \frac{c(x + \Delta x/2, t + \Delta t) - c(x + \Delta x/2, t)}{\Delta t}$$

$$\implies \frac{\partial \phi}{\partial x} = - \frac{\partial c}{\partial t}$$

Aside: Continuity Equation (REVISTED)



$$\implies \frac{\partial \phi}{\partial x} = -\frac{\partial c}{\partial t}$$

$$\frac{\partial J_n(x, t)}{\partial x} = -z_n F \frac{\partial c_n(x, t)}{\partial t}$$

Relationship between current density and flux:

$$J_n(x, t) = z_n F \phi_n(x, t)$$

Aside: Poisson's Equation

$$\frac{\partial^2 \psi(x, t)}{\partial x^2} = -\frac{1}{\epsilon} \sum_n z_n F c_n(x, t)$$

→ Stemming from Gauss' Law, relates the charge density and electric potential

charge density [C/m³]

$$\rho = \sum_n z_n F c_n(x, t)$$

Electrostatics [edit]

Main article: [Electrostatics](#)

One of the cornerstones of [electrostatics](#) is setting up and solving problems described by the Poisson equation. Solving the Poisson equation amounts to finding the [electric potential](#) ϕ for a given [charge](#) distribution ρ_f .

The mathematical details behind Poisson's equation in electrostatics are as follows (SI units are used rather than [Gaussian units](#), which are also frequently used in [electromagnetism](#)).

Starting with [Gauss's law](#) for electricity (also one of [Maxwell's equations](#)) in differential form, we have:

$$\nabla \cdot \mathbf{D} = \rho_f$$

where $\nabla \cdot$ is the [divergence operator](#), \mathbf{D} = [electric displacement field](#), and ρ_f = [free charge density](#) (describing charges brought from outside). Assuming the medium is linear, isotropic, and homogeneous (see [polarization density](#)), we have the [constitutive equation](#):

$$\mathbf{D} = \epsilon \mathbf{E}$$

where ϵ = [permittivity](#) of the medium and \mathbf{E} = [electric field](#). Substituting this into Gauss's law and assuming ϵ is spatially constant in the region of interest obtains:

$$\nabla \cdot \mathbf{E} = \frac{\rho_f}{\epsilon}$$

In the absence of a changing magnetic field, \mathbf{B} , [Faraday's law of induction](#) gives:

$$\nabla \times \mathbf{E} = -\frac{\partial \mathbf{B}}{\partial t} = 0$$

where $\nabla \times$ is the [curl operator](#) and t is time. Since the [curl](#) of the electric field is zero, it is defined by a scalar electric potential field, φ (see [Helmholtz decomposition](#)).

$$\mathbf{E} = -\nabla \varphi$$

The derivation of Poisson's equation under these circumstances is straightforward. Substituting the potential gradient for the electric field

$$\nabla \cdot \mathbf{E} = \nabla \cdot (-\nabla \varphi) = -\nabla^2 \varphi = \frac{\rho_f}{\epsilon},$$

directly obtains **Poisson's equation** for electrostatics, which is:

$$\nabla^2 \varphi = -\frac{\rho_f}{\epsilon}.$$

Solving Poisson's equation for the potential requires knowing the charge density distribution. If the charge density is zero, then [Laplace's equation](#) results. If the charge density follows a [Boltzmann distribution](#), then the [Poisson-Boltzmann equation](#) results. The Poisson-Boltzmann equation plays a role in the development of the [Debye-Hückel theory of dilute electrolyte solutions](#).

The above discussion assumes that the magnetic field is not varying in time. The same Poisson equation arises even if it does vary in time, as long as the [Coulomb gauge](#) is used. In this more general context, computing ϕ is no longer sufficient to calculate \mathbf{E} , since \mathbf{E} also depends on the [magnetic vector potential](#) \mathbf{A} , which must be independently computed. See [Maxwell's equation in potential formulation](#) for more on ϕ and \mathbf{A} in Maxwell's equations and how Poisson's equation is obtained in this case.

Electrodifusion

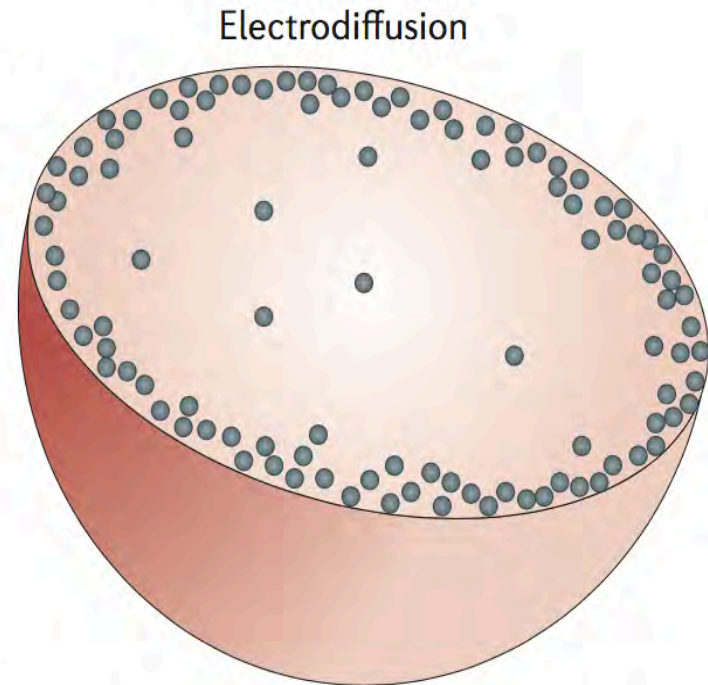
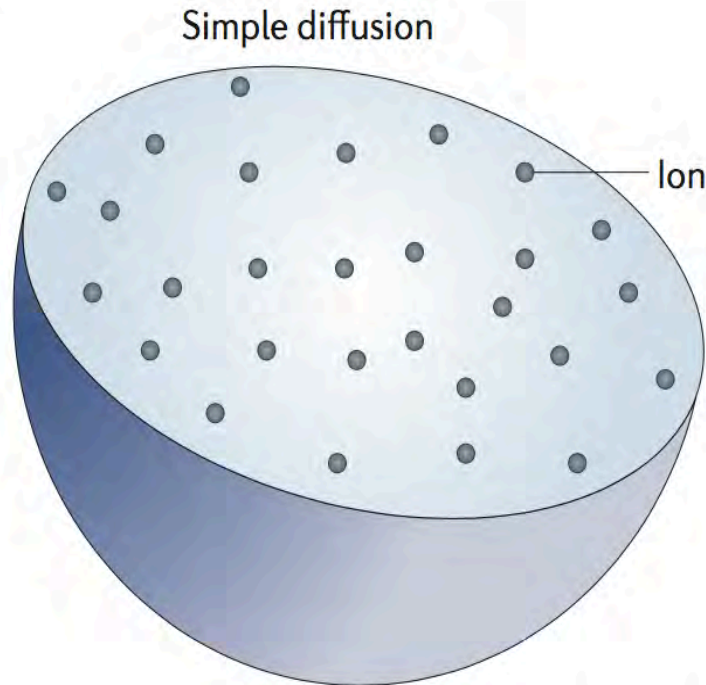
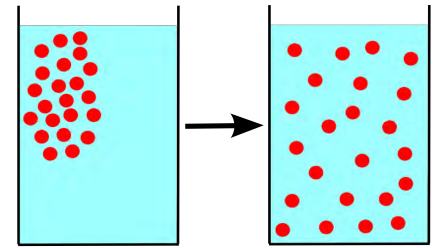


Figure 3 | **Comparison of simple diffusion and electrodiffusion theories.** Traditional diffusion theories and electrodiffusion theories make very different predictions about the distribution of ions within a three-dimensional structure such as a dendritic spine head.

Aside: Reaction-Diffusion (REVISITED)

Reaction-Diffusion equation

$$\frac{\partial \mathbf{c}}{\partial t} = \mathbf{f}(\mathbf{c}) + D\nabla^2 \mathbf{c},$$

Fick's Law & Diffusion equation

$$\phi = -D \frac{\partial c}{\partial x} \quad \frac{\partial c}{\partial t} = D \frac{\partial^2 c}{\partial x^2}$$

Electrodiffusion equation (Nernst-Planck)

$$J_n(x, t) = -z_n F D_n \frac{\partial c_n(x, t)}{\partial x} - u_n z_n^2 F^2 c_n(x, t) \frac{\partial \psi(x, t)}{\partial x}$$

$$J_n(x, t) = z_n F \phi_n(x, t)$$

- Close relationship between macroscopic descriptors, the notion of pattern formation, etc....

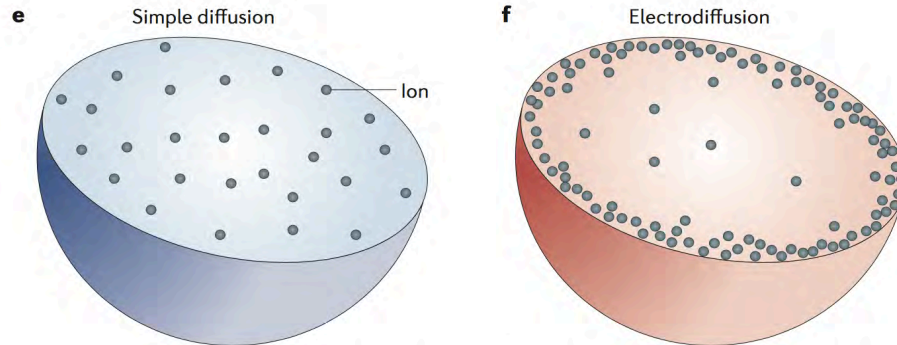
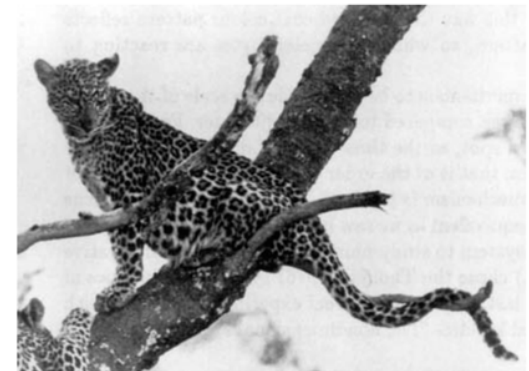
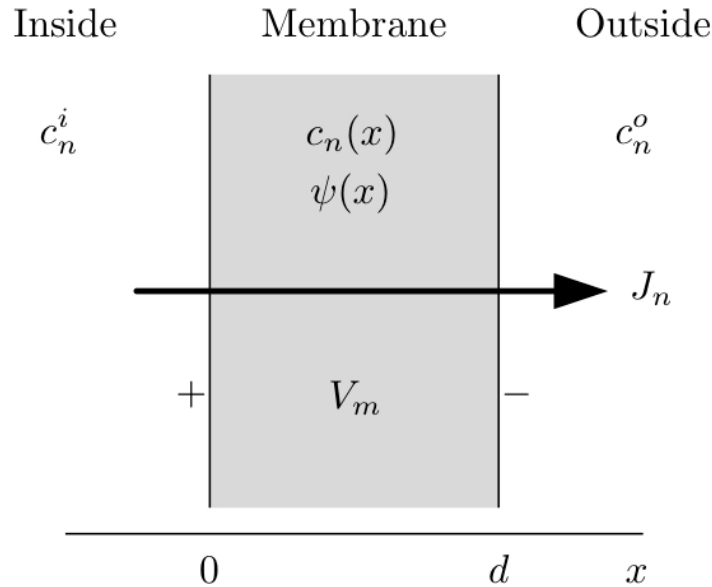


Figure 3 | Comparison of simple diffusion and electrodiffusion theories. Traditional diffusion theories and electrodiffusion theories make very different predictions about the distribution of ions within a three-dimensional structure such as a dendritic spine head. a-d | The change in the distribu-



Membrane Electrodiffusion

Steady-State Electrodiffusion through Membranes



Steady-state

$$\rightarrow \frac{\partial c_n(x, t)}{\partial t} = 0$$

$$\rightarrow \frac{\partial J_n(x, t)}{\partial x} = 0$$

$$\rightarrow J_n = \text{constant}$$

Electrolyte solutions \rightarrow Electroneutrality

$$\text{if } t \gg \tau_r \text{ and } x \gg \Lambda_D \text{ then } \sum_n z_n F c_n(x, t) = 0$$

$$\frac{\partial^2 \psi(x, t)}{\partial x^2} = -\frac{1}{\epsilon} \sum_n z_n F c_n(x, t)$$

\rightarrow Simplifies Poisson's equation such that ψ is a linear function across the membrane

Electrodiffusion phenomena in neuroscience: a neglected companion

Leonid P. Savtchenko¹, Mu Ming Poo² and Dmitri A. Rusakov¹

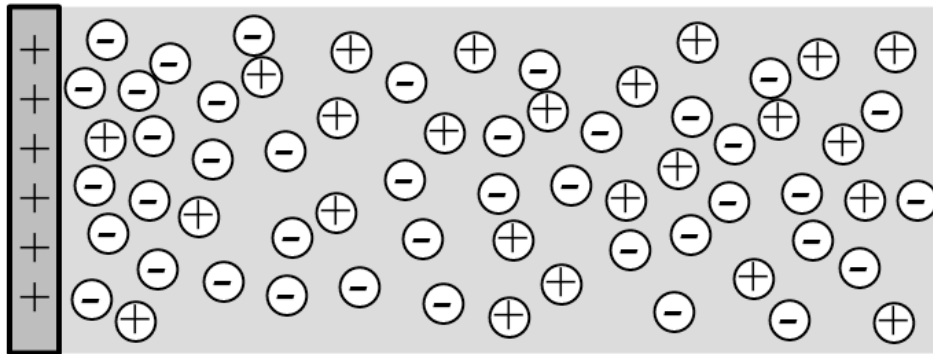
Abstract | The emerging technological revolution in genetically encoded molecular sensors and super-resolution imaging provides neuroscientists with a pass to the real-time nano-world. On this small scale, however, classical principles of electrophysiology do not always apply. This is in large part because the nanoscopic heterogeneities in ionic concentrations and the local electric fields associated with individual ions and their movement can no longer be ignored. Here, we review basic principles of molecular electrodiffusion in the cellular environment of organized brain tissue. We argue that accurate interpretation of physiological observations on the nanoscale requires a better understanding of the underlying electrodiffusion phenomena.

“We also endeavour to dispel some common misconceptions regarding the nature of the membrane potential while trying not to dwell too much on the well-established electrophysiological postulates.”

“...discuss where and how electroneutrality could be violated and what consequences this may have for our interpretation of empirical observations”

Aside: Assumptions re membrane electrodiffusion

- **Electrolytic solutions** → Fluids inside and outside cell are a stew of dissociated ionic species (e.g., K^+ , Na^+ , Ca^+ , etc...)
- **Electroneutrality** → Total charge per unit volume is zero



Clearly this is only going to be valid on a suitable set of scales...

→ Validity of these assumptions depends upon both a temporal scale (*charge relaxation time*) and spatial scale (*Debye length*)

Aside: Assumptions re membrane electrodiffusion

Electrolyte solutions → Electroneutrality

$$\text{if } t \gg \tau_r \text{ and } x \gg \Lambda_D \text{ then } \sum_n z_n F c_n(x, t) = 0$$

- Charge Relaxation Time τ_r

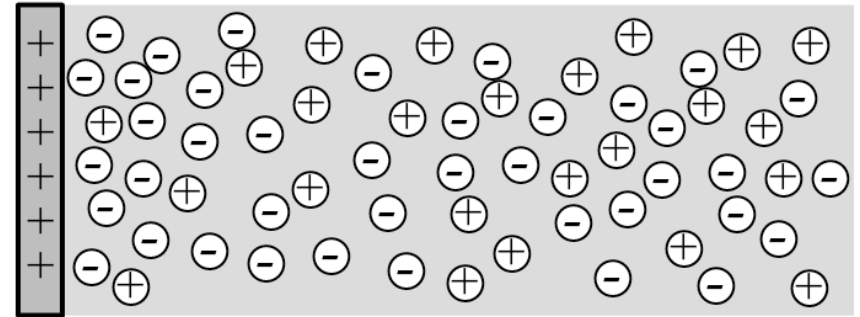
Measures temporal change in charge density

(i.e., relaxation time of charge distribution; also called the *Debye time*)

- Debye Length Λ_D

Measures spatial extent of electric potential

(i.e., distance over which electroneutrality is violated)



Aside: Debye length

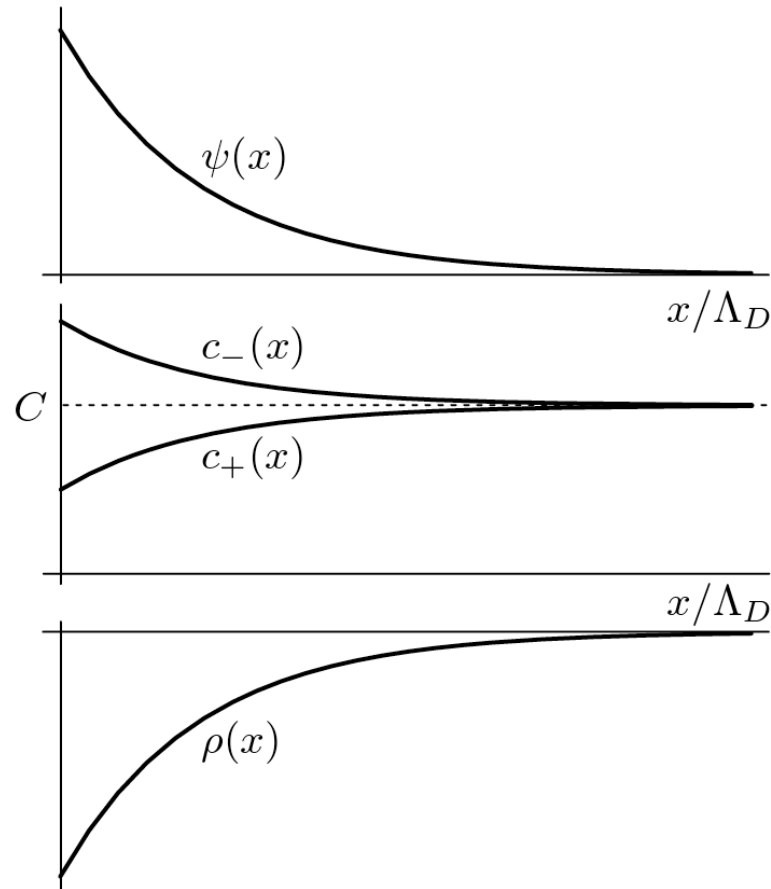
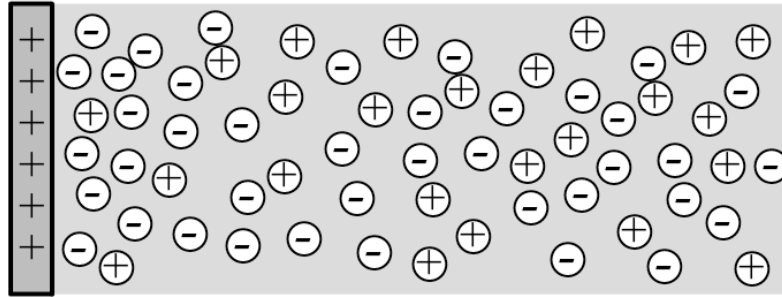


Figure 7.7 The spatial distribution of charge near a plate containing positive fixed charges. The counterions are anions and are in higher concentration near the plate than far from the plate. The cations are at a lower concentration near the plate than far from the plate. The spatial distributions of both mobile ions are exponential, with space constant equal to the Debye length.

Aside: Assumptions re membrane electrodiffusion

Electrolyte solutions → Electroneutrality

$$\text{if } t \gg \tau_r \text{ and } x \gg \Lambda_D \text{ then } \sum_n z_n F c_n(x, t) = 0$$

- Charge Relaxation Time τ_r

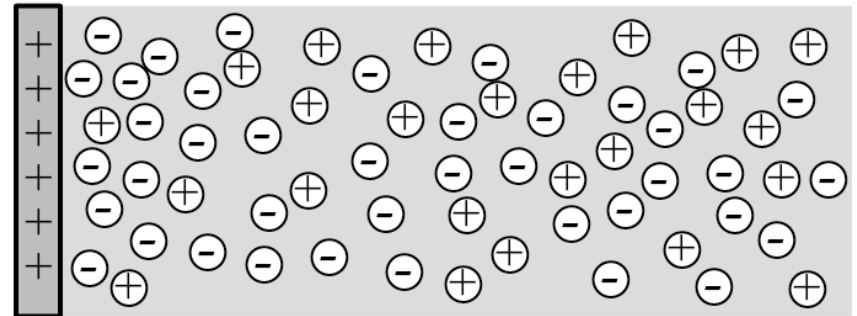
Measures temporal change in charge density

(i.e., relaxation time of charge distribution)

- Debye Length Λ_D

Measures spatial extent of electric potential

(i.e., distance over which electroneutrality is violated)



→ Both are very small (1 ns and 1 nm respectively; see Weiss v.1 7.2.3), justifying that ionic solutions obey electroneutrality

(further) Aside: Deviations from the ideal model....

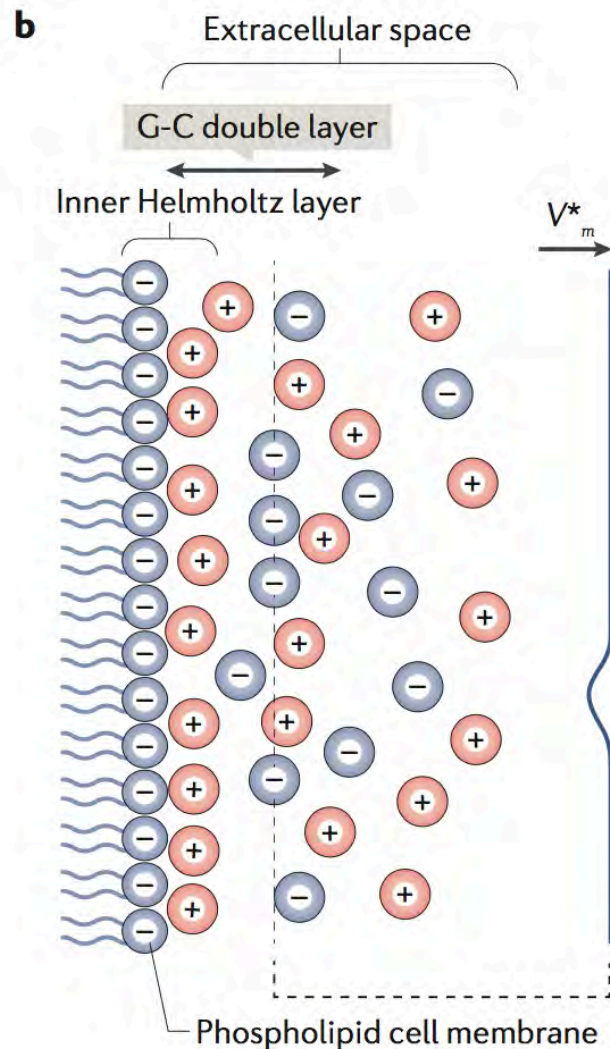
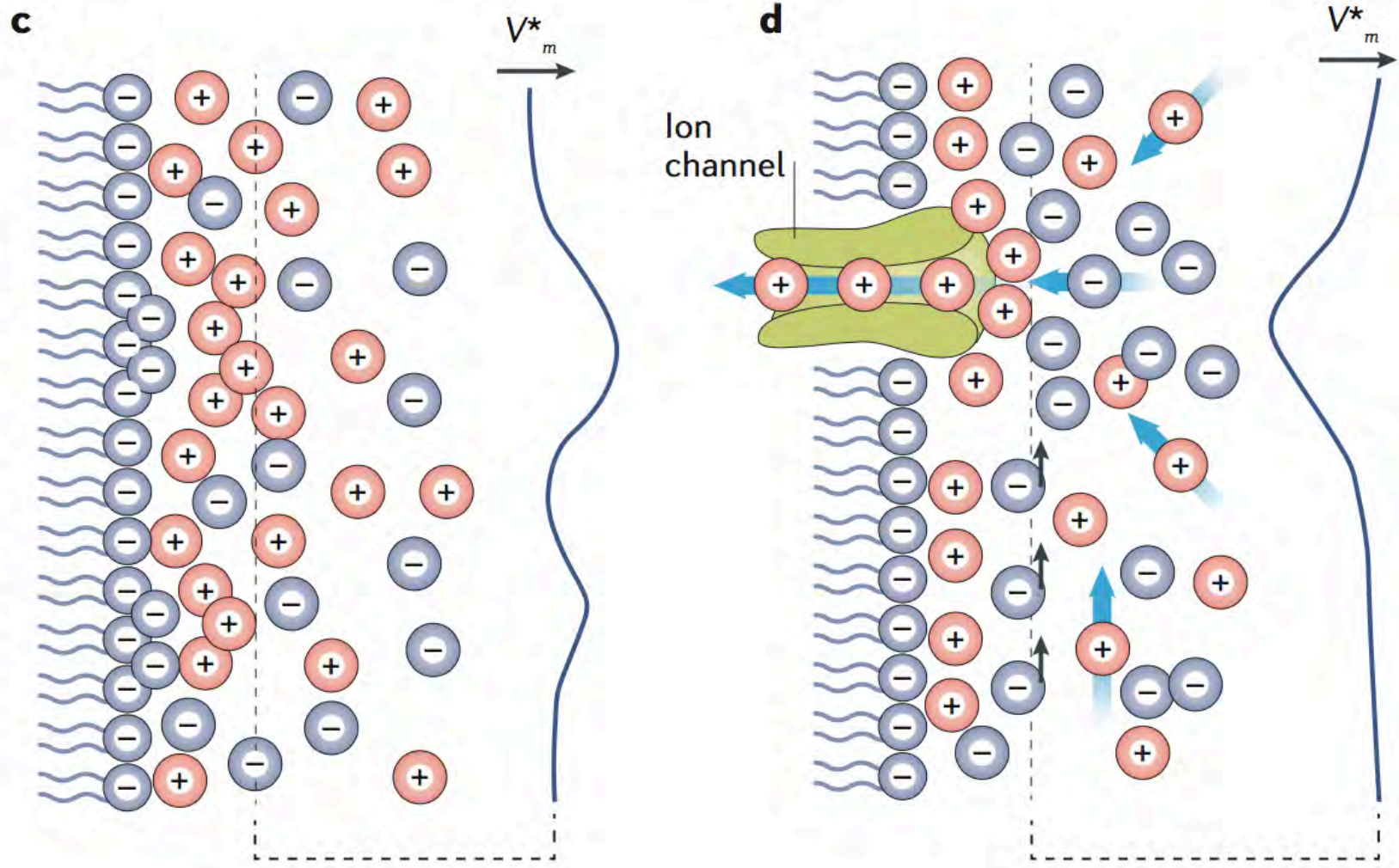


Figure 1 | **Electric charges and their fields in brain tissue: basic principles and two common deviations from common electrophysiological postulates.** **a** | The schematic depicts electrostatic electric fields generated by a local (point) charge and a charged plane, in either a vacuum (dielectric medium, top) or an electrolyte (bottom). The colour intensity illustrates the field strength. Whereas the field (depicted by arrows) in a vacuum extends into infinity, fields in electrolytes are highly localized. **b** | The panel shows ion distributions and the local voltage profile near a negatively charged phospholipid cell membrane surface; the inner Helmholtz layer (a layer of cations lined up next to the negatively charged membrane) and Gouy–Chapman double layer (G-C; includes the Helmholtz layer and a loose layer of anions adjacent to it) are indicated. V_m^* depicts the voltage profile (arrow indicates voltage scale) at a short distance from the membrane (dotted line, not to scale) from which signalling proteins such as ion channels may sense local electric fields (see below). The V_m^* profile shows a canonical case of a nearly evenly charged membrane. **c** | The schematic depicts heterogeneity in sub-membrane ion distribution and local voltage owing to excessive membrane charges (carried by either phospholipids or membrane proteins). The uneven occurrence of cations (red) and anions (blue) reflects the variable density of local electric fields and hence the heightened variability of the sub-membrane voltage V_m^* compared with that in part **b**. **d** | This panel depicts heterogeneity in sub-membrane ion distribution and local voltage owing to ion channel currents. Blue arrows depict the current direction (an ion channel is shown in green). Black arrows depict drag forces exerted by the cation current flow; these forces tend to drag particles alongside the sub-membrane ion layers.

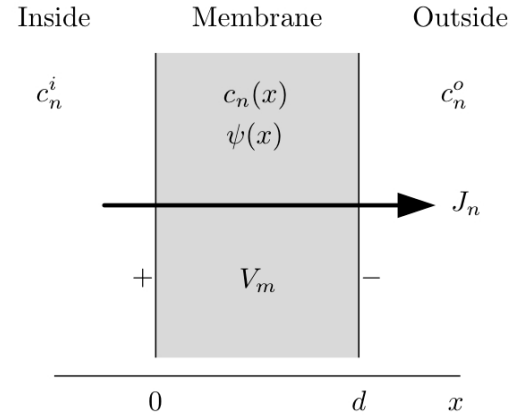
Savtchenko et al

(further) Aside: Deviations from the ideal model....



Membrane Electrodifusion

Steady-State Electrodiffusion through Membranes



Steady-state

$$\begin{aligned} \rightarrow \frac{\partial c_n(x, t)}{\partial t} &= 0 \\ \rightarrow \frac{\partial J_n(x, t)}{\partial x} &= 0 \\ \rightarrow J_n &= \text{constant} \end{aligned}$$

Rearrange Nernst-Planck Equation

$$J_n = -z_n F D_n \frac{dc_n(x)}{dx} - u_n z_n^2 F^2 c_n(x) \frac{d\psi(x)}{dx} = -u_n z_n^2 F^2 c_n(x) \left[\frac{D_n}{u_n z_n F c_n(x)} \frac{dc_n(x)}{dx} + \frac{d\psi(x)}{dx} \right]$$

Integrate across membrane

$$J_n \underbrace{\int_0^d \frac{dx}{u_n z_n^2 F^2 c_n(x)}}_{\frac{1}{G_n}} = - \int_0^d \frac{d}{dx} \left[\frac{RT}{z_n F} \ln c_n(x) + \psi(x) \right] dx$$

Rearrange/Rename

$$J_n \frac{1}{G_n} = - \overbrace{\frac{RT}{z_n F} \ln \frac{c_n(d)}{c_n(0)}}^{V_n} + \overbrace{\psi(0) - \psi(d)}^{V_m}$$

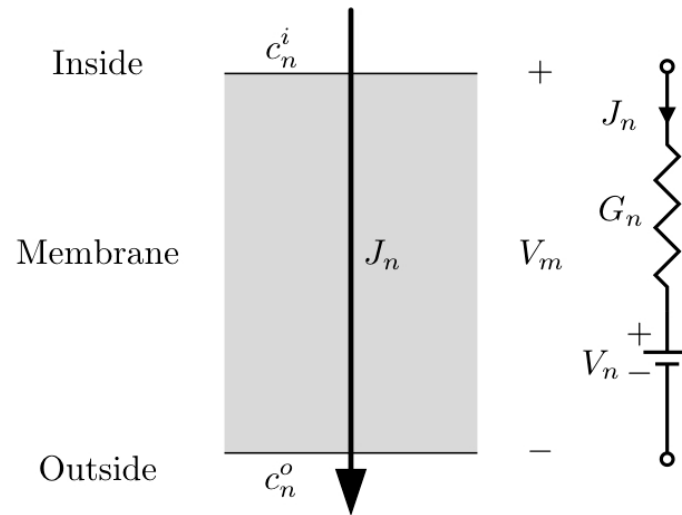


$$J_n = G_n (V_m - V_n)$$

Basically Ohm's law!

Key Idea: Membrane modeled as an electric circuit

Model of Steady-State Electrodiffusion through Membranes



$$\text{Nernst Equilibrium Potential } V_n = \frac{RT}{z_n F} \ln \frac{c_n^o}{c_n^i}$$

$$\text{Electrical Conductivity } G_n = \frac{1}{\int_0^d \frac{dx}{u_n z_n^2 F^2 c_n(x)}} \geq 0$$

Membrane Electrodiffusion: Different charged solutes as parallel paths

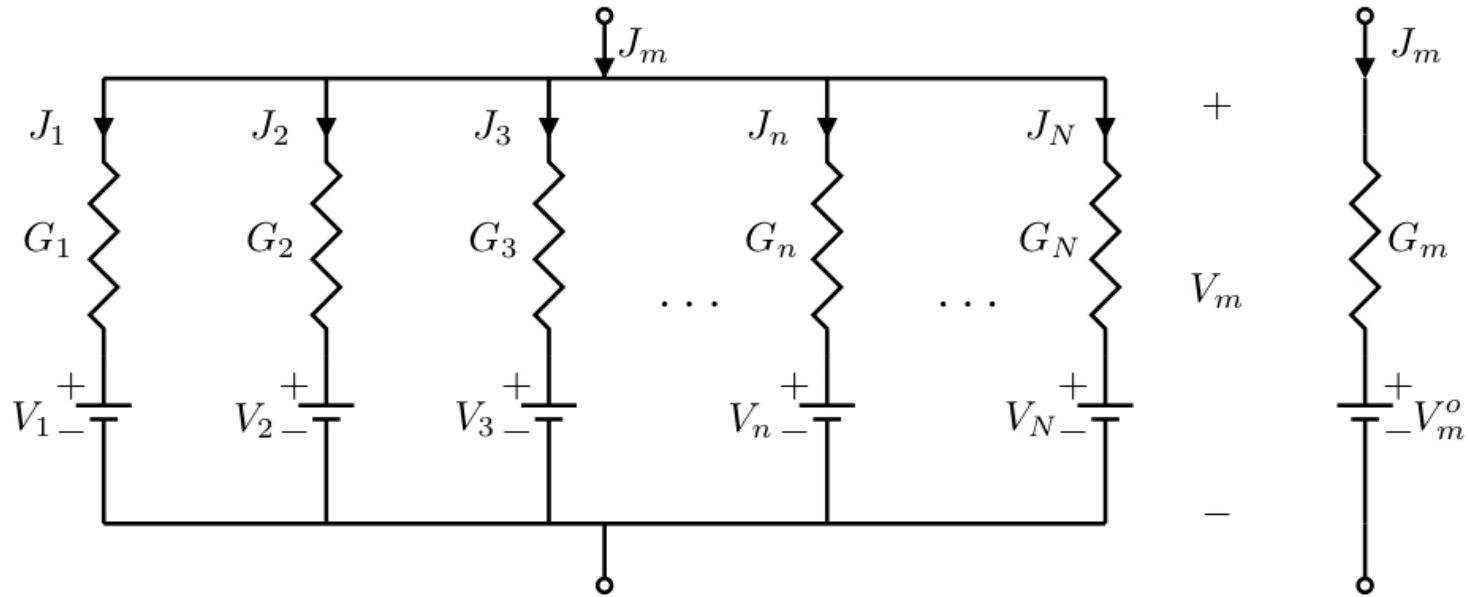
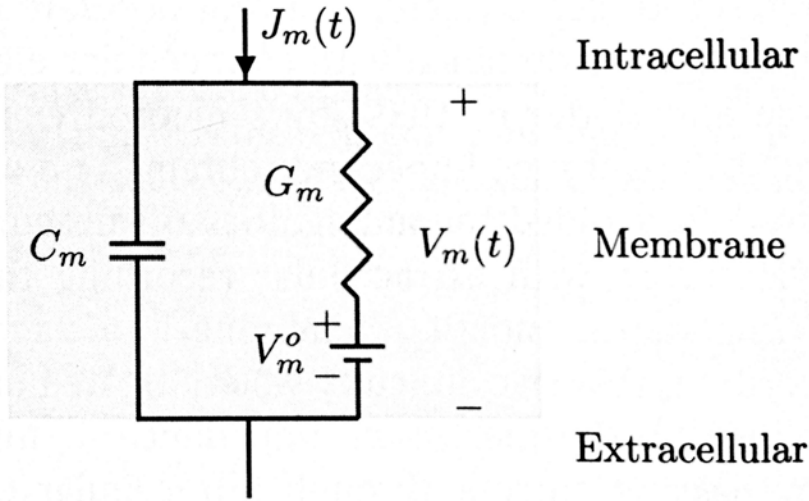
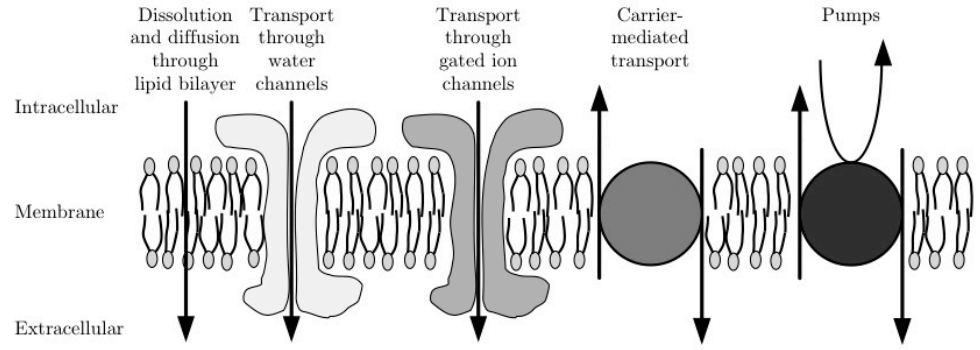


Figure 7.24

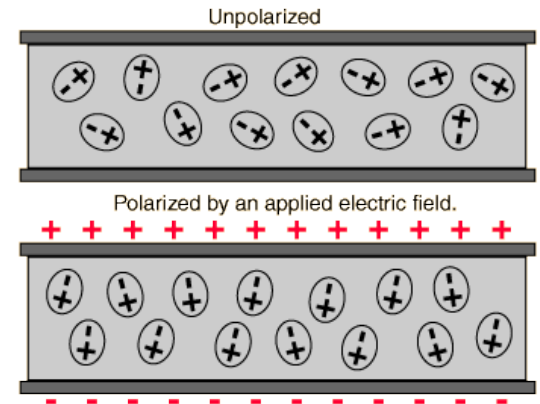
Equivalent

Key Idea: Lipid bilayer acts as a capacitor

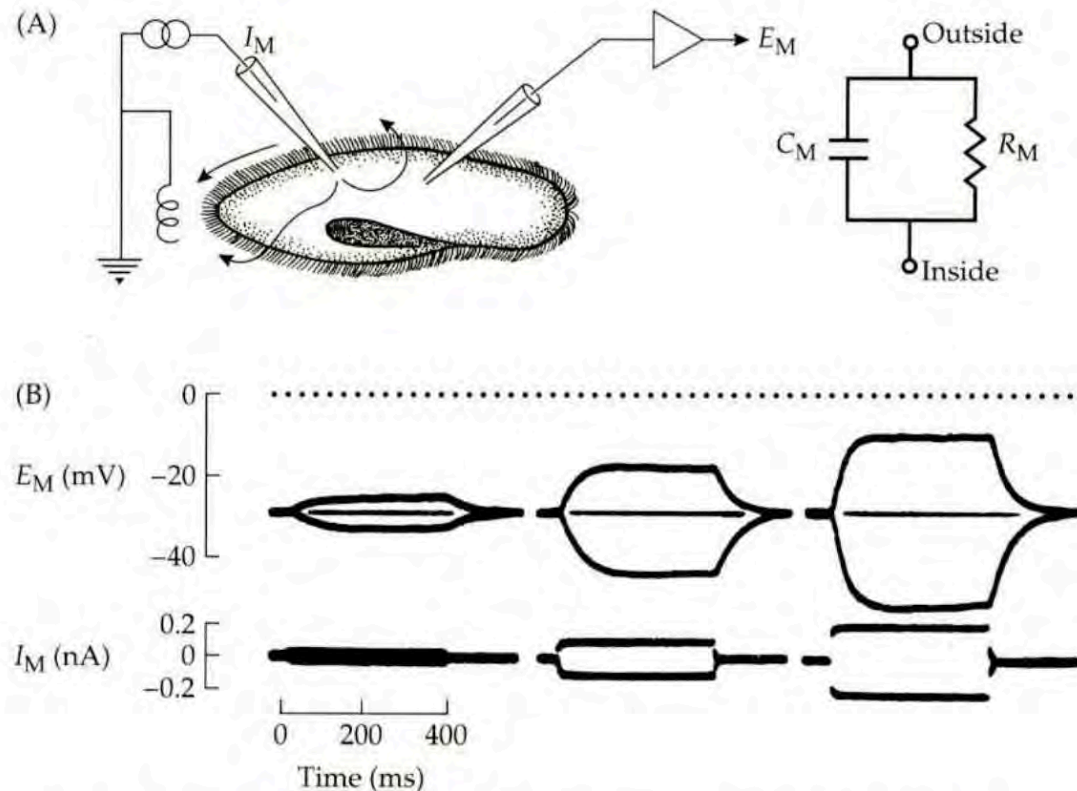
Cell membrane separates charge
(and thereby can act like a pair of parallel plates)



Has dielectric properties as well...



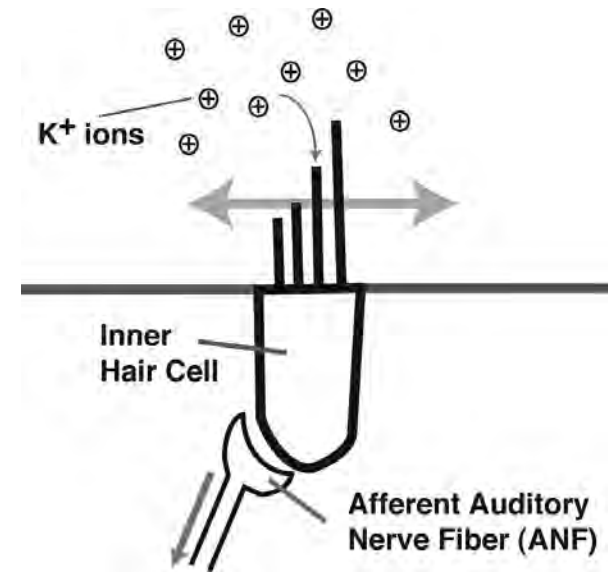
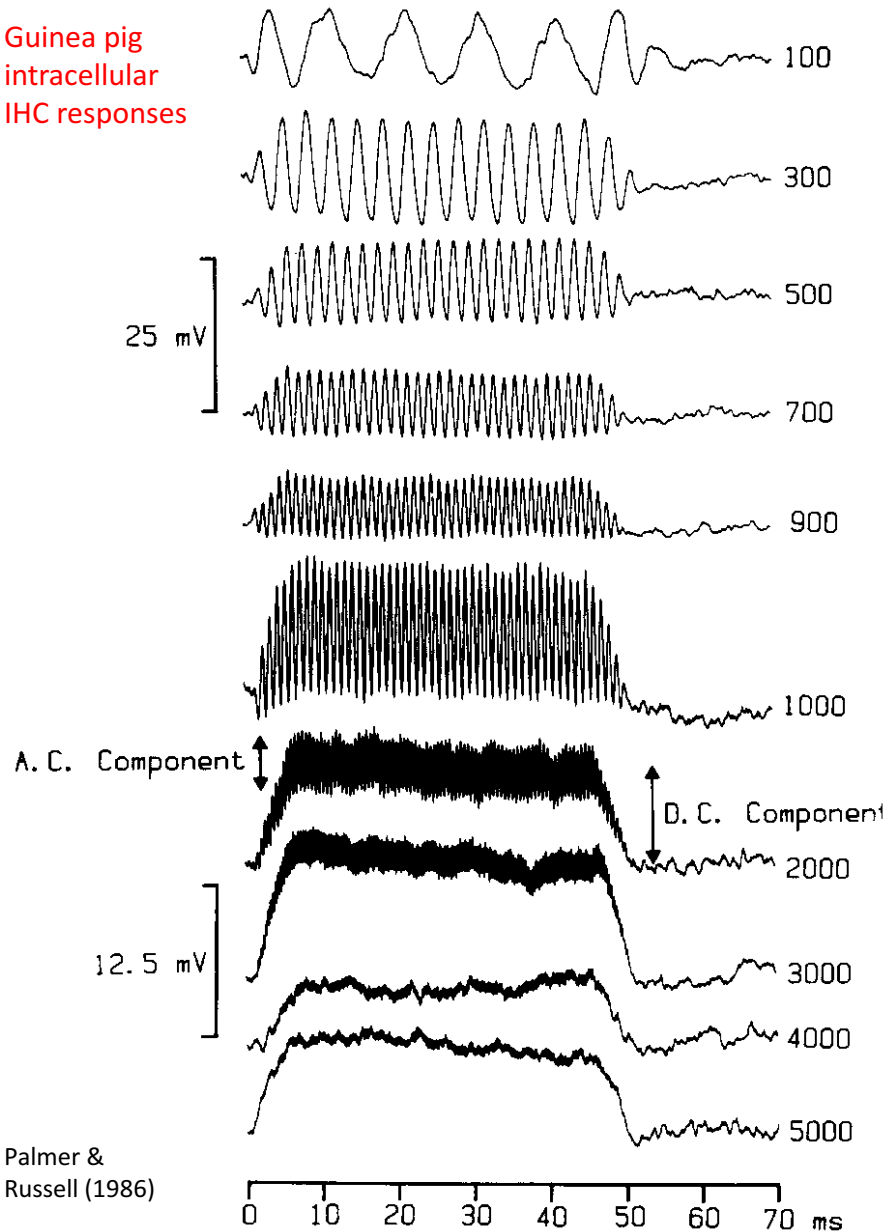
Aside: Empirical basis for membrane as an RC circuit



1.3 The Cell Membrane as an RC Circuit An experiment to study membrane electrical properties of *Paramecium*. The cell is impaled with two intracellular electrodes. One of them passes steps of current I_M across the membrane to an electrode in the bath; the other records the changes of membrane potential E_M with an amplifier (symbolized as a triangle). On the right, a current of 0.23 nA makes a voltage deflection of 23 mV, corresponding from Ohm's law to a membrane resistance of 100 M Ω ($10^8 \Omega$). The exponential time constant τ_M of the rise and fall of the voltage response is approximately 60 ms. The responses of this *Paramecium* to current steps are simpler than for wild-type *Paramecium* because it contains a genetic mutation of the normal excitability mechanism. [After Kung and Eckert 1972.]

Aside: Auditory hair cells

Guinea pig
intracellular
IHC responses



Transduction is nonlinear

➤ Hair cells act as low-pass filters
(due to membrane capacitance)

Hair cells (graded potentials) act as
front end to auditory neurons (action
potentials)

Aside: Two basic flavors of membrane currents

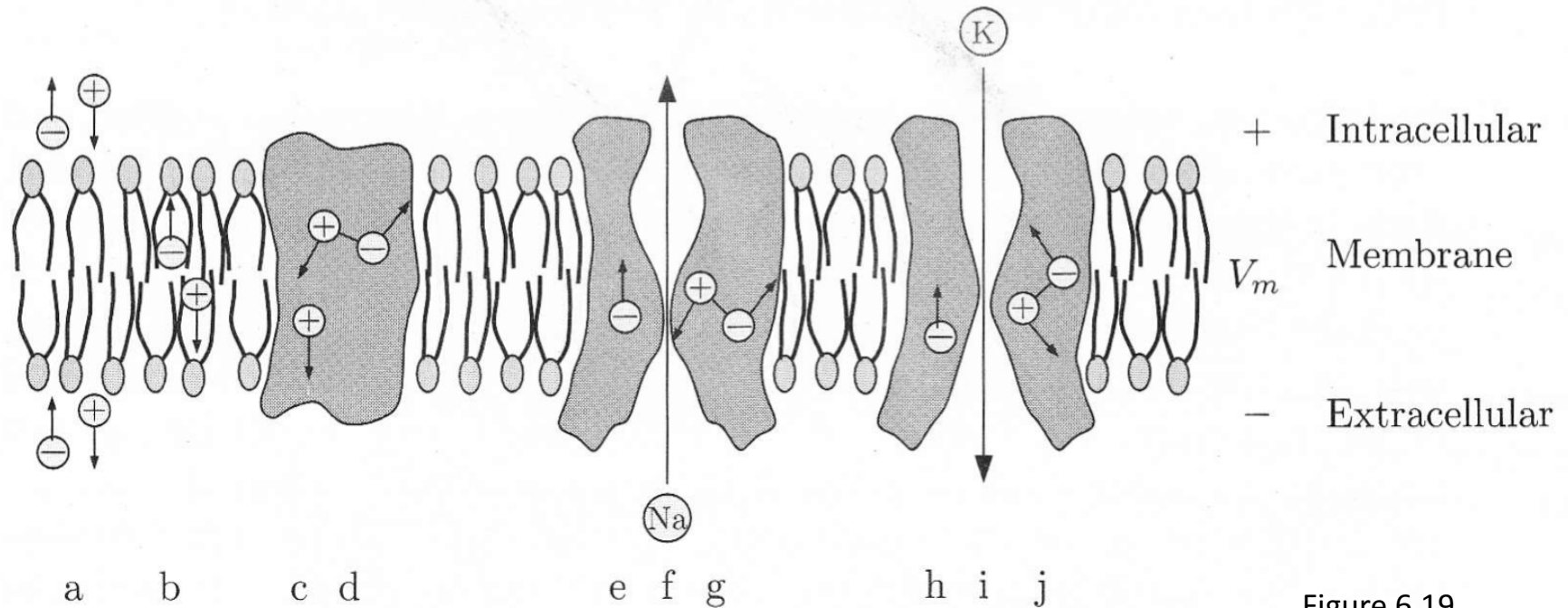


Figure 6.19

- **f, i – Ionic currents** (due to charge “flow” across membrane)
- **a-e, g, h, j – Capacitive currents** (due to charge “displacement” or redistribution along/inside membrane)

Aside: Gating currents

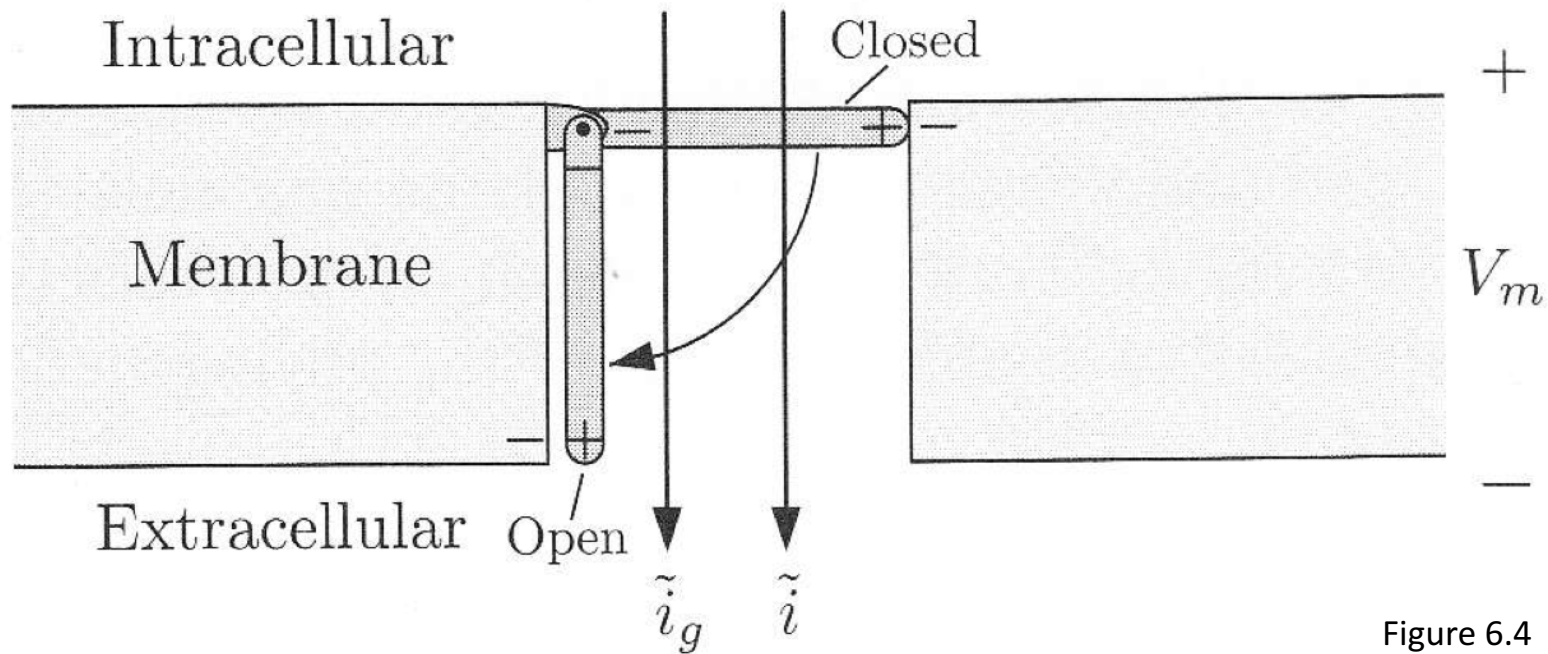
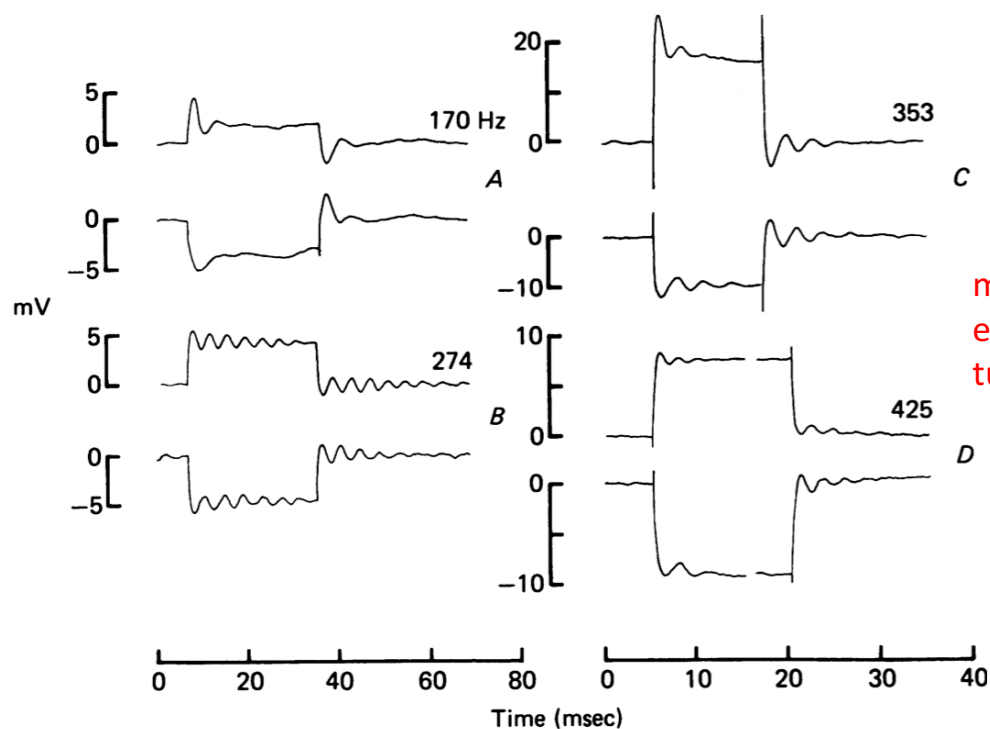
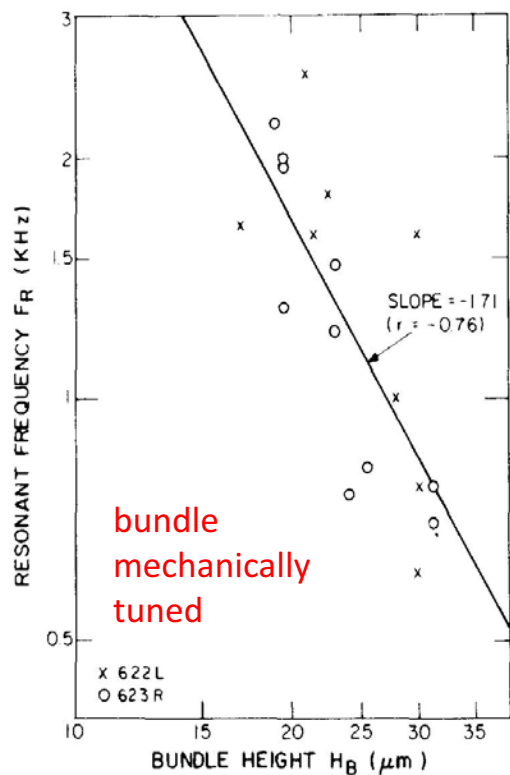


Figure 6.4

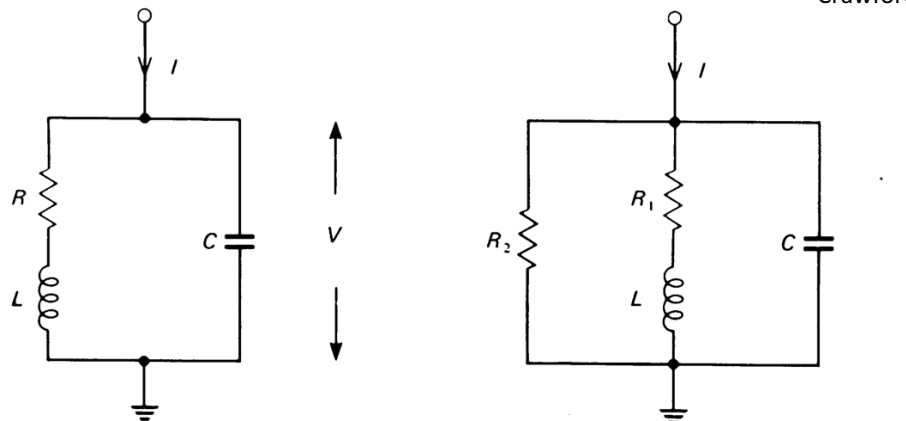
- Component (i_g) of the capacitive current
- Due to channel (molecule with non-uniform charge distribution) moving open/closed

Aside: Auditory hair cells exhibit mechanical & electrical resonances



Crawford & Fettiplace (1981)

Frishkopf & DeRosier (1983)



Aside: Auditory hair cells can behave like RLC circuits

- Voltage-gated channels (e.g., calcium-activated “BK” potassium channels) have intrinsic dynamics that can give rise to electric tuning

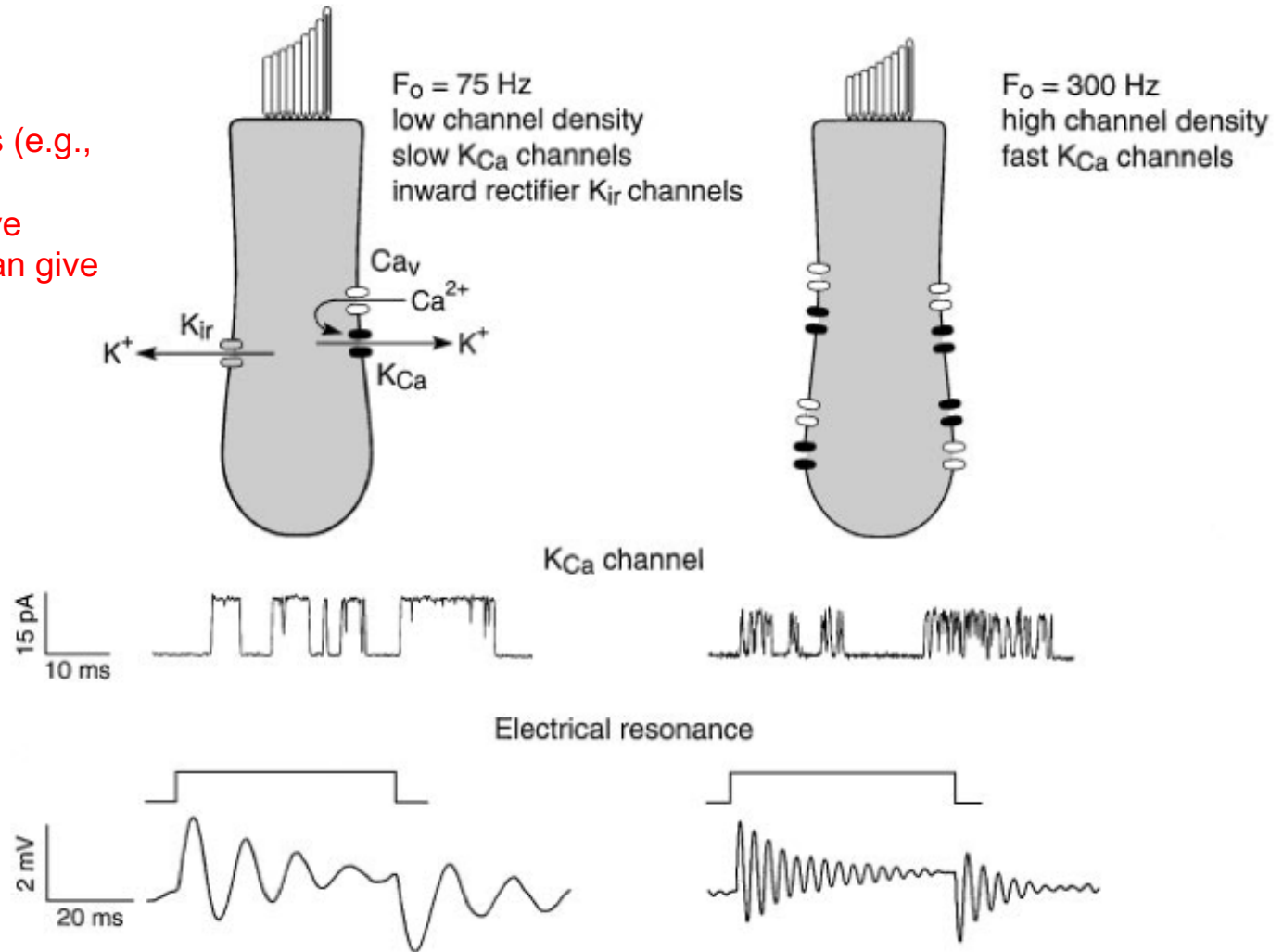


Figure 1 Schematic drawing of two hair cells from the turtle basilar papilla, with resonant frequencies (F_0) of 75 and 300 Hz. The low-frequency cell has a longer hair bundle, and a low density of Ca^{2+} and Ca^{2+} -activated K^+ (K_{Ca}) channel complexes. The number of channel complexes increases with (F_0). Beneath each cell are shown representative K_{Ca} (BK) single-channel records and ringing voltage responses to extrinsic current steps for cells tuned approximately to these two frequencies. The timing of the extrinsic current is shown above the voltage records. The single-channel records and the voltage ringing were from different sets of experiments (22, 23).

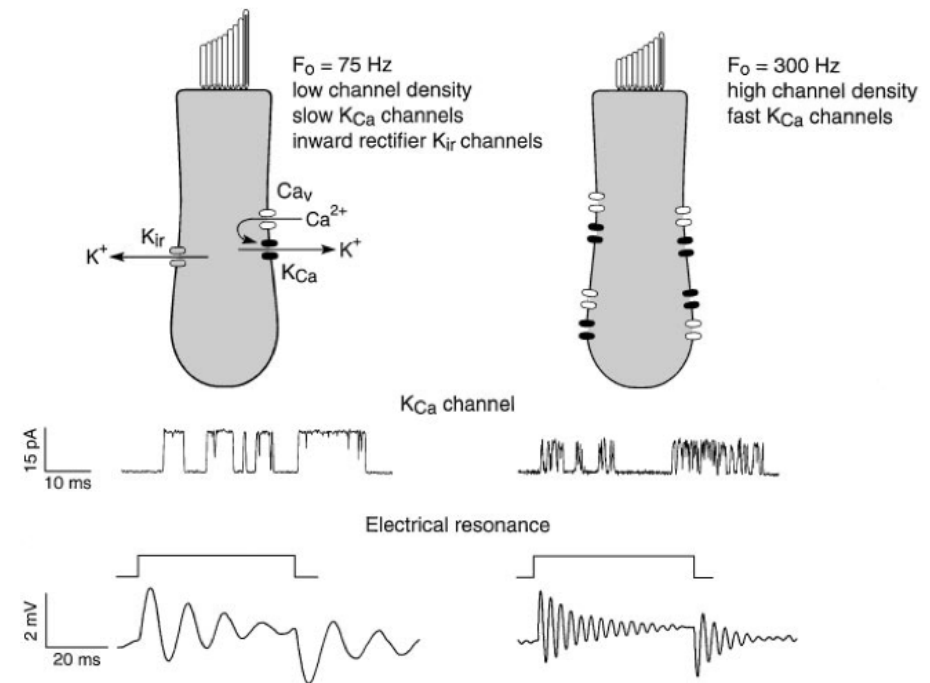
Aside: Auditory hair cells can behave like RLC circuits

1. Mechanical motion deflects bundle, causing a transduction current to depolarize the cell

2. “Depolarization opens voltage-gated Ca^{2+} channels, promoting a rise in internal Ca^{2+} that activates BK channels”

3. “The large outward K^+ current hyperpolarizes the membrane, closing the Ca^{2+} channels, which leads to the first cycle of the oscillation”

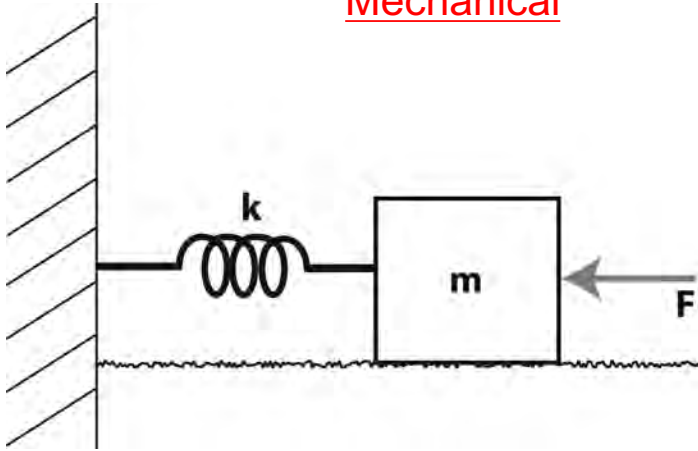
4. “As the cell hyperpolarizes and intracellular Ca^{2+} transients dissipate, the BK channels partially close, but due to the continued extrinsic current, the membrane swings positive to initiate another cycle of Ca^{2+} influx.”



“Since the BK channels are already partly activated, a smaller fraction of K^+ current is recruited on the second cycle, which will have a smaller amplitude than the first. Because the K^+ equilibrium potential (-80 mV) is negative to the resting potential (-50 mV), the BK channels behave as part of a negative feedback loop, but the time course of their activation delays the feedback and hence generates damped oscillatory responses. Such negative feedback also produces sharp tuning for sinusoidal stimuli, and the frequency at which the cell is maximally sensitive, the resonant frequency, should be influenced by the size and speed of the feedback.”

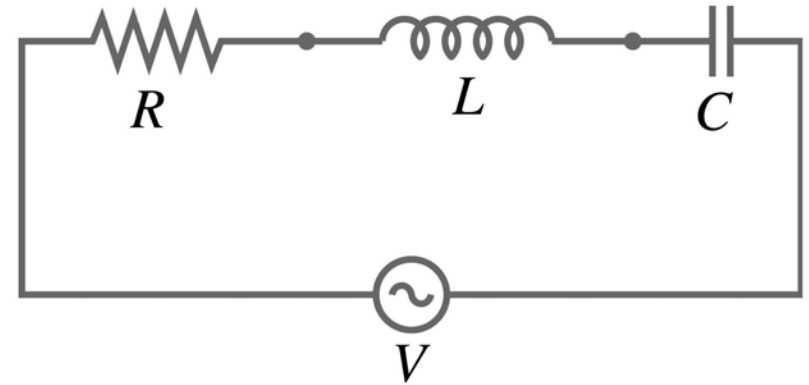
Aside: RLC circuit = damped harmonic oscillator

Mechanical



$$m\ddot{x} + b\dot{x} + kx = F_0 e^{i\omega t}$$

Electrical



$$L\ddot{q} + R\dot{q} + \frac{q}{C} = V_0 e^{i\omega t}$$

Aside: RLC connection back to harmonic oscillator

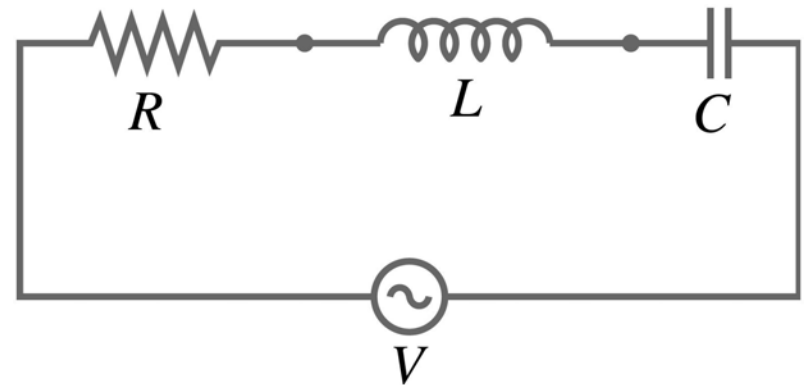
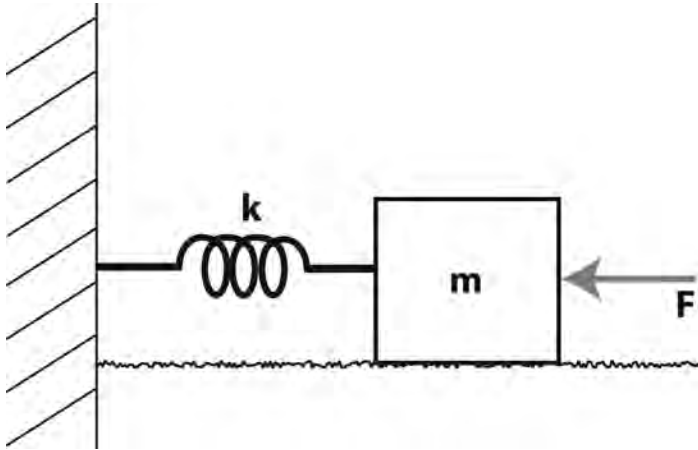
Mechanical

F (force) \leftrightarrow
 v (velocity) \leftrightarrow
 x (position) \leftrightarrow
 m (mass) \leftrightarrow
 b (damping) \leftrightarrow
 k (spring) \leftrightarrow

Electrical

V (potential)
 I (current)
 q (charge)
 L (inductance)
 R (resistance)
 $1/C$ (capacitance)

state
variables



Aside: Complex version of Ohm's Law

'Simple' Version

$$V = IR$$

$$V, I \in \mathbb{R}$$

'Complete' Version

$$\mathbf{V} = \mathbf{I}\mathbf{Z}$$

$$\mathbf{V}, \mathbf{I} \in \mathbb{C}$$

→ Note that DC (direct current) can be considered a special case of AC (alternating current). The 'complete' version of Ohm's Law thus allows for more dynamical behavior to be accounted for in an efficient fashion when using Fourier or Laplace transforms (and reduces to the 'simple' case for uni-directional currents).

Aside: Impedance (mechanical & electrical)

Mechanical
Impedance

$$Z \equiv b + i \left[m\omega - \frac{k}{\omega} \right]$$

Electrical
Impedance

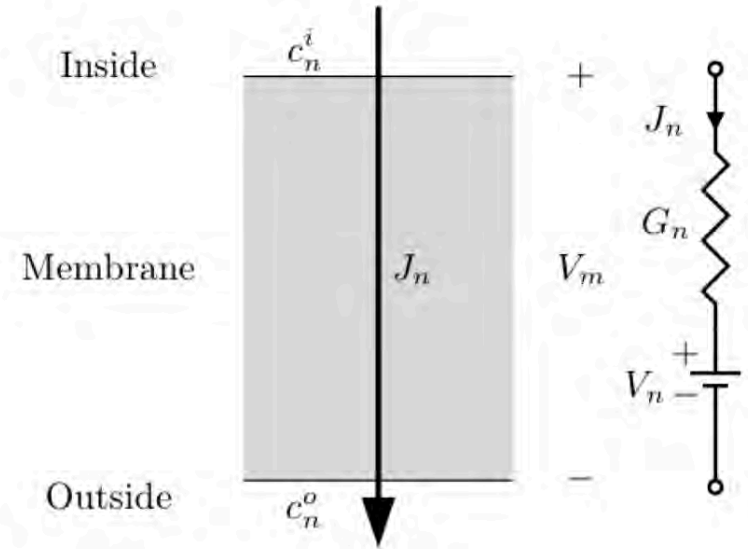
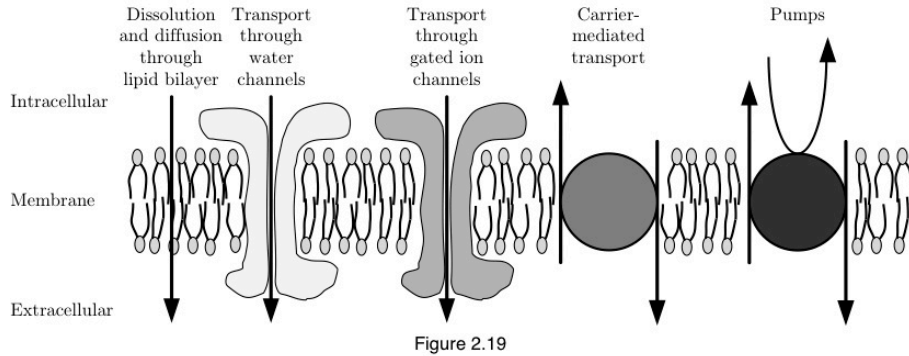
$$Z \equiv R + i \left[\omega L - \frac{1}{\omega C} \right]$$

→ Admittance (Y) = (Impedance)⁻¹

→ Conductance (G) = (Resistance)⁻¹

Key Idea: Membrane permeability as a (variable) conductance

$$\text{Electrical Conductivity } G_n = \frac{1}{\int_0^d \frac{dx}{u_n z_n^2 F^2 c_n(x)}} \geq 0$$



$$\phi_n(t) = P_n (c_n^i(t) - c_n^o(t)) ; P_n = \frac{D_n k_n}{d}$$

Fick's law for membranes

P_n = permeability of membrane to solute n

→ Electrodifusion drives movement of various ionic species across cell membrane, but *permeability* and *conductance* are two sides of the same coin...

Key Idea: Nernst potential

Steady-State Electrodiffusion through Membranes

$$J_n \frac{1}{G_n} = - \overbrace{\frac{RT}{z_n F} \ln \frac{c_n(d)}{c_n(0)}}^{V_n} + \overbrace{\psi(0) - \psi(d)}^{V_m}$$



Steady-state

$$\begin{aligned} \rightarrow \frac{\partial c_n(x, t)}{\partial t} &= 0 \\ \rightarrow \frac{\partial J_n(x, t)}{\partial x} &= 0 \\ \rightarrow J_n &= \text{constant} \end{aligned}$$

$$J_n = G_n (V_m - V_n)$$

Nernst Equilibrium Potential

$$V_n = \frac{RT}{z_n F} \ln \frac{c_n(d)}{c_n(0)} = \frac{RT}{z_n F} \ln \frac{c_n^o}{c_n^i}$$

$$G_n = \frac{1}{\int_0^d \frac{dx}{u_n z_n^2 F^2 c_n(x)}} \geq 0$$

Aside: How is the Nernst potential generated?

Assumption: Single permeable ionic species (positively charged)

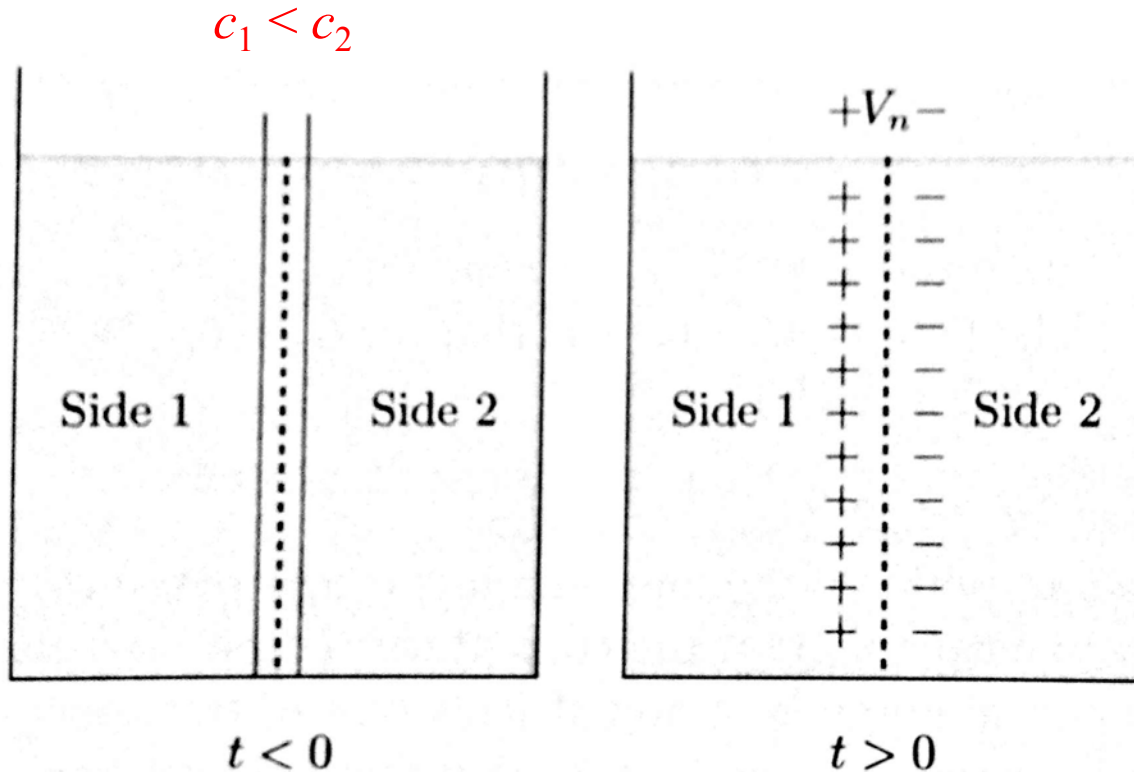


Figure 7.16 Illustration of the generation of the Nernst equilibrium potential. A bath is separated into two compartments by a membrane permeable only to ion n .

→ Note that the creation of a significant V_n need not require significant concentration changes

Key Idea (REVISITED): Statistical mechanics bridges “micro” & “macro”

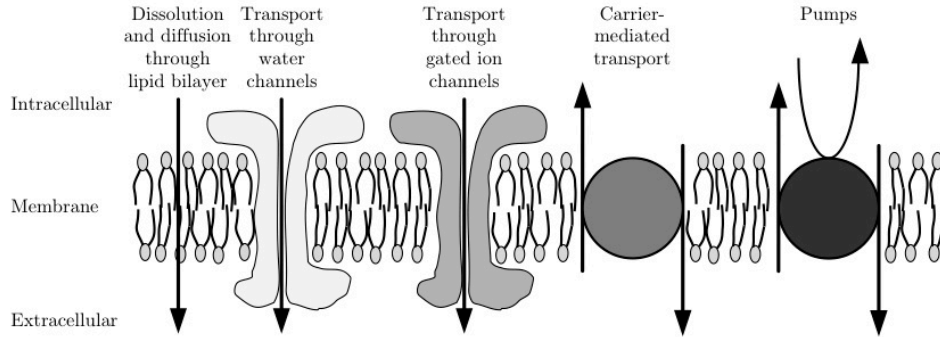


Figure 2.19

Model of Steady-State Electrodiffusion through Membranes

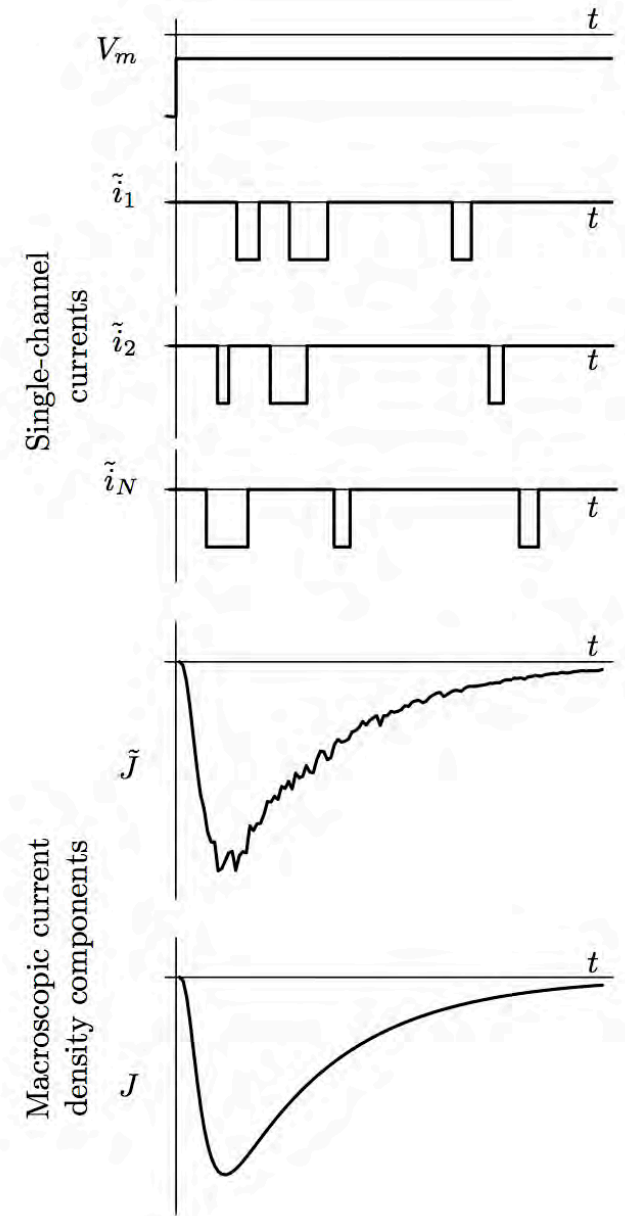
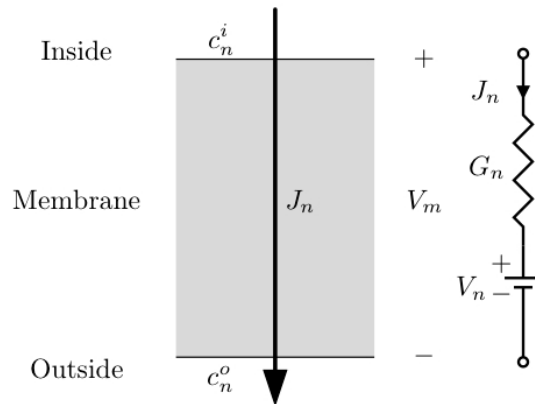


Figure 6.50 (mod)

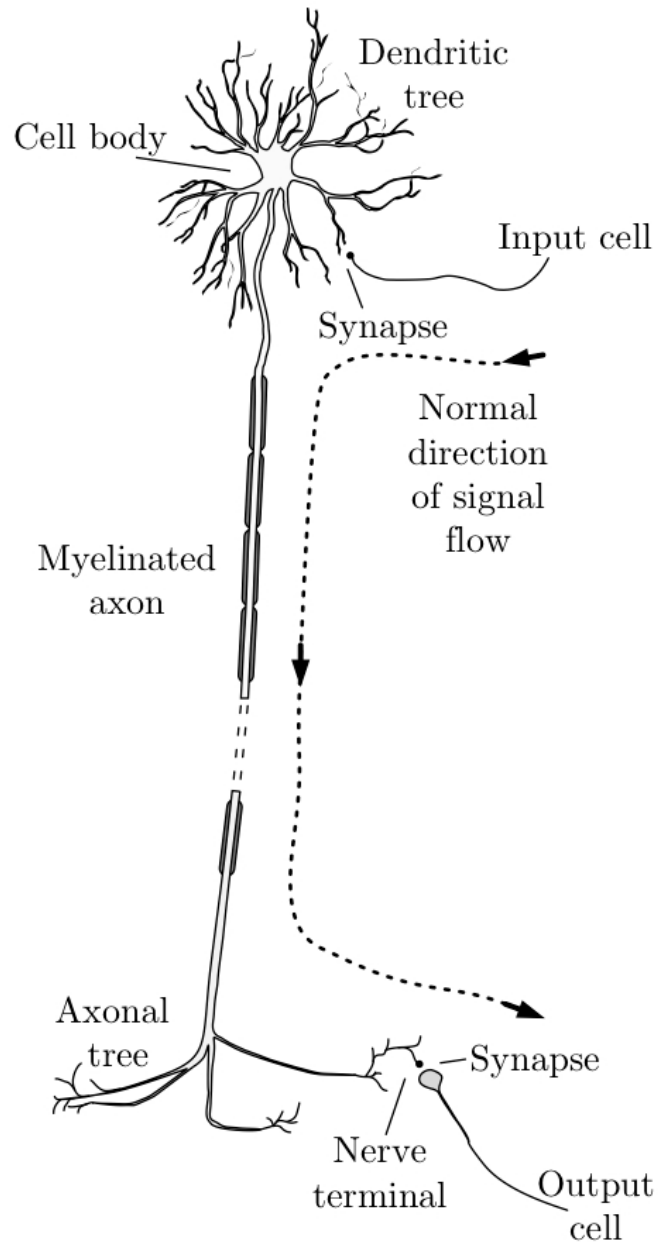
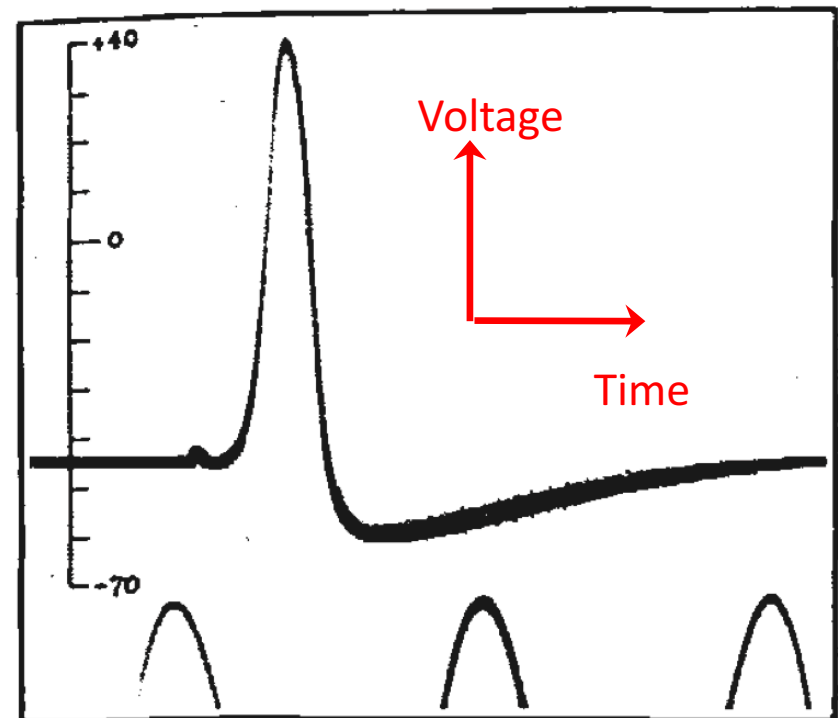
Recall

Figure 1.22

Key Point: Electrical properties of cells are important



Aside: Graded vs action potentials

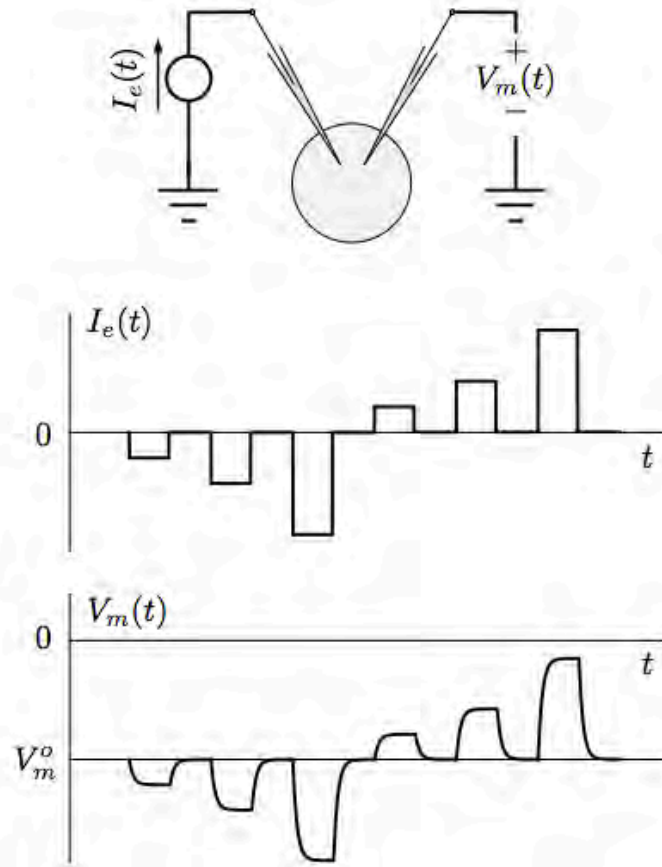


Figure 1.1

Electrically inexcitable cell

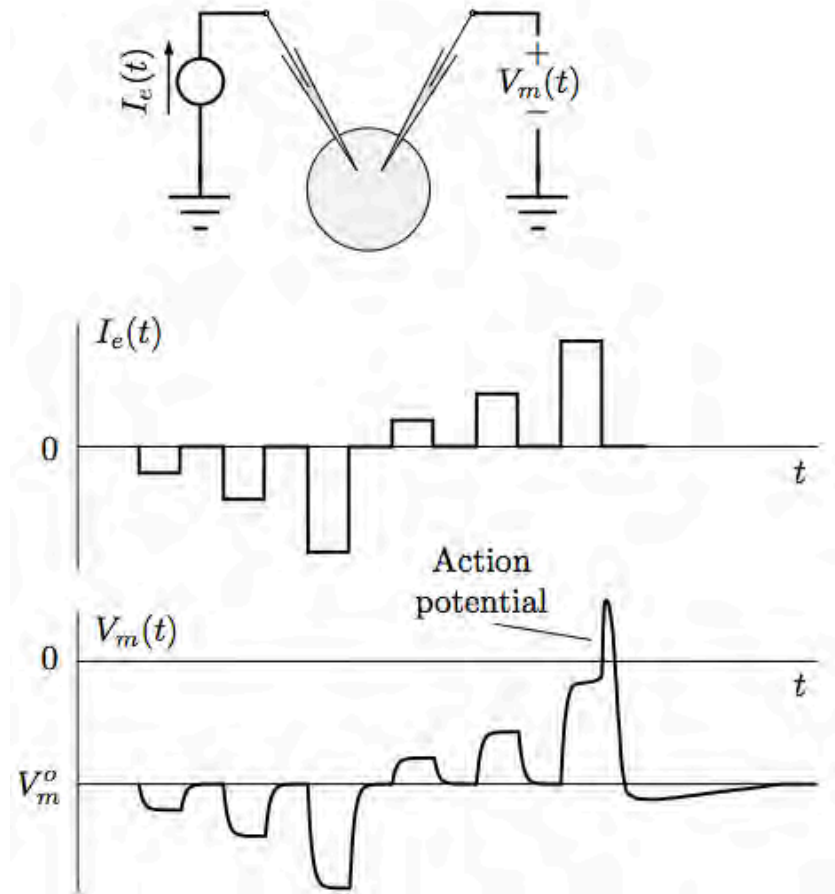


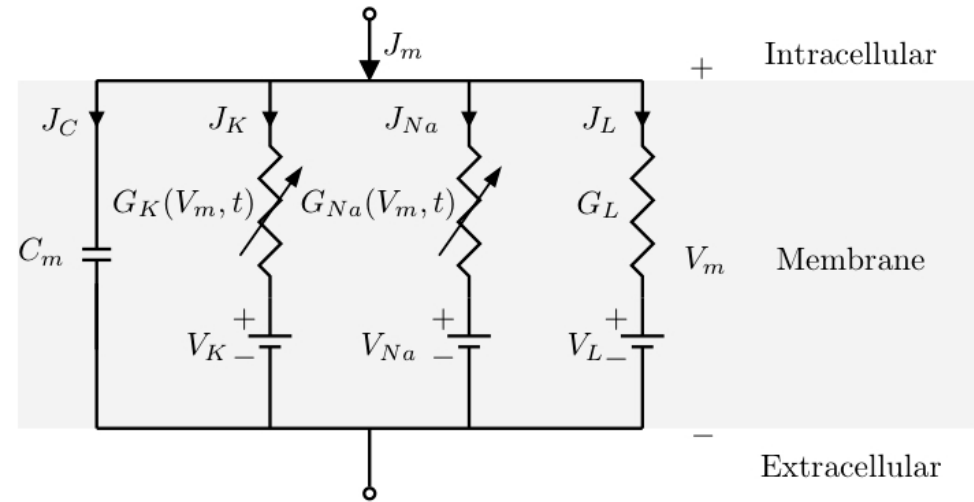
Figure 1.8

Electrically excitable cell

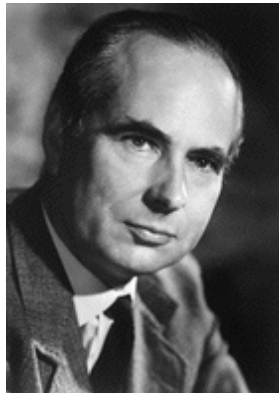
Key Idea: Neuron membrane dynamically/selectively “gates”

Hodgkin Huxley model

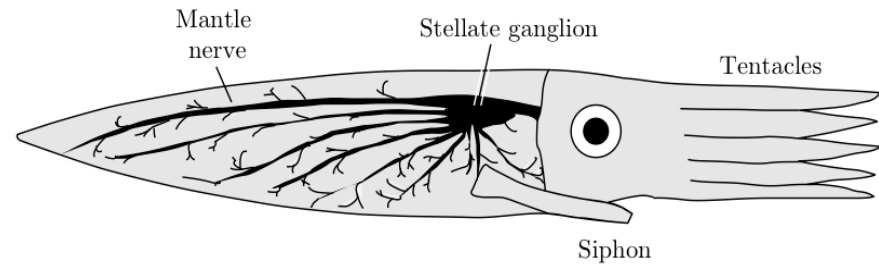
Variable Na⁺ and K⁺ conductances



Alan Hodgkin



Andrew Huxley



1963 Nobel Prize

Hodgkin-Huxley Equations

$$\frac{1}{2\pi a(r_o + r_i)} \frac{\partial^2 V_m}{\partial z^2} = C_m \frac{\partial V_m}{\partial t} + G_K(V_m, t) (V_m - V_K) + G_{Na}(V_m, t) (V_m - V_{Na}) + G_L(V_m - V_L)$$

$$G_K(V_m, t) = \bar{G}_K n^4(V_m, t)$$

$$G_{Na}(V_m, t) = \bar{G}_{Na} m^3(V_m, t) h(V_m, t)$$

$$n(V_m, t) + \tau_n(V_m) \frac{dn(V_m, t)}{dt} = n_\infty(V_m)$$

$$m(V_m, t) + \tau_m(V_m) \frac{dm(V_m, t)}{dt} = m_\infty(V_m)$$

$$h(V_m, t) + \tau_h(V_m) \frac{dh(V_m, t)}{dt} = h_\infty(V_m)$$

$$\tau_x \frac{dx}{dt} + x = x_\infty \quad \frac{dx}{dt} = \alpha_x(1-x) - \beta_x x$$

$$x_\infty = \alpha_x / (\alpha_x + \beta_x) \text{ and } \tau_x = 1 / (\alpha_x + \beta_x)$$

$$\alpha_m = \frac{-0.1(V_m + 35)}{e^{-0.1(V_m + 35)} - 1},$$

$$\beta_m = 4e^{-(V_m + 60)/18},$$

$$\alpha_h = 0.07e^{-0.05(V_m + 60)},$$

$$\beta_h = \frac{1}{1 + e^{-0.1(V_m + 30)}},$$

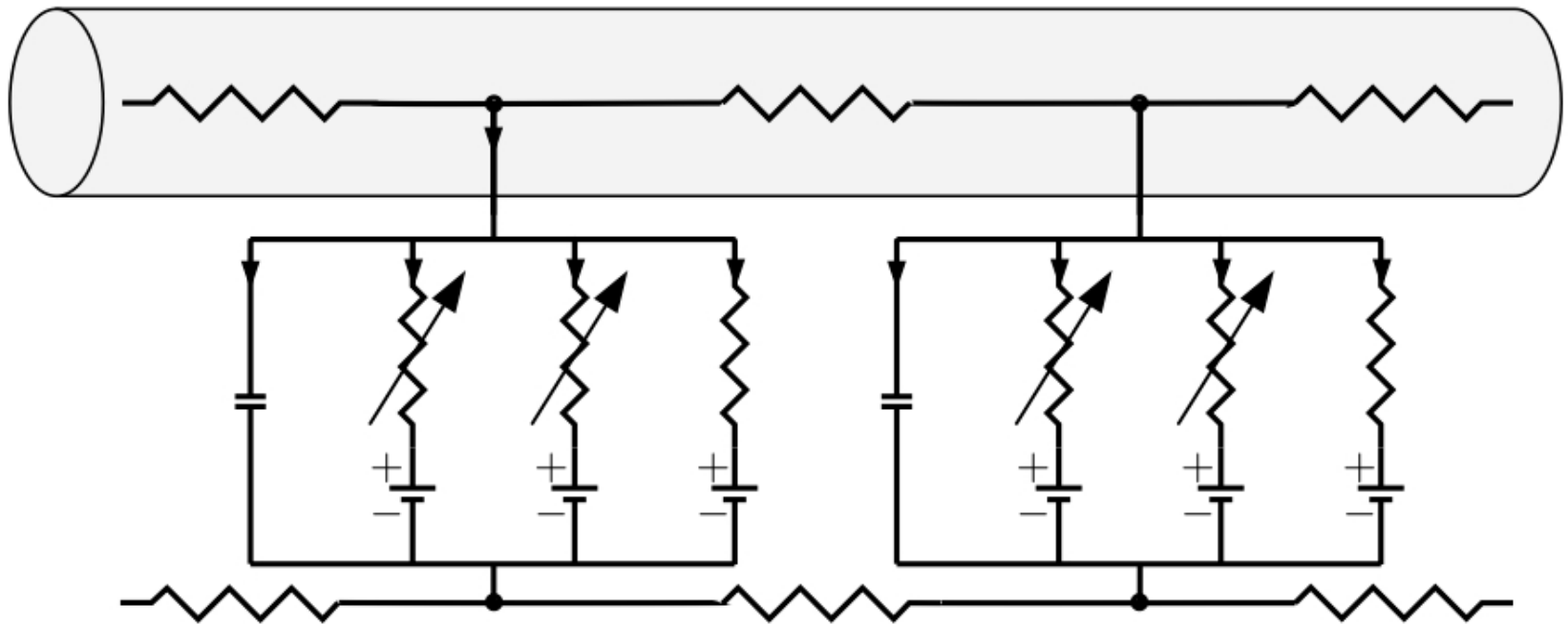
$$\alpha_n = \frac{-0.01(V_m + 50)}{e^{-0.1(V_m + 50)} - 1},$$

$$\beta_n = 0.125e^{-0.0125(V_m + 60)},$$

Finally there was the difficulty of computing the action potentials from the equations which we had developed. We had settled all the equations and constants by March 1951 and hoped to get these solved on the Cambridge University computer. However, before anything could be done we learnt that the computer would be off the air for 6 months or so while it underwent a major modification. Andrew Huxley got us out of that difficulty by solving the differential equations numerically using a hand-operated Brunsviga. The propagated action potential took about three weeks to complete and must have been an enormous labour for Andrew. But it was exciting to see it come out with the right shape and velocity and we began to feel that we had not wasted the many months that we had spent in analysing records.

—Hodgkin, 1977

HH + “Cable Model”

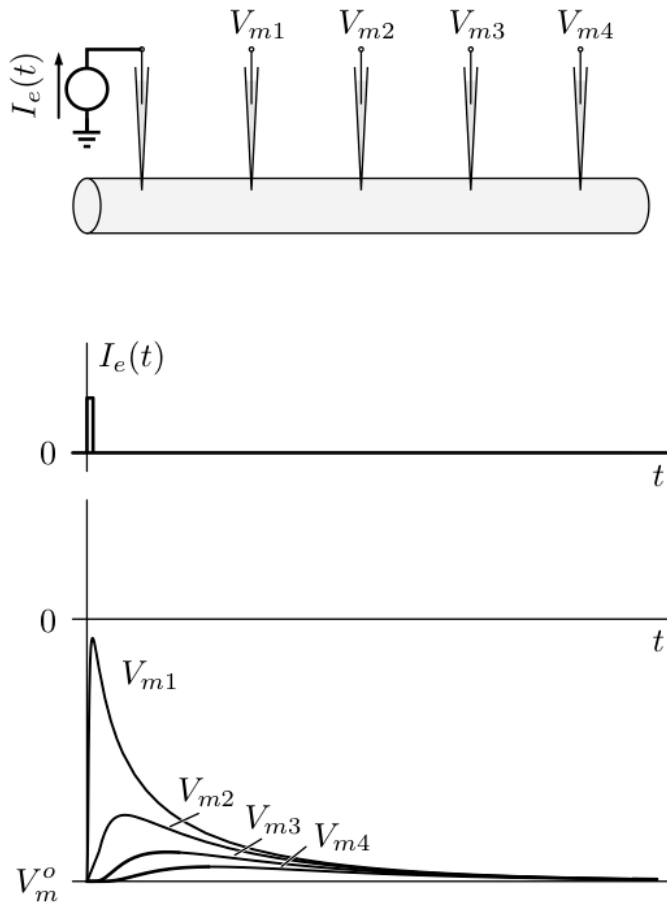


Weiss (1996)

“In the history of the biological sciences, there exists no mathematical model that has been welcomed with such a broad consensus as the Hodgkin-Huxley model.”

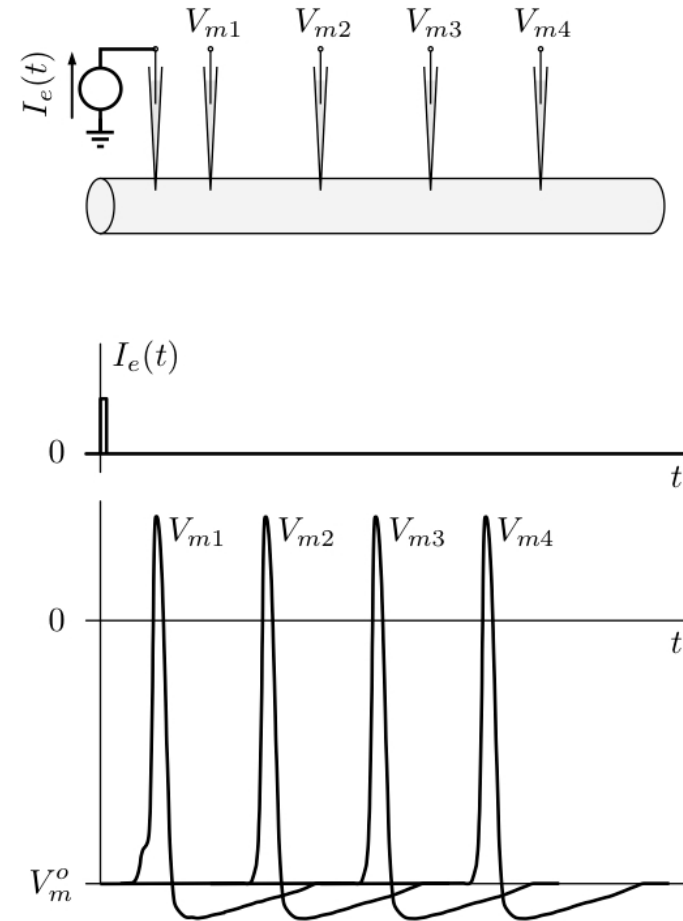
Aside: Spatial conduction → Propagation

Decremental conduction



Electrically inexcitable cell

Decrement-free conduction



Electrically excitable cell

Aside: Hodgkin-Huxley is not without criticism...

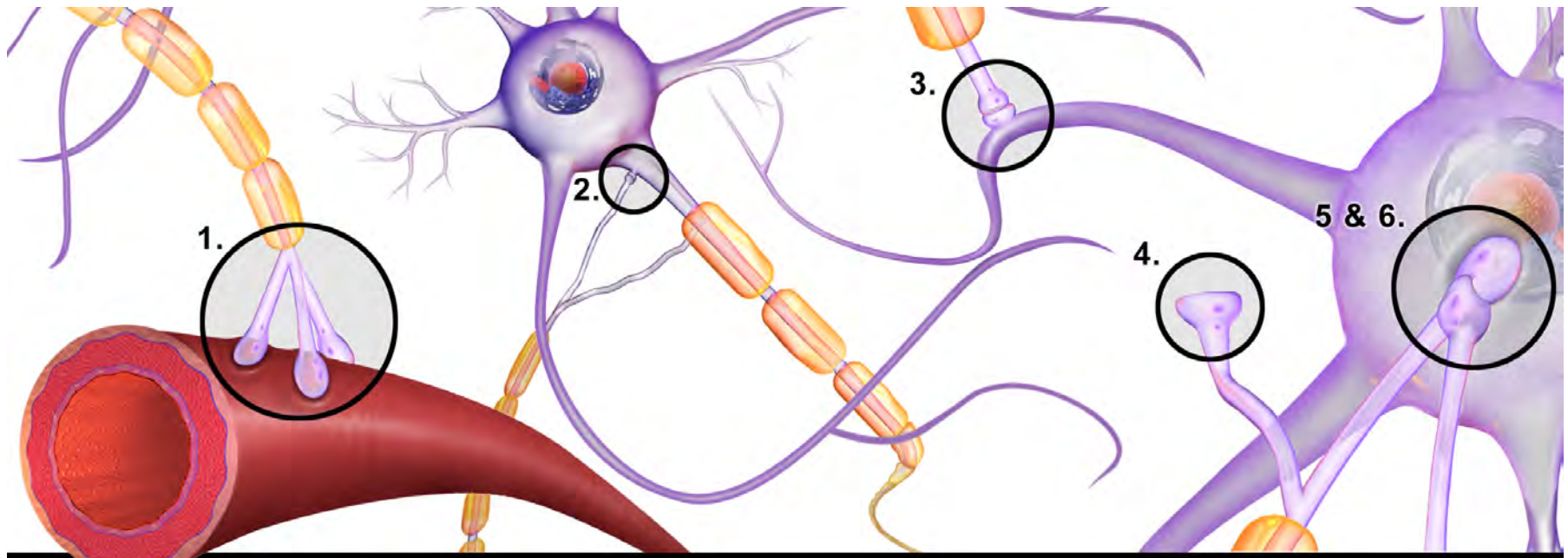
- Simplifications were made & widely employed (e.g., Fitzhugh-Nagumo, Morris-Lecar)
- Neurons appears to have more than just one kind of Na⁺ and K⁺ channel (e.g., inward-rectifier potassium channels, Ca²⁺ channels, etc...)
- Even the “sodium hypothesis” (i.e.,) has been challenged, much like the “potassium hypothesis” of Julius Bernstein

[Faraci et al, 2013]

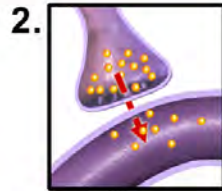
“Despite of its inconsistencies, the sodium hypothesis has received broad acceptance in time up to the point that it constitutes nowadays one of the basic principles of our understanding of how neurons function. The reason why this could be defended by the vast majority of the scientific community in face of the experimental evidence is at least in part (if not mainly) due to the the attractive mathematical formalism used by Hodgkin and Huxley.”

“Given that the Hodgkin-Huxley model has been ruled out, it becomes natural to wonder which could be then an interpretation of action potentials consistent with experimental evidence.”

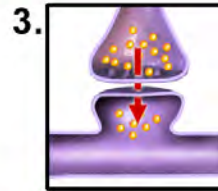
Chemical Synapses



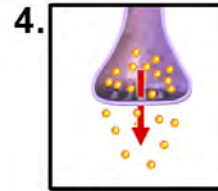
1. Axosecretory
Axon terminal secretes directly into bloodstream



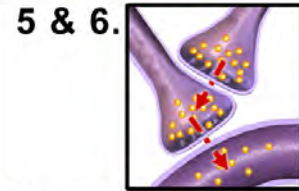
2. Axoaxonic
Axon terminal secretes into another axon



3. Axodendritic
Axon terminal ends on a dendrite spine

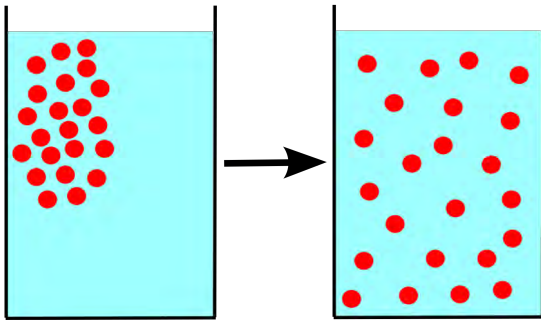


4. Axoextracellular
Axon with no connection secretes into extracellular fluid



5 & 6. Axosomatic
Axon terminal ends on soma
Axosynaptic
Axon terminal ends on another axon terminal

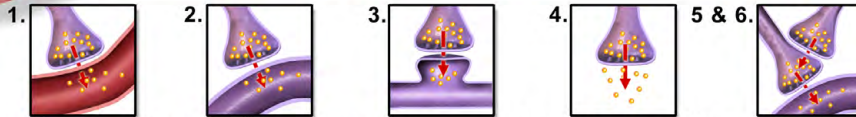
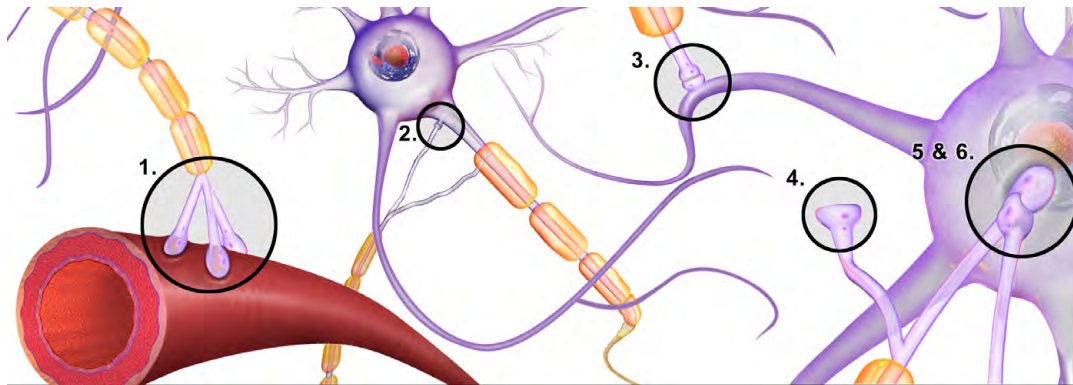
Key Idea: Diffusion is a fundamental aspect by which neurons “communicate”



Chemical synapses
“communicate” via diffusion
of neurotransmitter(s)

Recall: $\Rightarrow t_{1/2} \approx \frac{x_{1/2}^2}{D}$

	$x_{1/2}$	$t_{1/2}$
membrane sized	10 nm	$\frac{1}{10}$ μ sec
cell sized	10 μ m	$\frac{1}{10}$ sec
dime sized	10 mm	10^5 sec \approx 1 day



1. Axosecretory
Axon terminal secretes directly into bloodstream

2. Axoaxonic
Axon terminal secretes into another axon

3. Axodendritic
Axon terminal ends on a dendrite spine

4. Axoextracellular
Axon with no connection secretes into extracellular fluid

**5 & 6. Axosomatic
Axosynaptic**
Axon terminal ends on another axon terminal

Rough calculation:

Diffusion across the synaptic cleft (~20 nm) takes ~ 1 μ s

(i.e., diffusion is plenty fast!)

Recall: Role of physicists?

U.S. Department of Health & Human Services

NIH National Institutes of Health
Turning Discovery Into Health

The BRAIN Initiative® About | Resources | Funding | BRAIN & News | BRAIN Update ¹ | Contact Us

The BRAIN Initiative®



BRAIN Update
New Funding Opportunity Announcements and a Pre-Application Webinar for the BRAIN Initiative Advanced Postdoctoral Career Transition Award to Promote Diversity (K99/R00)
Program for BRAIN Initiative K99/R00 Career Transition Award to Promote Diversity

Cell Type ✨ | Circuit Diagrams ↵ | Monitor Neural Activity 🧠 | Interventional Tools 🗨️ | Theory and Data Analysis Tools 📊 | Human Neuroscience 🗣️ | Integrated Approaches 🌐

WHAT IS THE BRAIN INITIATIVE?

The Brain Research through Advancing Innovative Neurotechnologies® (BRAIN) Initiative is aimed at revolutionizing our understanding of the human brain. By accelerating the development and application of innovative technologies, researchers will be able to produce a revolutionary new dynamic picture of the brain that, for the first time, shows how individual cells and complex neural circuits interact in both time and space. Long desired by researchers seeking new ways to treat, cure, and even prevent brain disorders, this picture will fill major gaps in our current knowledge and provide unprecedented opportunities for exploring exactly how the brain enables the human body to record, process, utilize, store, and retrieve vast quantities of information, all at the speed of thought.

Highlights of The BRAIN Initiative®

- Re-visiting BRAIN's Strategic Plan**
Accepting input using BRAINfeedback@nih.gov
- 2017 Funded Awards**

- BRAIN Initiative Funding Opportunities**


- BRAIN 2025 Report**
- BRAIN Alliance**

BRAIN Initiative Partners

Federal

- National Science Foundation (NSF)
- Defense Advanced Research Projects Agency (DARPA)
- U.S. Food and Drug Administration (FDA)
- The Intelligence Advanced Research Projects Activity (IARPA)

Photon Upmanship: Why Multiphoton Imaging Is More than a Gimmick

Winfried Denk and Karel Svoboda
Bell Laboratories
Lucent Technologies
Murray Hill, New Jersey 07974

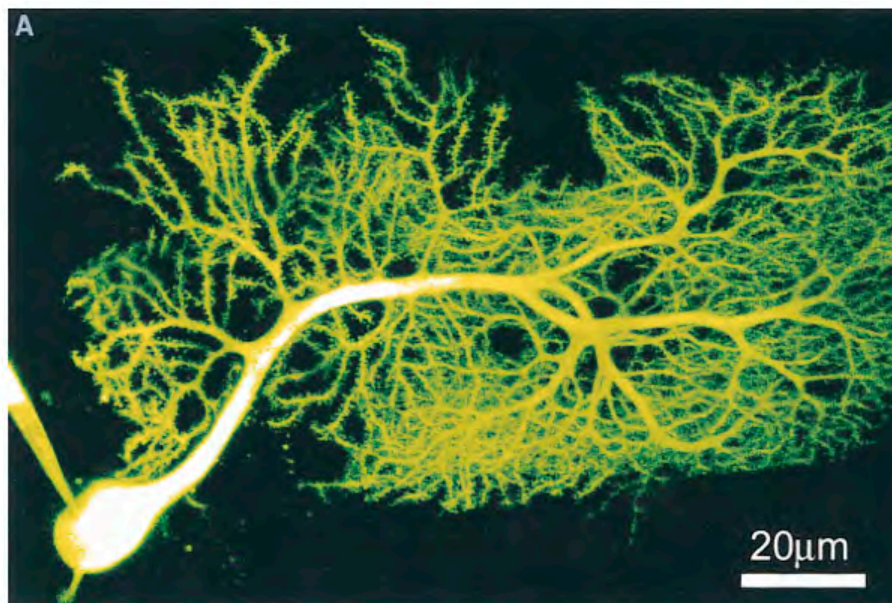
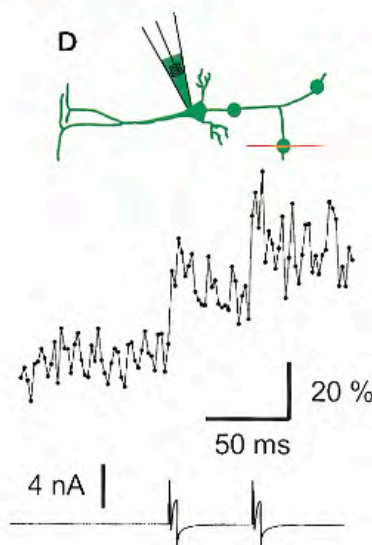
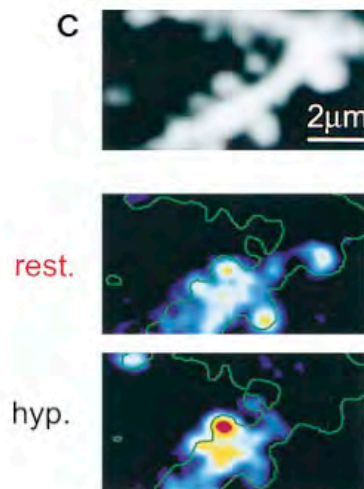
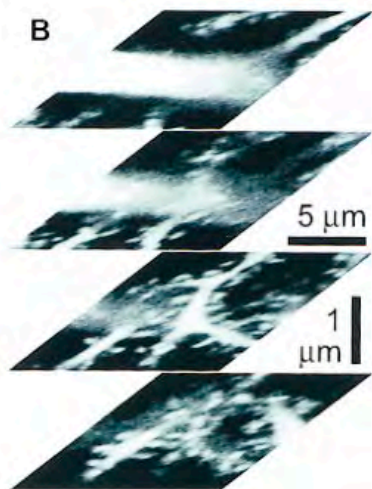


Figure 3. Three-Dimensional Functional Imaging in Brain Slices

2-photon excitation without and 1-photon excitation with confocal detection are (aside from the wavelength dependence of resolution) equivalent in their optical point-spread functions, including their optical sectioning properties (Sheppard and Gu, 1990). This figure shows images acquired using 2PLSM

(A) Maximum projection of a stack of optical sections through a living Purkinje cell filled with fluorescein dextran (400 μm).

(B) At higher resolution, a sequence of sections taken at 1.8 μm focus intervals (objective lens: 63 \times , 0.9 NA, water immersion, Zeiss) of a piece of dendrite belonging to the same cell.

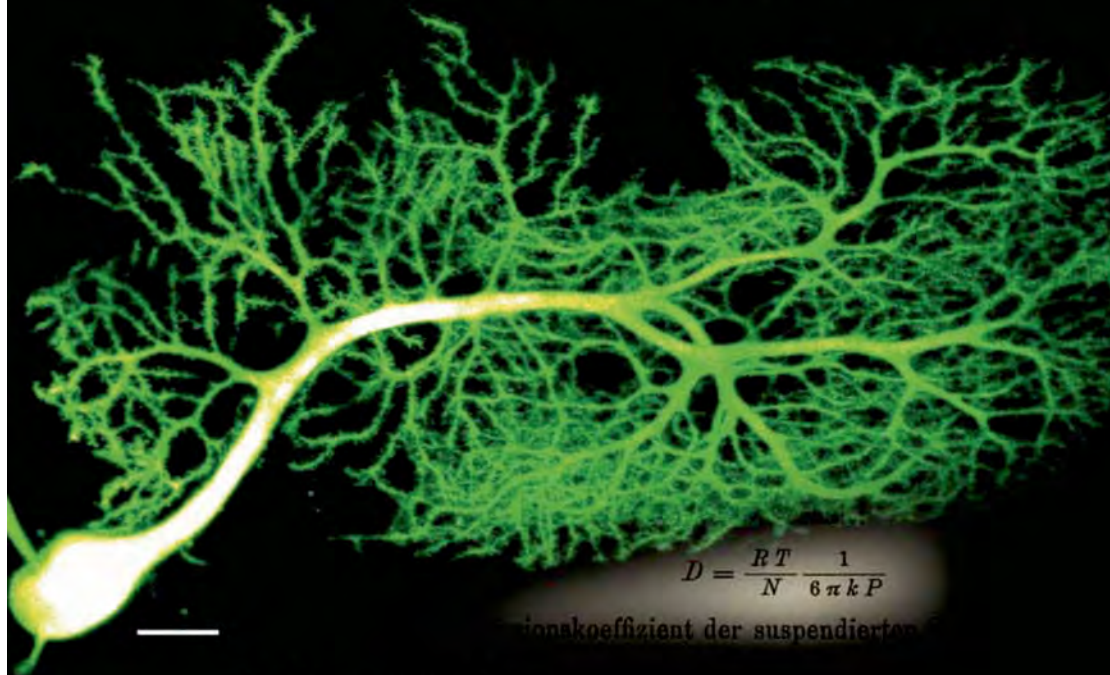
(C) The anatomy of a spiny branchlet and its response to focal stimulation of parallel fibers while the cell is held at its resting potential (rest.) and at strongly hyperpolarized levels (hyperpol.; Denk et al., 1995c).

(D) The calcium dynamics in a presynaptic terminal during a pair of action potentials (bottom trace) in a neocortical pyramidal cell is shown (single trial). Calcium concentration was measured using fluorescence (100 μM Calcium Green 1) recorded in line-scan mode. The excitation source was a prototype diode-pumped Cr:LiSrAlF₄ laser (Svoboda et al., 1996a) in (A) and (B) and a Ti:sapphire laser in (C) and (D).

BIOLOGICAL PHYSICS

Energy, Information, Life

WITH NEW ART BY DAVID GOODSSELL

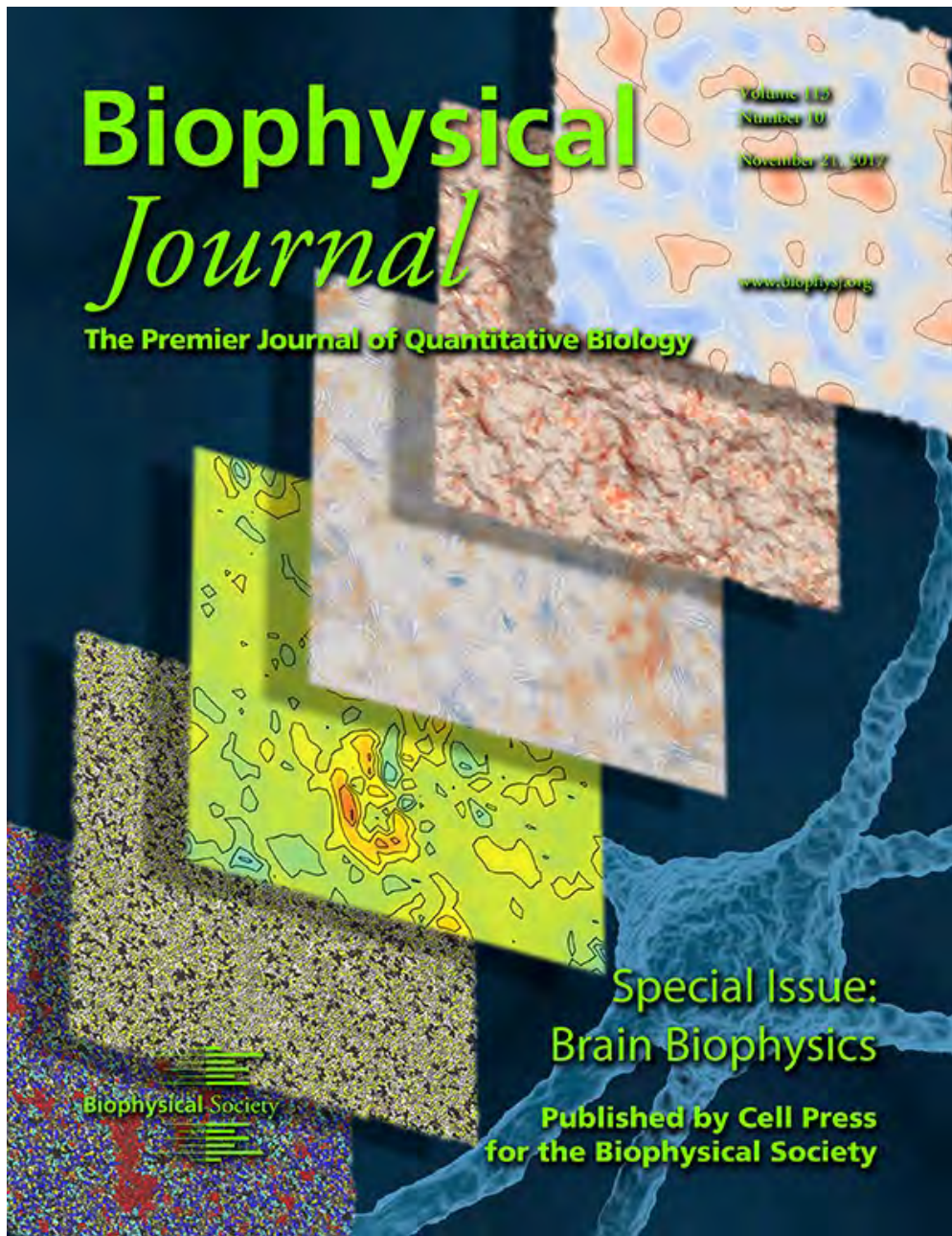


$$D = \frac{RT}{N} \frac{1}{6\pi kP}$$

Diffusionskoeffizient der suspendierten

Philip Nelson

Aside (re Light & the Brain)



Nov. 2017 “Special Issue”
of Biophysical Journal

Biophysics of the Brain: From Molecules to Networks

Vasanthi Jayaraman¹

¹*University of Texas-Houston Medical School, Houston, Texas*

Biophysical Journal 113, E01, November 21, 2017

The brain, with billions of neurons making trillions of connections, still largely remains an enigma. The last decade has seen the development of new biophysical tools, including optical methods for mapping neuronal connections and high-resolution imaging. These new biophysical tools, along with electrophysiological, structural, and computational methods, have brought the understanding of the brain into better focus. This special issue of Biophysical Journal on brain biophysics highlights research in these areas.

Probing the Interplay between Dendritic Spine Morphology and Membrane-Bound Diffusion

Max Adrian,¹ Remy Kusters,² Cornelis Storm,^{2,3} Casper C. Hoogenraad,¹ and Lukas C. Kapitein^{1,*}

¹Division of Cell Biology, Faculty of Science, Utrecht University, Utrecht, the Netherlands; ²Department of Applied Physics and ³Institute for Complex Molecular Systems, Eindhoven University of Technology, Eindhoven, the Netherlands

ABSTRACT Dendritic spines are protrusions along neuronal dendrites that harbor the majority of excitatory postsynapses. Their distinct morphology, often featuring a bulbous head and small neck that connects to the dendritic shaft, has been shown to facilitate compartmentalization of electrical and cytoplasmic signaling stimuli elicited at the synapse. The extent to which spine morphology also forms a barrier for membrane-bound diffusion has remained unclear. Recent simulations suggested that especially the diameter of the spine neck plays a limiting role in this process. Here, we examine the connection between spine morphology and membrane-bound diffusion through a combination of photoconversion, live-cell superresolution experiments, and numerical simulations. Local photoconversion was used to obtain the timescale of diffusive equilibration in spines and followed by global sparse photoconversion to determine spine morphologies with nanoscopic resolution. These morphologies were subsequently used to assess the role of morphology on the diffusive equilibration. From the simulations, we could determine a robust relation between the equilibration timescale and a generalized shape factor calculated using both spine neck width and neck length, as well as spine head size. Experimentally, we found that diffusive equilibration was often slower, but rarely faster than predicted from the simulations, indicating that other biological confounders further reduce membrane-bound diffusion in these spines. This shape-dependent membrane-bound diffusion in mature spines may contribute to spine-specific compartmentalization of neurotransmitter receptors and signaling molecules and thereby support long-term plasticity of synaptic contacts.

Aside (re Light & the Brain)



OPTOGENETICS

[sequence info](#) [virus preparation](#) [hardware](#) [request materials](#) [references](#) [d-lab](#)

Brain tissue light transmission calculator
Angeled Stereotax coordinate calculator (MatLab)
Opsin and fluorophore spectra tool

Clarity Resource Site
Optogenetic courses
Fiber photometry resources

2016 Perspective
Cell
Targeting circuits

2015 Commentary
nature neuroscience
Optogenetics 10 year history

2016 Primer
Cell
Communication in the brain

2014
nature
Circuit dynamics of behavior

2015
Neuron
Closed-loop optogenetics

2014 Annual Review of
Biomedical Engineering
Optical neural interfaces

2012 Analysis
nature methods
Quantitative opsin properties

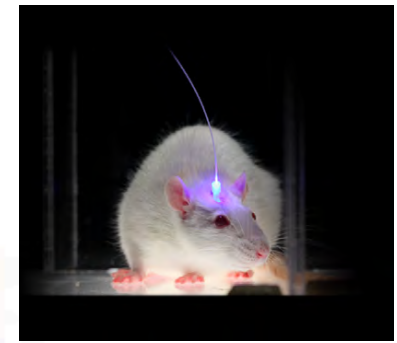
2012
nature REVIEWS
Optogenetics & neural circuits in
brain disease

2011 Primer
Neuron
Optogenetics in neural systems

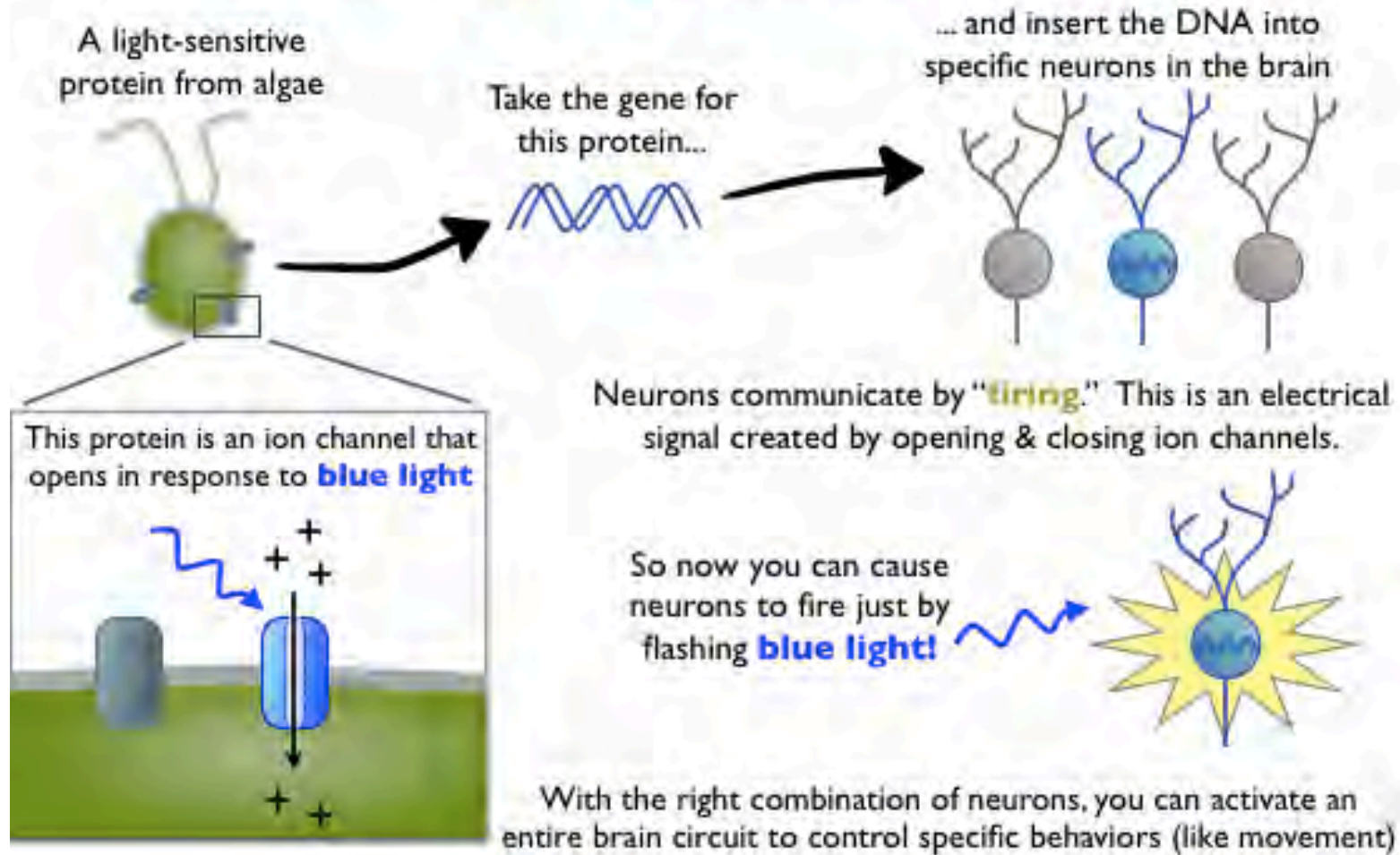
2011 Annual Review of
Neuroscience
Development & application of
optogenetics

2010 Method of the year
nature methods

2010
SCIENTIFIC AMERICAN
Controlling the brain with light



How optogenetics works



ARTICLE

doi:10.1038/nature14322

Structural basis for Na⁺ transport mechanism by a light-driven Na⁺ pump

Hideaki E. Kato^{1†}, Keiichi Inoue^{2,3,4}, Rei Abe-Yoshizumi², Yoshitaka Kato², Hikaru Ono², Masae Konno², Shoko Hososhima^{5,6}, Toru Ishizuka^{5,6}, Mohammad Razuanul Hoque^{5,6}, Hirofumi Kunitomo³, Junpei Ito⁷, Susumu Yoshizawa⁸, Keitaro Yamashita⁹, Mizuki Takemoto¹, Tomohiro Nishizawa¹, Reiya Taniguchi¹, Kazuhiro Kogure⁸, Andrés D. Maturana⁷, Yuichi Iino^{1,6}, Hiromu Yawo^{5,6}, Ryuichiro Ishitani¹, Hideki Kandori^{2,3} & Osamu Nureki¹

Krokinobacter eikastus rhodopsin 2 (KR2) is the first light-driven Na⁺ pump discovered, and is viewed as a potential next-generation optogenetics tool. Since the positively charged Schiff base proton, located within the ion-conducting pathway of all light-driven ion pumps, was thought to prohibit the transport of a non-proton cation, the discovery of KR2 raised the question of how it achieves Na⁺ transport. Here we present crystal structures of KR2 under neutral and acidic conditions, which represent the resting and M-like intermediate states, respectively. Structural and spectroscopic analyses revealed the gating mechanism, whereby the flipping of Asp116 sequesters the Schiff base proton from the conducting pathway to facilitate Na⁺ transport. Together with the structure-based engineering of the first light-driven K⁺ pumps, electrophysiological assays in mammalian neurons and behavioural assays in a nematode, our studies reveal the molecular basis for light-driven non-proton cation pumps and thus provide a framework that may advance the development of next-generation optogenetics.

Many organisms capture light energy and information using the rhodopsin family of proteins, which comprise the heptahelical transmembrane (7-TM) proteins called opsins covalently linked to retinal. Based on their primary sequences, the opsin genes are classified into two groups: the microbial and animal opsins. The animal rhodopsins primarily work as G-protein-coupled receptors, whereas the microbial rhodopsins have divergent functions, such as ion pumps, ion channels, sensors and kinases^{1–3}. Recently, the pump-and-channel-type rhodopsins have attracted broad attention, since these microbial rhodopsins can be used as powerful tools in the neuroscience field to control neuronal activity in a wide range of living animals (optogenetics)^{4,5}.

As compared to the light-gated ion channel channelrhodopsin (ChR), the light-driven ion pumps have a long research history. Since the discoveries of the light-driven proton pump bacteriorhodopsin (BR) and the light-driven chloride pump halorhodopsin (HR)^{2,6}, several light-driven ion pumps, such as proteorhodopsins (PRs), xanthorhodopsin (XR), and archaerhodopsins (ARs), have been cloned and studied in diverse research fields, including optogenetics^{7–12}. However, these light-driven ion pumps were basically classified into only two groups: outward proton pumps and inward chloride pumps, and no non-proton cation pumps have been discovered. Almost all of the known microbial rhodopsins are covalently bound to all-trans retinal (ATR) via the protonated Schiff base in the resting state, and the positively charged Schiff base proton in the middle of the ion transport pathway prevents cation transport (Extended Data Fig. 1). In the case of proton pumps, the Schiff base proton itself works as the substrate, and retinal photoisomerization alters the pK_a values of the Schiff base and the carboxylates located on the extracellular side (historically called the 'Schiff base counterions'), consequently leading

to the proton transfer from the Schiff base to the extracellular side (Extended Data Fig. 1a)¹³. In the case of chloride pumps, Cl⁻ binding stabilizes the protonated Schiff base and retinal photoisomerization flips the N-H dipole, thus driving the movement of Cl⁻ from the extracellular environment to the intracellular side (Extended Data Fig. 1b)¹⁴. Therefore, it was widely believed that the absence of light-driven non-proton cation pumps was reasonable, because a non-proton cation would experience electrostatic repulsion from the Schiff base proton (Extended Data Fig. 1c).

However, in 2013, a new microbial rhodopsin, containing the unique NDQ (Asn112, Asp116 and Gln123) motif, was cloned from the marine flavobacterium *Krokinobacter eikastus*, and was characterized as the first light-driven Na⁺ pump¹⁵. Although the new rhodopsin, *Krokinobacter eikastus* rhodopsin 2 (KR2), transports protons in the absence of Na⁺ and Li⁺, under physiological conditions it works solely as an outward Na⁺ pump. A previous study revealed its cyclic photochemical reaction (photocycle) involving four spectroscopically distinguishable intermediates (K, L, M and O) and identified some of the functionally important residues^{15,16}, but the mechanism of Na⁺ transport remained elusive. Understanding the structural basis of non-proton cation transport by KR2 would be enormously valuable, not only to enhance our knowledge of rhodopsin family proteins, but also to facilitate the design of novel light-driven ion pumps with desired ion selectivity, such as K⁺ and Ca²⁺ pumps. Such ion pumps, as well as Na⁺ pumps, would be useful as next-generation optogenetics tools.

Overall structure and comparison with BR

To understand the structural basis for Na⁺ transport, we expressed, purified and crystallized KR2 lacking the five carboxy-terminal amino acid residues (residues 1–275). The crystals were obtained by the lipidic

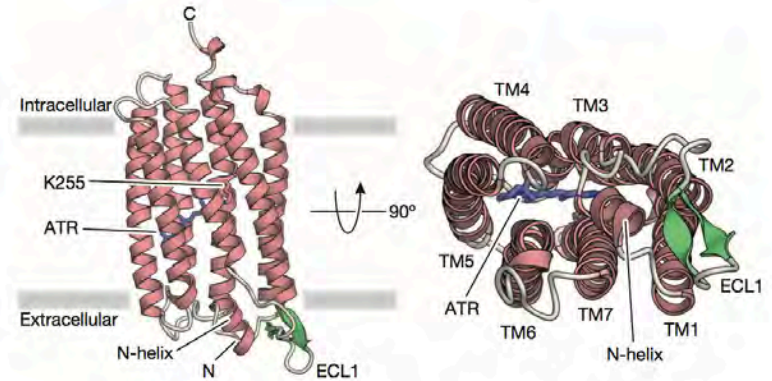
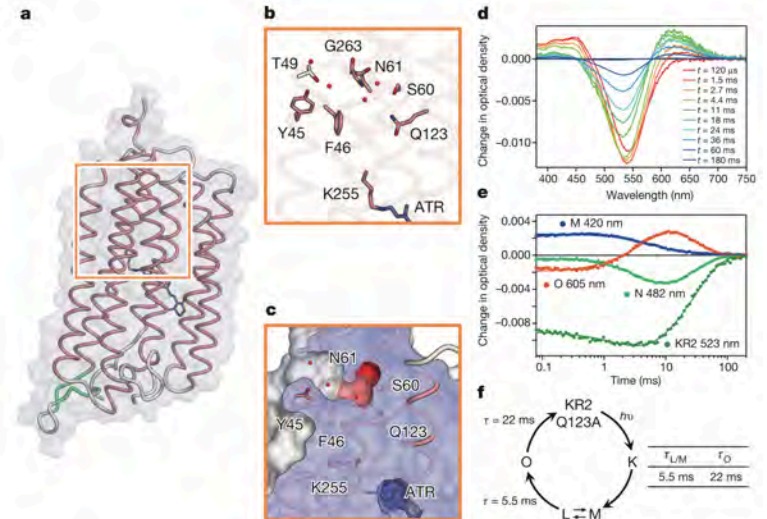


Figure 1 | Overall structure of KR2 and comparison with BR. Crystal structure of KR2, viewed parallel to the membrane (left), and from the extracellular side (right). KR2 consists of the N-helix and the seven transmembrane helices (TM1–TM7) connected by extracellular loops (ECL1–ECL3) and intracellular loops (ICL1–ICL3). ATR, depicted by stick models, is coloured blue, and ECL1 is coloured green.



¹Department of Biological Sciences, Graduate School of Science, The University of Tokyo, 2-11-16 Yayoi, Bunkyo-ku, Tokyo 113-0032, Japan. ²Department of Frontier Materials, Nagoya Institute of Technology, Showa-ku, Nagoya 466-8555, Japan. ³OptoBioTechnology Research Center, Nagoya Institute of Technology, Showa-ku, Nagoya 466-8555, Japan. ⁴PRESTO, Japan Science and Technology Agency, 4-1-8 Honcho, Kawaguchi, Saitama 332-0012, Japan. ⁵Department of Developmental Biology and Neuroscience, Tohoku University Graduate School of Life Sciences, Sendai 980-8577, Japan. ⁶CREST, Japan Science and Technology Agency, 4-1-8 Honcho, Kawaguchi, Saitama 332-0012, Japan. ⁷Department of Bioengineering Sciences, Graduate School of Biocultural Sciences, Nagoya University, Furo-cho, Chikusa-ku, Nagoya 464-8601, Japan. ⁸Atmosphere and Ocean Research Institute, The University of Tokyo, 5-1-5 Kashiwanoha, Kashiwa, Chiba 277-8564, Japan. ⁹RIKEN SPring-8 Center, Hyogo 679-5148, Japan. [†]Present address: Department of Molecular and Cellular Physiology, Stanford University School of Medicine, Stanford, California 94305, USA.

Aside (re Light & the Brain)

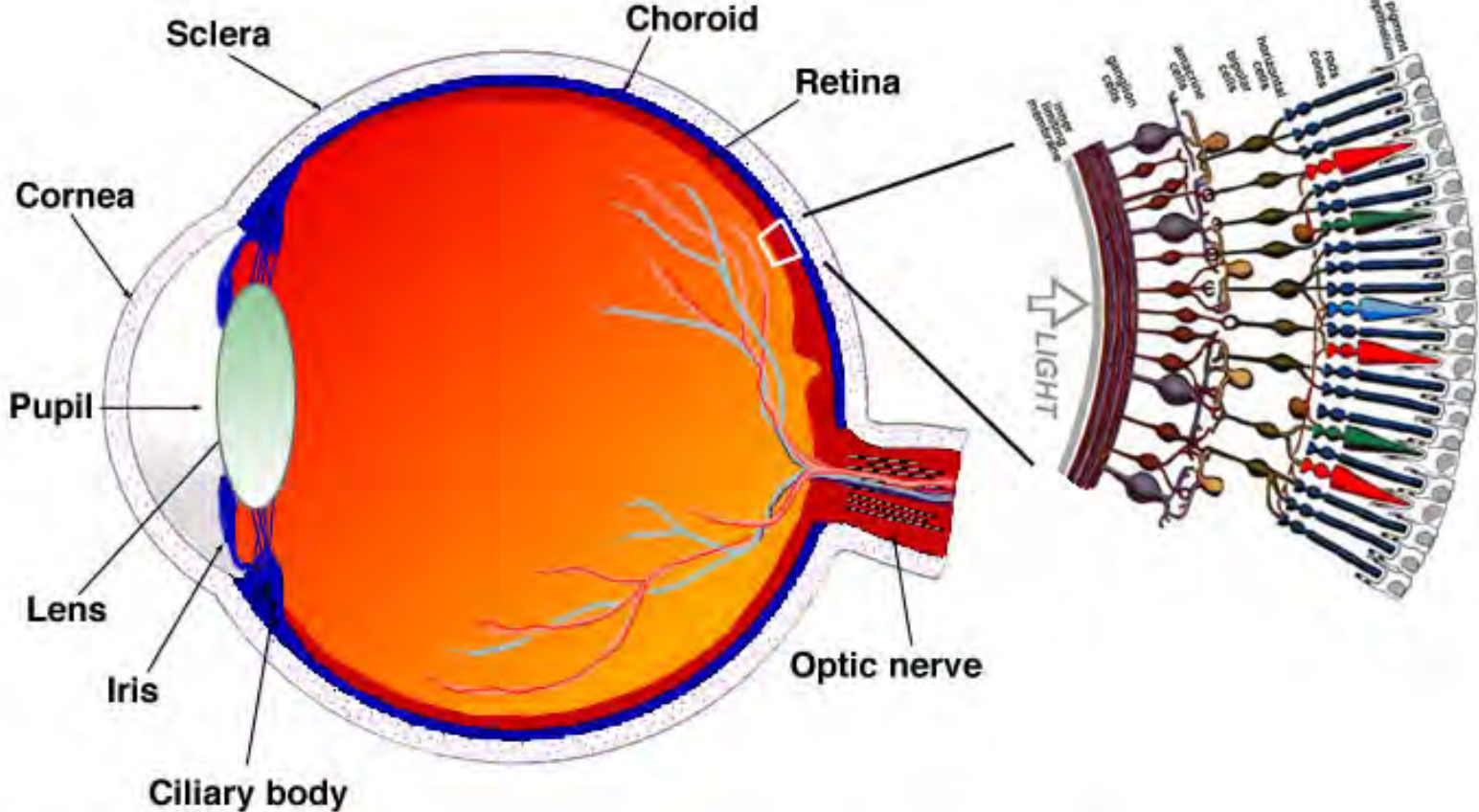
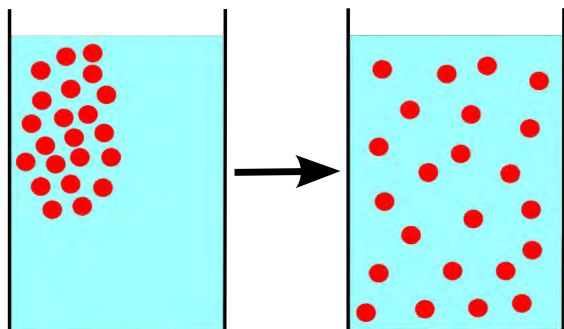
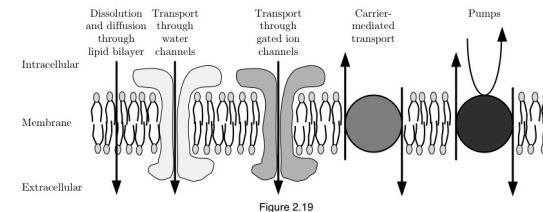
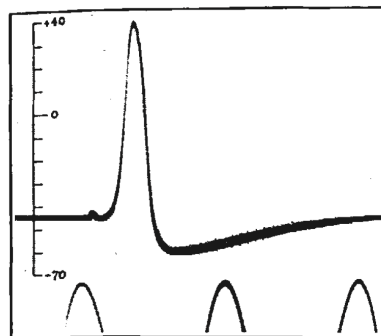
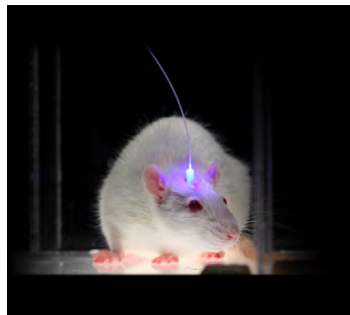


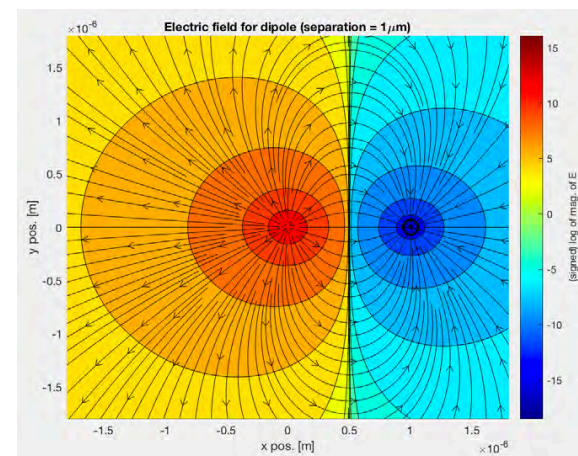
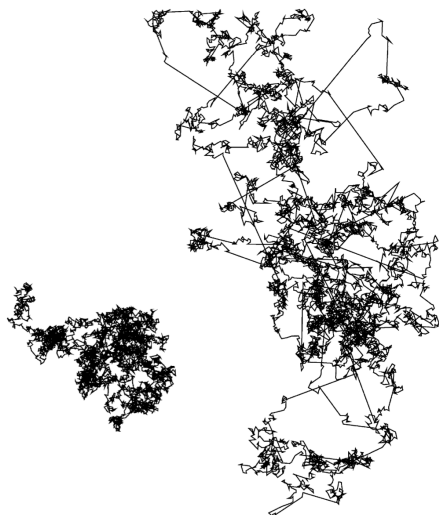
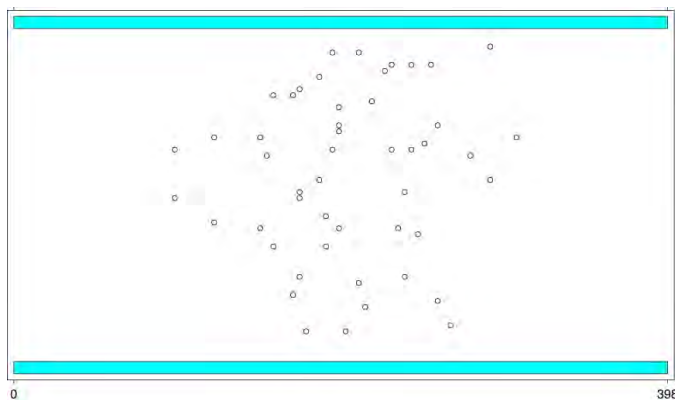
Fig. 1.1. A drawing of a section through the human eye with a schematic enlargement of the retina.

Summary



$$\frac{\partial c}{\partial t} = D \frac{\partial^2 c}{\partial x^2}$$

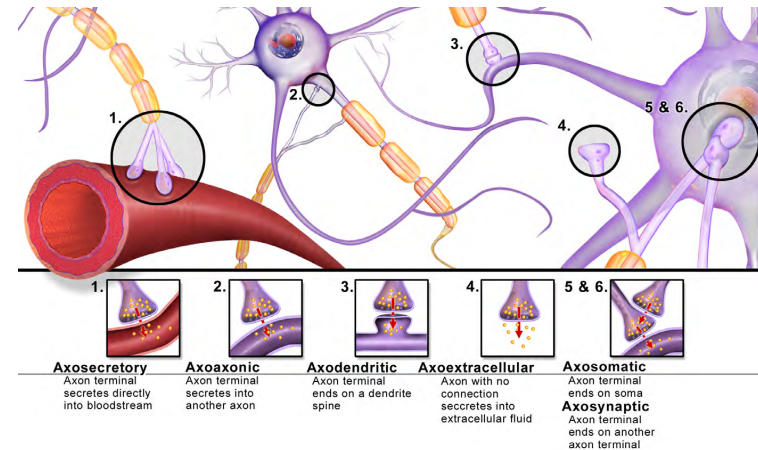
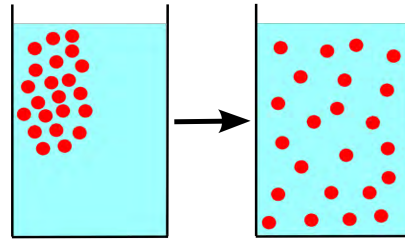
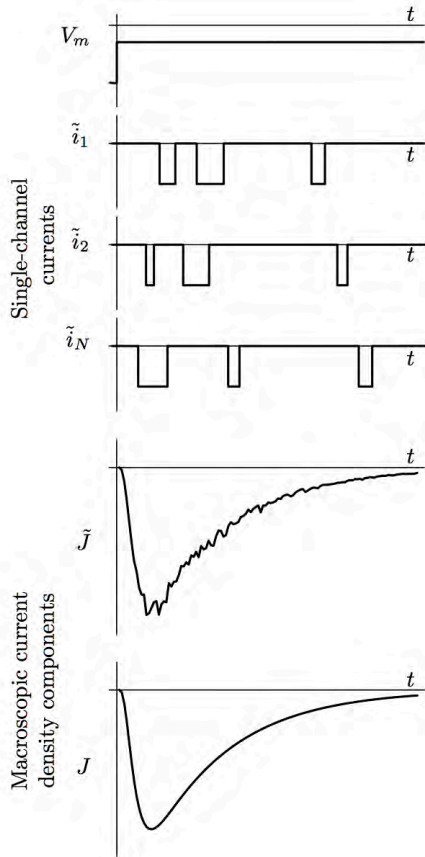
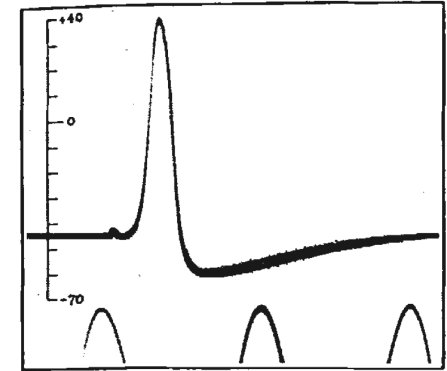
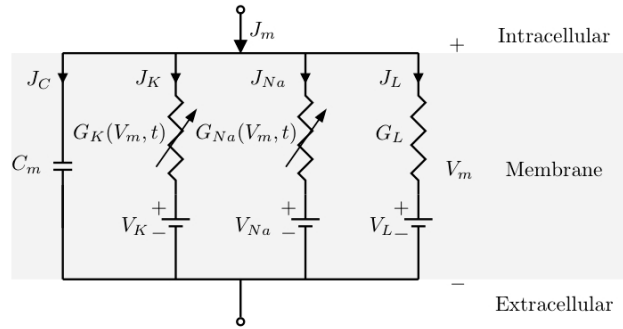
	$x_{1/2}$	$t_{1/2}$
membrane sized	10 nm	$\frac{1}{10} \mu\text{sec}$
cell sized	10 μm	$\frac{1}{10} \text{sec}$
dime sized	10 mm	$10^5 \text{sec} \approx 1 \text{day}$



Summary

$$J_n(x, t) = -z_n F D_n \frac{\partial c_n(x, t)}{\partial x} - u_n z_n^2 F^2 c_n(x, t) \frac{\partial \psi(x, t)}{\partial x}$$

Hodgkin Huxley model





Random Walk with Drift (Marius Lehene)



BIOPHYSICS @ YORK



redefine THE POSSIBLE.

Fini

Slides available at:
<http://www.yorku.ca/cberge/>

The new nanophysiology: regulation of ionic flow in neuronal subcompartments

David Holcman and Rafael Yuste

Abstract | Cable theory and the Goldman–Hodgkin–Huxley–Katz models for the propagation of ions and voltage within a neuron have provided a theoretical foundation for electrophysiology and been responsible for many cornerstone advances in neuroscience. However, these theories break down when they are applied to small neuronal compartments, such as dendritic spines, synaptic terminals or small neuronal processes, because they assume spatial and ionic homogeneity. Here we discuss a broader theory that uses the Poisson–Nernst–Planck (PNP) approximation and electrodiffusion to more accurately model the constraints that neuronal nanostructures place on electrical current flow. This extension of traditional cable theory could advance our understanding of the physiology of neuronal nanocompartments.


```

% ### EXwalker2D.m ###          07.15.15 CB
% Simulates a 2-D Brownian walker
% - polar coords. for computing a step
% - step size is unit value with normally distrib. val.
% - direction-wise, allows for either (via A.Pbias):
% o step direction is uniformly distributed over circle
% o Gaussian-like directional bias (kinda kludgy, but works)
% - [IN PROGRESS] allow for a (circular) boundary condition (via A.Pbound)
% that either reflects or is periodic

clear
% =====
walkerNum= 200; % # of walkers to compute
steps= 500; % # of steps to take by walker
A0= 0.1; % limiting stochastic factor (re 1) for unit step size (A0=0 --> unit radial steps, A0>0 introduce Gaussian variance)
% ---
A.Pbias= 0; % boolean to create a directional bias
A.alpha= 0.2; % bias factor [0,1] --> small (~0.1 means stronger bias)
A.offset= 0.75; % offset direction for bias[cy]
% ---
A.force1D= 0; % boolean to force angle to be 0 or pi (thus making this 1-D)
% ---
A.Pbound= 1; % boolean to create circular boundary (i.e., walkers constrained)
A.bndR= 20; % radius of bounding wall (re origin)
A.boundType= 0; % boundary condtion (req. A.Pbound=1): 0-"hard" (reflecting), 1-periodic
% ---
axLim= 25; % bounds for plotting (Fig.66)
kk= 1; % particle ID to visualize a single walker (Fig.66)
animate= 1; % boolean to turn on/off movie for an individual walker (Fig.66)
numWplot= 5; % # of walkers to plot individual (r^2) paths (Fig.4)
% =====

% ---
% if a constrained walk, force bounding condition (A.bndR) to be much
% larger than mean unit step size (helps avoid some coding headaches below)
if (A.Pbound==1 && A.bndR <= 5), disp('Make larger bounding condition'); end

for m= 1:walkerNum
% walker m initially at origin [i.e., cartesian (0,0)]
P(m).coord(1,:)= [0 0];

for nn=2:steps
% ----
P(m).A(nn)= 1+ A0*randn(1); % (radial) size of nn'th step for m'th walker
if (P(m).A(nn)<0), P(m).A(nn)=0; end % make zero size step if negative (introduces bias?)
% ----
% direction of nn'th step for m'th walker (allows possibility of bias)
if A.Pbias==0
P(m).theta(nn)= rand(1)*2*pi; % no bias
else
if (m==1 && nn==2), disp('Radial bias in effect'); end
P(m).theta(nn)= (A.offset + A.alpha.*randn(1))*2*pi; % w/ radial bias
end
end

```

```

% ----
% constrain angle such that movement is essentially 1-D
if A.force1D==1
    P(m).theta(nn)= round(P(m).theta(nn)/(2*pi))*pi;
end
% ----
% update re last position and store away in Cartesian and radial coords.
P(m).coord(nn,:) = [P(m).coord(nn-1,1)+P(m).A(nn)*cos(P(m).theta(nn)) P(m).coord(nn-1,2)+P(m).A(nn)*sin(P(m).theta(nn))];
P(m).rsq(nn)= P(m).coord(nn,1)^2 + P(m).coord(nn,2)^2; % new radial position (squared)
P(m).phi(nn)= atan2(P(m).coord(nn,2),P(m).coord(nn,1)); % angle of new position re origin
% ----
% if constrained, check that new coords. aren't past wall (otherwise "reflect")
if A.Pbound==1
    if (m==1 && nn==2 && A.boundType==0), disp('Circular hard/reflecting boundary in effect'); end
    if (m==1 && nn==2 && A.boundType==1), disp('Circular periodic boundary in effect'); end
    temp1= sqrt(P(m).rsq(nn)); % dummy to reduce re-computation
    if temp1 >= A.bndR
        if A.boundType==0
            % ### HARD REFLECTION ###
            % angle stays the same, only radius changes (and in a simple way)
            temp2= 2*A.bndR- temp1; % reflected radial length
            %disp([temp1 P(m).A(nn) P(m).theta(nn) P(m).phi(nn) temp2]); % for debugging
        elseif A.boundType==1
            % ### PERIODIC B.C. ###
            % both radius changes and angle flips 180
            temp2= 2*A.bndR- temp1; % reflected radial length
            P(m).phi(nn)= mod(P(m).phi(nn)+pi,2*pi);
        end
        P(m).rsq(nn)= temp2^2; % squared version
        % revised Cartesian version
        P(m).coord(nn,1)= temp2*cos(P(m).phi(nn));
        P(m).coord(nn,2)= temp2*sin(P(m).phi(nn));
    end
end
% ----
% determine MSD
P(m).time(nn)= nn; % "time" is simply the step number (can rescale as needed)
%P(m).MSD(nn)= sqrt(P(m).coord(nn,1)^2 + P(m).coord(nn,2)^2); % radial position (not squared)
%P(m).MSD(nn)= P(m).coord(nn,1)^2 + P(m).coord(nn,2)^2; % squared to get the "S" in MSD
P(m).MSD(nn)= P(m).rsq(nn); % note that this is the radial position squared (hence "S" in MSD)
end
end

% -----
% compute mean MSD (across all walkers) --> KLUDGE (better way to do this sans loops??)
for nn=1:steps
    for m= 1:walkerNum
        val(m)= P(m).MSD(nn);
    end
    meanMSD(nn)= mean(val);
end
end

```

```

% -----
% plot vals. for a (specified) individual walker
if l==1
    figure(1); clf;
    subplot(211); plot(P(kk).coord(:,1),P(kk).coord(:,2),'k.-');
    xlabel('x'); ylabel('y'); grid on; hold on; title('Walker position')
    axis([-axLim axLim -axLim axLim])
    % --- (plot a bounding circle)
    if A.Pbound==1
        th= 0:pi/50:2*pi; xunit= A.bndR*cos(th); yunit= A.bndR*sin(th); h66= plot(xunit, yunit,'r-');
    end
    % --- (plot MSD for an individual walker)
    subplot(212); plot(P(kk).time,P(kk).MSD,'k-');
    xlabel('Time'); ylabel('Radial displacement (squared)'); grid on; hold on;
end

% -----
% plot MSD for the ensemble
figure(2); clf;
plot(P(m).time,meanMSD,'k-');
xlabel('Time'); ylabel('MSD'); grid on; hold on;
% if constrained, visualize effective bounding limit
if (A.Pbound==1), h2B= stem(A.bndR^2,max(meanMSD),'r--','LineWidth',1);
    legend(h2B,'Bounding radius (squared)','Location','SouthEast'); end

% -----
% plot distribution of angular values (polar histogram)
if l==0
    figure(3); clf;
    % == (single walker) directions taken for each step for an individual walker
    subplot(221); h3= rose(P(kk).theta,30);
    set(h3,'LineWidth',1.5); x = get(h3,'Xdata'); y = get(h3,'Ydata'); g=patch(x,y,'y');
    title('All steps for a single walker'); grid on; hold on;
    % == (all walkers) directions taken for all steps of all walkers
    subplot(223); h3= rose([P(:).theta],30);
    set(h3,'LineWidth',1.5); x = get(h3,'Xdata'); y = get(h3,'Ydata'); g=patch(x,y,'y');
    title('All steps for all walkers'); grid on; hold on;
    % == (all walkers) final position for all walkers [KLUDGE: not sure how to do sans loop]
    for mm=1:numel(P) bank(mm)= P(mm).phi(end); end
    subplot(224); h3= rose(bank,floor(numel(P)/15));
    set(h3,'LineWidth',1.5); x = get(h3,'Xdata'); y = get(h3,'Ydata'); g=patch(x,y,'y');
    title('Final ang. position of all walkers'); grid on; hold on;
end

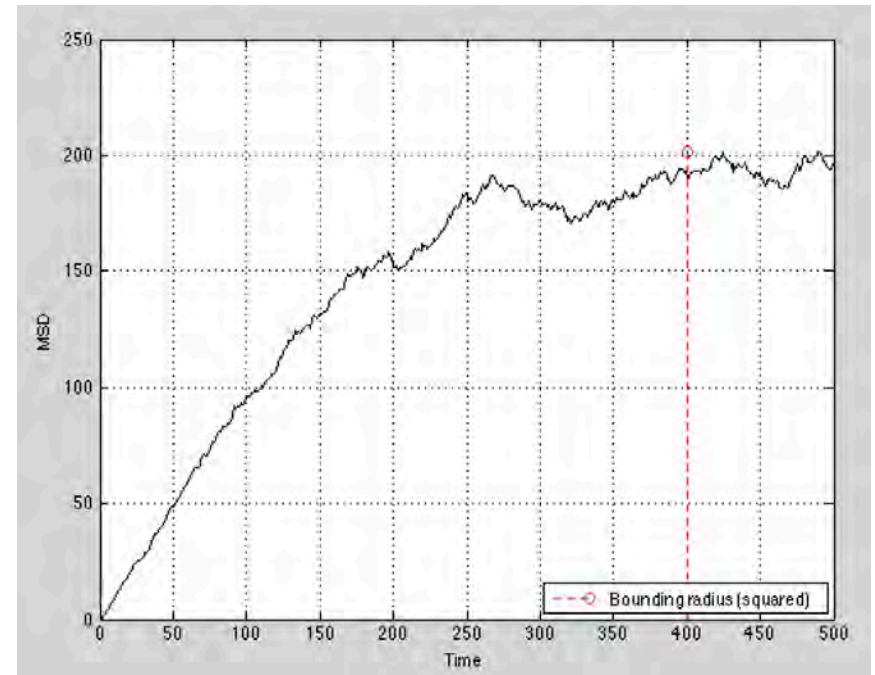
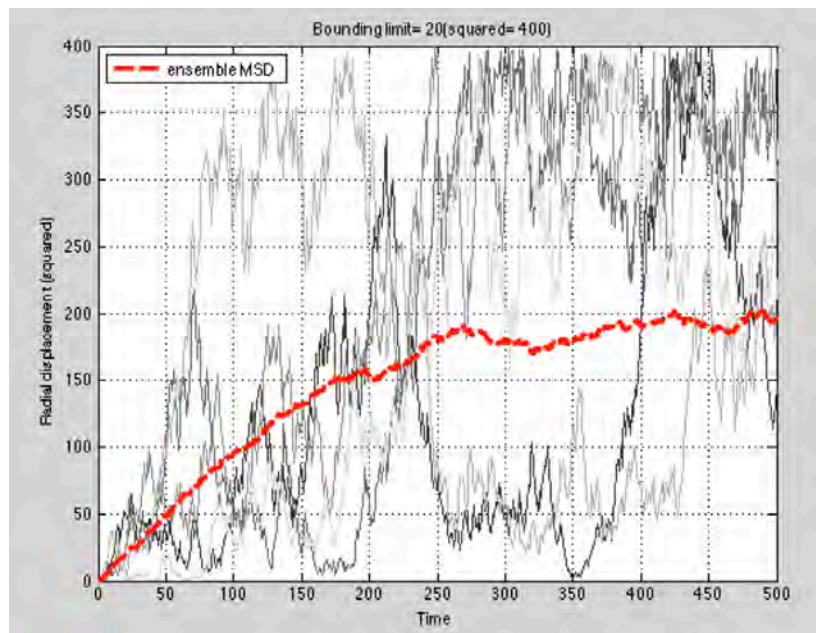
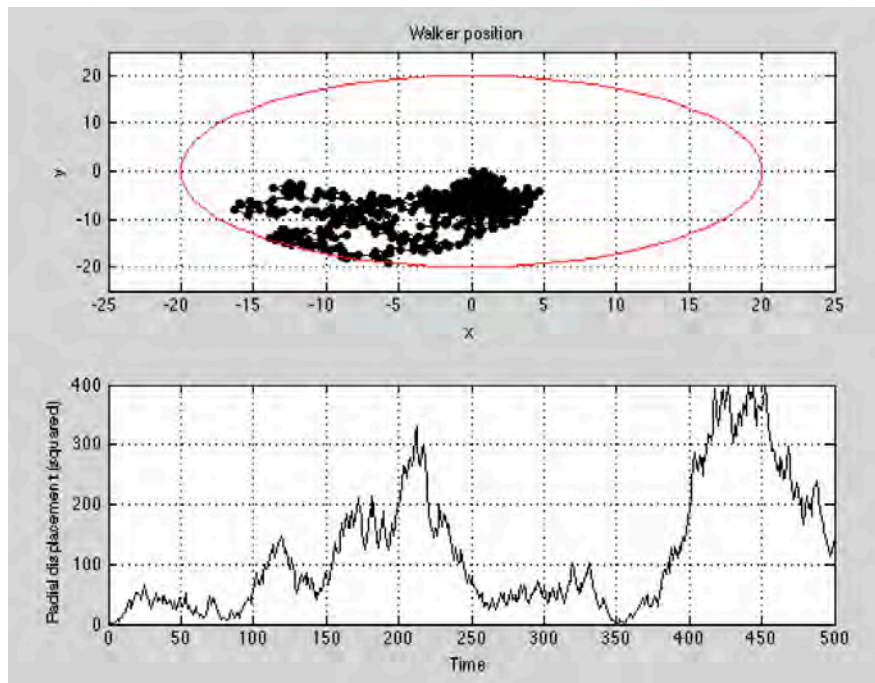
```

```

% -----
% plot time course (or r^2) for several walkers? (see also Fig.1B)
if l==1
    figure(4); clf;
    for n=1:numWplot
        hh= 0.8*n/numWplot; % shading factor (to discern different traces)
        plot(P(n).time,P(n).MSD,'-', 'Color',hh*[1 1 1]); grid on; hold on;
    end
    leg= plot(P(m).time,meanMSD,'r--', 'LineWidth',2); % also plot ensemble MSD
    xlabel('Time'); ylabel('Radial displacement (squared)');
    title(['Bounding limit= ',num2str(A.bndR), '(squared= ',num2str(A.bndR^2),')']);
    legend(leg,'ensemble MSD','Location','NorthWest');
end

% -----
% movie for an individual walker
if animate==1
    figure(66); clf; axis([-axLim axLim -axLim axLim]); grid on; hold on;
    for nn=2:steps
        % --- (plot a bounding circle)
        if A.Pbound==1
            th= 0:pi/50:2*pi; xunit= A.bndR*cos(th); yunit= A.bndR*sin(th); h66= plot(xunit, yunit,'r-');
        end
        % --- (plot/update the track)
        %plot(P(kk).coord(nn,1),P(kk).coord(nn,2),'ko-');
        plot([P(kk).coord(nn-1,1) P(kk).coord(nn,1)], [P(kk).coord(nn-1,2) P(kk).coord(nn,2)], 'k.-');
        pause(0.04); % {0.04}
    end
end
end

```



➤ Introducing a bias.....

